ELECTRONIC PROPERTIES OF AMORPHOUS SEMICONDUCTORS

A Thesis

Submitted to the

Faculty of Graduate Studies and Research

The University of Manitoba

In Partial Fulfillment

of the Requirements for the Degree of

Master of Science

by

Gino Angelo Petrillo

April, 1973

ACKNOWLEDGEMENT

The author wishes to express his grateful appreciation to Dr. K.C. Kao for suggesting the thesis subject and for his supervision throughout the entire work.

Sincere thanks must be given to the students and staff of the Department of Electrical Engineering of the University of Manitoba for their assistance and co-operation throughout the work of this thesis.

Finally, this research was supported by the National Research Council of Canada under grant number A 3339, and the Defence Research Board of Canada under grant number 5501-65.

ABSTRACT

The electrical switching and memory properties of the amorphous composition Te_{48} As_{30} Si_{12} Ge_{10} have been investigated, and emphasis has been placed on the initial switching behaviour of new devices, the durability of devices when subjected to continuous operation, and the energy required to obtain the memory state. It has been found that the degree of stability in the switching threshold voltage, both initially and after many thousands of switching cycles, depends on the operating current levels, switching involving higher current being less stable than that involving a smaller current. It has also been found that the durability of the devices which were investigated depends on operating current levels; operating currents of 1 mA resulted in stable switching for more than $5X10^4$ switching cycles, whereas operating currents of 18 mA resulted in rapid deterioration after only several switching cycles. The transition from threshold switching without memory, to threshold switching with memory, depends mainly on the energy input to the device, and for the devices used in the present investigation this energy is about 0.03 Joules. All of the results can be explained on the basis that the transition which occurs in conductivity for both ordinary switching and memory switching is due to the formation of conductive filaments, and that their formation is preceded by a diffusion of certain constituent atoms away from the filament region and other atoms towards the region, so that the final composition of atoms along the filamentary path is more favourable to structural changes towards a more crystalline structure.

TABLE OF CONTENTS

Chapter 1	Introduction	1
Chapter 2	Review Of Previous Work On Amorphous Semiconductors	5
	2.1 Electronic states and energy bands	5
	2.2 Mechanisms of electronic conduction	9
	2.3 Switching and memory behaviour	17
	2.3.1 The amorphous threshold switch	20
	2.3.2 The amorphous memory switch	23
	2.4 Mechanisms of switching	25
	2.4.1 Switching due to electronic processes	25
	2.4.2 Switching due to electrically induced thermal processes	29
	2.5 Some important experimental results	31
	2.5.1 Conductivity and I-V characteristics for the Te-As-Si-Ge system	31
	2.5.2 The dependence of threshold voltage on sample thickness	33
	2.5.3 The dependence of threshold voltage on temperature	34
	2.5.4 The dependence of switching delay time and recovery time on applied voltage	37
Chapter 3	Theoretical Approaches	42
	3.1 Carrier mobility and conductivity in disordered structures	42
	3.2 The current-voltage (I-V) characteristics for covalent amorphous semiconductors	50
	3.3 Calculation of the threshold voltage and the delay time based on thermal switching	54

3.4 Switching due to electronic processes-avalanche ionization 59

Chapter 4 Experimental Techniques 67

4.1 Sample preparation 67

4.2 Experimental procedures 69

4.2.1 Switching instabilities in new devices 69

4.2.2 The effect of long-term continuous cycling on the properties of threshold switches 75

4.2.3 The effect of peak current on the durability of amorphous threshold switches 77

4.2.4 Memory behaviour of threshold devices in the Te-As-Si-Ge system 79

4.2.5 The effect of temperature on the switching voltage and switching time 82

Chapter 5 Experimental Results and Discussion 83

5.1 General switching and memory characteristics 83

5.1.1 The current-voltage characteristics 83

5.1.2 The switching time 85

5.1.3 The memory phenomenon 87

5.2 The initial switching behaviour of new devices 89

5.3 The effects of long-term continuous switching on the properties of threshold devices 96

5.4 The effect of peak current on the durability of threshold switches 100

5.5 Memory behaviour of threshold devices in the Te-As-Si-Ge system 104

5.6 The effects of temperature on electrical switching properties 108

Chapter 6 Conclusions 111

6.1 Switching properties 111

6.2 Memory properties 112

References 115

LIST OF MOST USED SYMBOLS

A	activation energy for electrical conduction (expressed in temperature units)
a	interatomic separation
C	heat capacity per unit volume
D	carrier diffusion constant
d	thickness of active material (electrode separation)
E_c	energy at the conduction band edge
E_v	energy at the valence band edge
E_F	energy at the Fermi level
E_g	band gap energy
E_h	average activation energy required for hopping
E_p	energy of polarization near a localized state of order
E_{K_i}	energy of state K_i
ΔE	activation energy for electrical conduction
F_{cr}	critical electric field required for switching
f	jump frequency between two states
$f(E)$	Fermi-Dirac function
I_H	holding current required to maintain the high conductivity state
K_B	Boltzmann constant
K_c	degree of compensation
ℓ	current distubution factor (ratio of filament current to total current)
m_n	effective electron mass

N_m	concentration of majority carriers
N_τ	total trap density
N_τ'	fraction of charged traps
$N(E)$	density of states at energy level E
P_h	hopping probability per unit time
$p(R)$	tunnel factor
q	electronic charge
R	mean separation between trapping centers
R_T	thermal resistance
R_{pp}	average rate of electron-hole production
r	hydrogenic radius of a state
T_e	electron temperature
T_{cr}	critical temperature reached during switching
ΔT	incremental temperature changes
t_D	switching delay time
t_R	switching recovery time
V_c	conduction voltage
V_o	average random potential for state localization
V_{TH}	switching threshold voltage
v_d	carrier drift velocity
v_τ	thermal velocity of carriers
ε	dielectric constant
ε_o	dielectric constant of free space
λ	mean free path of carriers
σ	electrical conductivity

σ_o	pre-expoential conductivity factor
σ_T	thermal conductivity
ν_σ	frequency factor for potential fluctuation
ν_{ph}	phonon frequency
ν_{el}	electron frequency
τ_{pp}	time constant for electron-hole pair production
θ	temperature of the switching filament
ρ_T	thermal resistance of switching filament
μ	carrier mobility

CHAPTER 1

INTRODUCTION

The properties of crystalline semiconductors have been extensively investigated in the past two decades. Quantum theory, supported by experiments, has resulted in the understanding of conduction processes and many other important phenomena in crystals. The development of the transistor, for example, is the result of the research in the field of crystalline semiconductors. Until recently, solid state physics and electronics have been primarily concerned with the properties of materials having crystalline structure (i.e. with long range order and periodicity). Non-crystalline materials, or more specifically amorphous semiconductors however, have no long range order (i.e. no regular periodicity) although local short range order does exist. This means that each atom sees its neighbouring atoms in much the same relative positions as in a crystal.

Several aspects of amorphous semiconductors may be considered as characteristic of the disordered phase. For example, anomalous Hall effects, temperature activated drift mobilities, frequency dependence of conductivities, and electric field dependence of quantum efficiencies, to mention but a few properties, have all been widely reported in the literature (Male 1967, Mott 1967, Cohen 1968). Also, several investigators have proposed a number of models and theories in an attempt to explain the observed facts (Anderson 1958, Mott 1967, Boer 1970, Cohen 1970). It has been postulated that conduction in amorphous semiconductors is due to the coexistence of two basic mechanisms-band conduction and conduction due to hopping,

and that in the amorphous phase a material may have a continuous range of energy states in which all of the wave functions are localized.

One of the important factors which has stimulated the present interest in amorphous materials is the apparent inability of the present theory of solid state physics to explain the optical, electrical, and thermal properties of these materials. The concept of energy bands and Fermi surface, which have been formulated and developed based on the periodic nature of the crystal lattice, cannot be applied directly to amorphous materials. Another factor which has resulted in a great deal of research in this field is the potentiality of amorphous semiconductors for switching and memory devices. The switching phenomenon in these materials has been reported by many investigators over the past decade. Pearson (1962) has reported switching amd memory effects in the As-Te-I system. Kolomiets and Lebedev (1963) has observed the switching phenomenon in $TlAs\ (Se,\ Te)_2$, and Simmons and Verberder (1967) have reported that amorphous silicon monoxide could be used for memory switches. Switching in amorphous films of various semiconducting materials has also been observed by Chopra (1965). Some details of the Ovonic switch based on evaporated films of a mixture of tellurium, arsenic, germanium, and silicon have been reported by several investigations (Ovshinsky 1968, Mott and Davis 1972).

The most important elements in amorphous semiconductors and those which have been extensively investigated are Si and Ge in Group IV; P, As, Sb, and Bi in Group V; and S, Se, and Te in Group VI. The methods

on preparation include: evaporation and condensation on a cold substrate, cathode sputtering, exposing crystalline materials to very high doses of high energy radiation, rapid quenching techniques, anodic oxidation, and, in some cases, cooling the material from the melt. The two most commonly used procedures are: (1) the formation of films by evaporation and condensation onto a cold substrate, by cathode sputtering or other techniques, and (2) by rapid cooling of the melt. The variety of materials and methods of preparation has made it possible to obtain a wide range of configurational structures ranging from the quasi-crystalline state to the highly disordered state. The structural properties of these materials depends greatly on the specific elements used, and on the method of preparation.

In the investigation being reported in this thesis the covalent alloy Te_{48} As_{30} Si_{12} Ge_{10} was used. All of the devices used had an active material thickness of 100 μm between two vacuum evaporated electrodes. The specific properties to be studied are: (1) the initial switching characteristics of new devices under various operating currents and switching rates, (2) the characteristics and lifetime of devices when subjected to continuous switching over a long period of time, (3) the effect of operating current on the durability, and reliability of switching devices, (4) the memory behaviour and the conditions required to obtain and to erase memory, and (5) the variations of switching threshold voltage, switching time, and holding current with temperature. The primary purpose of the investigation is to gain a better understanding of the actual mechanisms responsible for the switching and memory phenomena in amorphous materials, and to determine some guidelines with respect to

the practical applications of devices made of amorphous semiconductors.

Chapter 2 of this thesis gives a brief systematic review of previous theoretical and experimental work. Chapter 3 presents several mathematical models for elucidating the properties of amorphous semiconductors with emphasis on models for switching and memory behaviour. The experimental procedures and circuits are described in detail in Chapter 4, and the results and discussion are given in Chapter 5. Tentative conclusions arising from this investigation are given in Chapter 6.

CHAPTER 2

REVIEW OF PREVIOUS WORK ON AMORPHOUS SEMICONDUCTORS

The first part of this chapter will deal with several of the more fundamental and widely accepted explanations and models for the basic phenomena observed in amorphous semiconductors including the energy band model for these materials and a review of several mechanisms responsible for conduction, switching, and memory behaviour. The second part of this chapter will be devoted to a review of experimental work with particular emphasis on the Te-As-Si-Ge system. Throughout the present chapter a strong emphasis will be given on the correlation between the theoretical and experimental results. It should be noted, however, that although some models have been highly successful in elucidating certain isolated observations, there is no unified theoretical approach capable of explaining all experimental results.

2.1 ELECTRONIC STATES AND ENERGY BANDS

The simplest possible model for an amorphous semiconductor is shown in Fig. 2.1 (a). There is a valence band with a tail of localized states above E_V and a conduction band with a tail of localized states below E_C. Thus only a pseudogap exists between the valence and conduction bands. The simple model presented in Fig. 2.1 (a) is probably only adaquate for elemental and compound amorphous semiconductors. Though these materials are transitionally disordered, the short range order is in general so well defined that only structural defects can occur. Examples of such defects are broken bonds in a covalently bonded network, nonbridging atoms, and chain ends. Being structurally well defined,

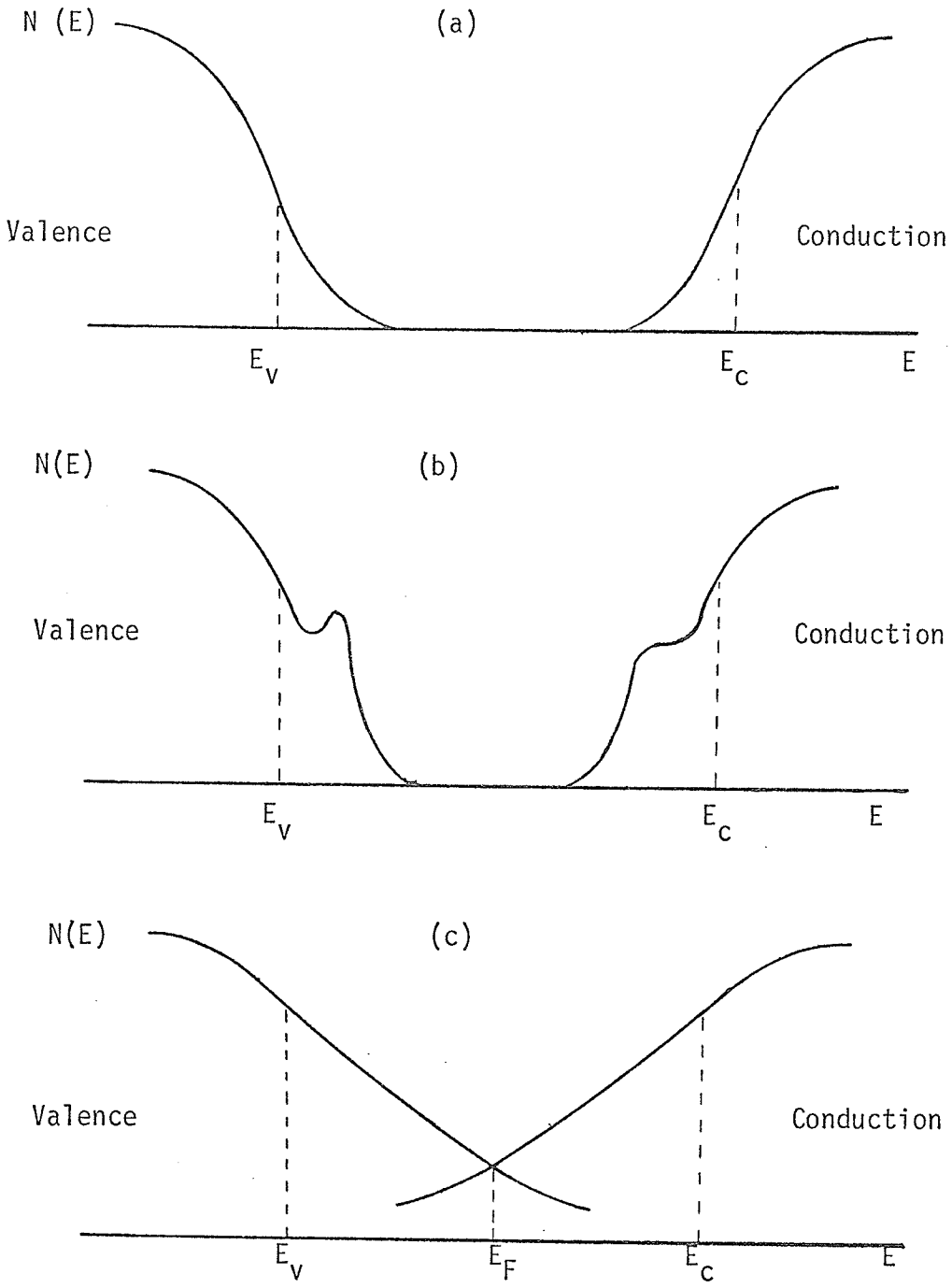

Fig. 2.1 Band models for amorphous semiconductors.
(a) Valence and conduction bands with extended states for $E>E_c$ and tails of localized states on each band.
(b) Local order leads to the presence of well defined structural defects and nonmonotonoicity in N(E) in or near the tails.
(c) The tails of the conduction and valence bands overlap, leading to a finite density of states at the Fermi energy and a finite concentration of localized charged states near E_F (after Cohen 1970).

these defects can be expected to have well defined energy levels associated with them. These would not be sharp as in a crystal but would vary somewhat with local environment giving rise to peaks in the density of states as illustrated in Fig. 2.1 (b).

Neither of Fig. 2.1 (a) and (b) is adaquate for concentrated amorphous covalent alloys such as those based on the chalcogenides Se and Te. Such alloys contain atoms of varying valences in large concentrations. The original work by Anderson (1958), and Mott (1967), has led Cohen et al. (1970) to formulate the CFO (Cohen-Fritzsche-Ovshinsky) model which has been quite successful for the covalent amorphous semiconducting alloys. The CFO model is based on four signicicant postulations: 1) amorphous semiconducting alloys with widely varying valences behave as intrinsic materials because the individual atoms have their valence requirements satisfied locally, i.e., all valence bonds are saturated, 2) these alloys are characterized by valence and conduction bands of extended states as shown in Fig. 2.1 (c), 3) both bands of extended states have tails of localized states, and 4) there exists a well defined energy, E_v or E_c , in each band at which a transition from extended to localized states occurs. The CFO model incorporated with these four points formulates four additional features. 5) In amorphous semiconducting alloys the disorder is sufficiently great that the tails of the conduction and valence bands overlap. Because bonding conditions and hence valence requirements are satisfied locally, the connectivity of the atomic structure varies randomly throughout the material. There are not merely the typical translational disorder of an amorphous material and the typical compositional disorder of an alloy, but also an enhanced

translational disorder because of the additional randomness of the structural network itself, forced by variations in its connectivity from site to site. 6) The localized states which come off the valence band and those which come off the conduction band are always identifiable as either valence band states or conduction band states even when their energy levels lie in the region of overlap. 7) There exists a continuous distribution of charged traps in the middle of the band gap. That is, valence band states are locally neutral when occupied. Therefore, an empty valence tail state above the Fermi level contributes a localized positive charge. Conversely, conduction band states are locally neutral when empty, and an occupied conduction tail state contributes a localized negative charge. 8) In the transition from extended states to localized states the transport processes change their character. It is speculated that above E_c in the conduction band, charge transport is achieved primarily through band conduction mechanisms, whereas below E_c transport occurs by phonon-assisted hopping between the localized states. A similar process also occurs in the valence band.

The eight features of the CFO model have been used to explain several experimental results with varying degrees of success. For example, this model has been used to explain the existence of a well defined activation energy in the conduction process i.e. , the apparent intrinsic character of the conductivity (Cohen et. al 1969). This model may also give some insight into the relationship between photoconductivity and frequency of incident radiation, and quantum efficiencies, observed by Fagen and Fritzsche (1970). Feature (8) of this model may explain the difference in the values of mobility caused by the various conduction

mechanisms and may therefore help to clarify the anomalous behaviour of the Hall effect reported in the literature (Pearson 1963, Kolomiets and Nazarowa 1960, Male 1967, Peck and Dewald 1964).

2.2 MECHANISMS OF ELECTRIC CONDUCTION

The electrical conductivities of many amorphous semiconductors, particularly bulk chalcogenide glasses produced by cooling a melt, follow the relation

$$\sigma = \sigma_o \exp(-\Delta E/K_B T) \quad , \tag{2.1}$$

where σ_o is the pre-exponential conductivity factor and is of the order $10^3 - 10^4\ \Omega^{-1}\ cm^{-1}$, and ΔE is the activation energy of the electrical conduction which is usually 0.2 eV larger than half the band gap of the material. A typical plot of the temperature dependence of conductivity for several amorphous semiconductors is given in Fig. 2.2. The insensitivity of these materials to doping suggests that the conduction is intrinsic so that the slope of these curves is proportional to one half of an energy gap. It seems as though the presence of short range order is sufficient to ensure that the electronic density of states in the amorphous phase is not significantly different from that of the crystalline phase, and that the concept of a forbidden gap, with an energy equal to that for breaking covalent bonds between atoms, is acceptable. It is reasonable to assume, on the basis of other properties of amorphous semiconductors, that the electronic states at the band edges are perturbed on going from the crystalline to the amorphous phase and that the density

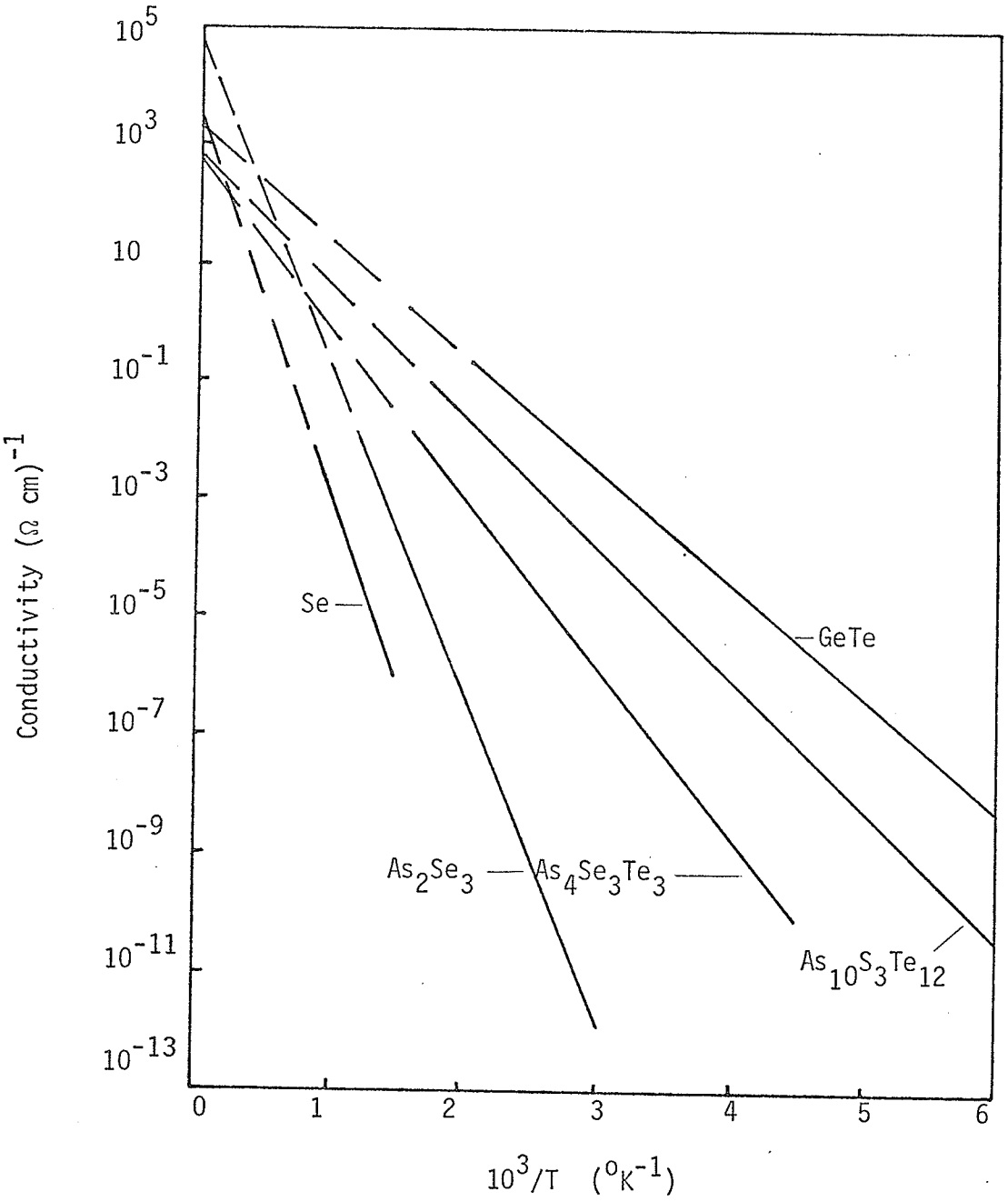

Fig. 2.2. Temperature variation of conductivity of a few amorphous semiconductors. (after Davis and Shaw 1970).

of states is finite in the energy gap (Banyai 1964, Mott 1967, Fagan and Fritzsche 1970). Fig. 2.3 shows schematically the tailing of the states into the gap to a degree in which valence states and conduction states overlap near the center of the gap. As mentioned previously, the states in these tails arise from structural defects, and large variations in density and composition throughout the material. The levels are distributed over a sufficiently wide energy range to satisfy the Anderson criterion for state localization (Anderson 1958, Anderson 1961). The Anderson criterion is

$$V_o > 10zI^o \exp(-\alpha R) , \qquad (2.2)$$

where V_o is the average random potential, z is the coordination number, I^o represents an overlap integral, R is the mean separation between centers, and α gives a measure of the extent of the wave function on isolated centers. In addition to these tails of localized states, the absence of long range order will, if the wave functions on the atoms are not s - like, lead to the localization of states at the band extremities up to well defined energies A and B where the density of states is perhaps equal to about 20% of the effective density of states associated with the band.

Because the states between A and B are localized, conduction can occur in these energy states only by a thermally activated tunneling process similar to that occuring between centers in a heavily doped semiconductor and commonly referred to as impurity conduction. The mobility associated with this process is generally quite small and may be expressed in the form

$$\mu = \frac{q\nu_{Ph} R^2 e^{-2\alpha R} e^{-E_h/K_BT}}{K_BT} , \qquad (2.3)$$

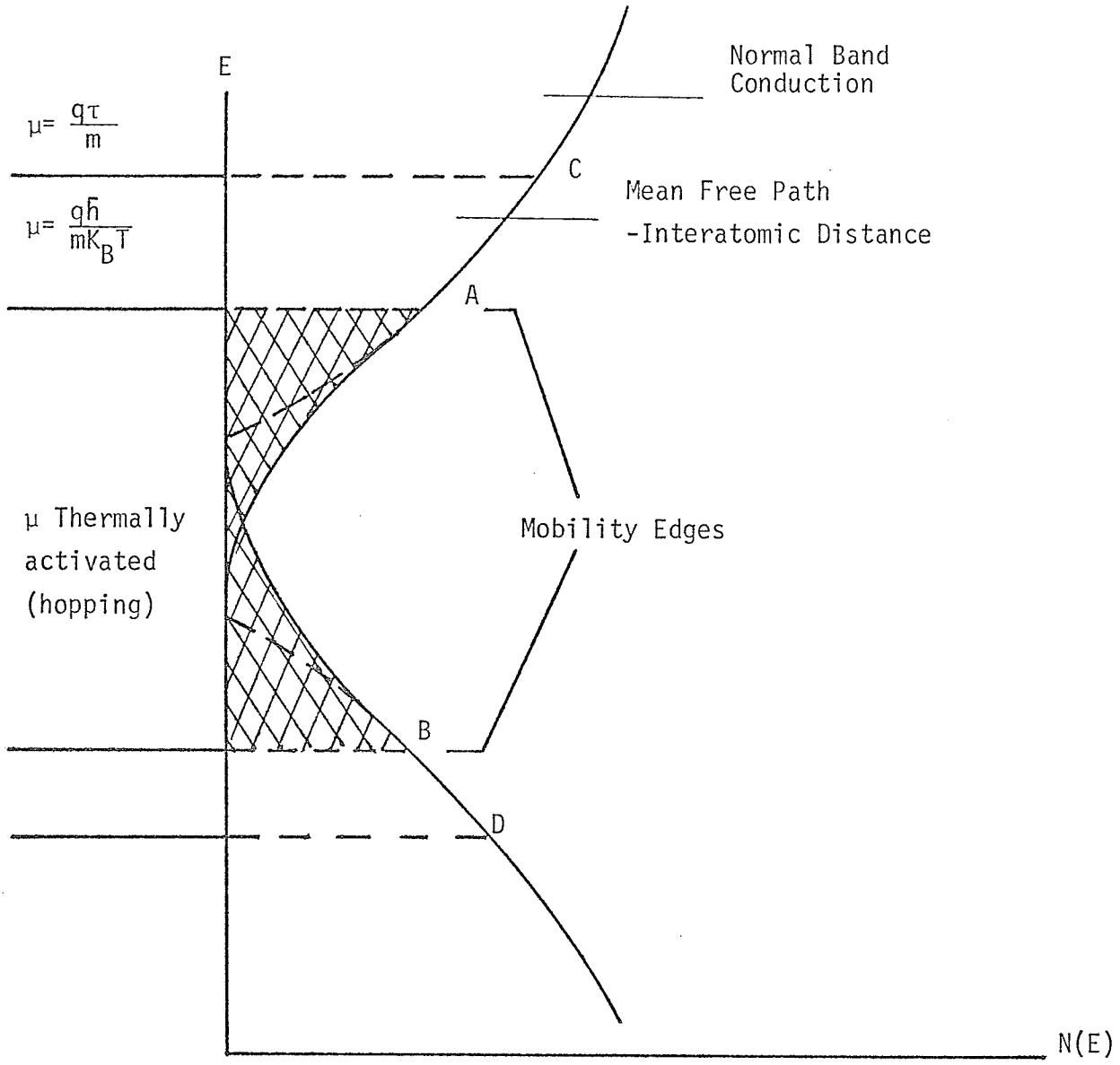

Fig. 2.3. Schematic representation of the density of states in an amorphous semiconductor, showing the regions (shaded) in which the electronic states are localized and the regions in which the carriers move with short mean free path. (after Davis and Shaw 1970).

where V_{Ph} is a phonon frequency, and E_h is the average activation energy required for hopping. For amorphous materials a quantitative calculation of μ is quite difficult. Near A and B, however, E_h is expected to be small and the tunneling factor exp $(-2\alpha R)$ approaches unity. Under these conditions the hopping mobility has its maximum value, typically $\sim$ 0.1 cm^2/V sec.

Immediately beyond A and B where the states are delocalized the carriers can move without thermal activation. In the region of delocalized states however, the mean free path is expected to be of the order of the interatomic separation and the appropriate expression for the mobility becomes

$$\mu = \frac{qa^2}{K_B T} \nu_{el} \quad . \tag{2.4}$$

ν_{el} is the electronic frequency which is equal to $\hbar$ / $ma^2 \sim 10^{15}$ sec^{-1}, and a is the interatomic separation. The mobility in this region is expected to be approximatly 40 cm^2/V sec. Deep into the bands, beyond C and D, band conduction with long mean free paths will occur and the normal formula for the mobility

$$\mu = \frac{q \tau}{m} \tag{2.5}$$

can be used.

The energy gap in a crystalline semiconductor is usually a gap between extremities in the density of states, whereas in amorphous solids it is really a gap between mobility edges A and B (Cohen et al. 1969). The conductivity curves of Fig. 2.2 therefore, represent intrinsic activation across a mobility gap AB. Extrapolation of these curves to 1/T=0 yields a value of σ_o which ranges between 10^3 and 10^4 Ω^{-1} cm^{-1} in most

amorphous materials, corresponding to values of mobility between 10 and 100 cm^2/V sec for a reasonable density of states. This substantiates the idea of a mean free path of the order of the inter - atomic separation.

One of the most important conduction mechanisms in amorphous materials involves the transport of carriers by a process of hopping from one localized state to another. In the evaluation of the conductivity due to hopping there are two basic points to consider. First of all it is necessary to evaluate the probability per unit time that the electron jumps from one localized state to another. Mott (1967) has formulated an expression for this probability and it is

$$P_h = \nu_{Ph}\, p\,(R)\, \exp\,[-(\Delta E_h + \tfrac{1}{2}E_p) \,/\, K_B T] \qquad (2.6)$$

In this expression p (R) is a tunnel factor which must be introduced if the distance R between states is large, ΔE_h is the difference in energy of the two levels, and E_p is the energy of polarization round a localized state of order. The energy of polarization is given by (Miller and Abrahams 1961)

$$E_p = \tfrac{1}{2}\,\frac{q^2}{r_o}\,\left(\frac{1}{\varepsilon_o} - \frac{1}{\varepsilon}\right), \qquad (2.7)$$

where r_o is the radius of the center belonging to a state, and ε_o and ε are the dielectric constants of free space and the amorphous material respectively. The second point is that the tunnel factor p (R) , and the energy difference between states ΔE_h, vary greatly from one jump to another and as a result it is necessary to average the hopping probability P_h over all possible jumps in order to obtain the a c or d c conductivity. By means of this averaging process it has been shown that the a c conductivity is higher than

the d c conductivity and increases with frequency (Pollak and Geballe 1961, Pollak 1962), and that the activation energy for conduction decreases with decreasing temperature.

Very closely associated with the hopping mechanism is the phenomenon known as impurity - band conduction. In the present context impurity - band conduction will refer to the motion of an electron from one impurity center to another under the condition that the overlap between the orbitals of neighbouring centers is great enough to allow tunneling but not great enough for a transition to the metallic state. This process can only occur if compensation is present and it usually but not always involves a hopping process. The phenomenon identified as impurity - band conduction was first observed by Hung (1950) and by Hung and Gleissman (1950, 1954). Latter Conwell (1956) and Mott (1956) emphasized that this process could only occur when compensation was present. The work of Fritzsche (1958, 1959, 1960) demonstrated experimentally the role of compensation. Mott (1956) was the first to emphasize that the process involved an activation energy.

At low concentrations, the states will certainly be localized and motion will be due to the hopping process. Under this condition two cases are of major interest: 1) Very small compensation - we then have a few vacancies in n-type centers (or electrons in p-type centers) which are bound to the nearest charged minority carrier with the binding energy ΔE equal to $q^2/\epsilon R$. The number of free carriers is proportional to exp $(-\frac{1}{2} \Delta E/K_B T)$ and ΔE is thus the activation energy of the hopping process. This case has been studied extensively by Mott (1956). 2) Moderate compensation- this is the case considered by Miller and Abrahams (1960) in which they used many different materials for their investigation.

In this case the energy difference ΔE between neighbouring centers depends on the random electric fields due to charged centers of both types. If K_c is the degree of compensation, then for small K_c Miller and Abrahams have found that the linking energy is given by the relation

$$\Delta E = (q^2/\varepsilon_o R)\ (1-1.35\ K_c^{1/3}) \quad , \tag{2.8}$$

where R is equal to $(4\pi N_m/3)^{-1/3}$, and N_m is the concentration of majority carriers. For larger values of K_c Eqn. (2.8) becomes

$$\Delta E = 0.285\ \frac{q^2}{\varepsilon_o R} \ , \tag{2.9}$$

when $K_c \sim \frac{1}{2}$.

The jump frequency between two states with energy difference ΔE is given by (Miller and Abrahams 1960)

$$f = \frac{1}{\tau} = 2x10^{12}\ (R/r)^{3/2} \exp\ (-2R/r)\ \tanh.\ (\Delta E/K_B T), \tag{3.10}$$

where r is the hydrogenic radius of each state. Using the averaging process Miller and Abrahams have calculated the d c conductivity and pointed out that: 1) the logarithm of the resistivity is proportional not to R, but to $R^{3/2}$; 2) the decrease in the apparent activation energy ΔE with T, which should occur in a random hopping process, does not appear in their investigation.

The Hall coefficient of impurity conduction in silicon and germanium

has been investigated in the hopping region by Amitay and Pollak (1966), but no Hall voltage was observed, and this has made it necessary to make some revisions of the averaging precedures of Holstein's (1961) theory.

Based on the averaging procedures the a c conductivity should be greater than the d c conductivity and should increase with frequency. This phenomenon has been investigated and confirmed both experimentally and theoretically by Pollak et al. (Pollak and Geballe 1961, Sewell 1963, Pollak 1964, 1965).

2.3 SWITCHING AND MEMORY BEHAVIOUR

It is well known that the majority of materials cannot withstand electric fields in excess of about 10^6 V/cm. In common insulators, fields of this magnitude invariably results in a destructive breakdown. This is, in general, a non-regenerative change of the material along the breakdown path. The amorphous semiconductors differ considerally from insulating materials because the abrupt change in electric conductivity in amorphous semiconductors can be regenerative and non-destructive (Ovshinsky 1965, Pearson 1962, Ovshinsky 1968). The physical processes which determine and sustain the conduction after the abrupt change in conductivity has taken place, may be quite different from those which initiate and lead to the transition. Before proceeding to the mechanisms leading to switching, as well as the processes taking place once the transition in conductivity has occurred, it may be desirable to classify some important types of switching characteristics.

There are basically four main current-voltage characteristics commonly

encountered in amorphous semiconductors and these are illustrated in Fig. 2.4. Fig. 2.4 (a) illustrates the negative differential resistance phenomenon. With a proper choice of the load resistor this negative differential resistance device can be kept at any point of the I-V curve. Fig. 2.4 (b) shows a typical characteristic of the amorphous semiconductor switch. Two states are possible, one of low conductivity and the other of high conductivity. The device can be switched from the low conductivity to the high conductivity state when the applied voltage reaches a characteristic value, termed the threshold voltage V_{TH}. The high conductivity state remains as long as the current does not fall below a typical limit known as the holding current I_H. This does not imply, however, that V_{TH} and I_H are the only parameters determining the switching behaviour. Fig. 2.4 (c) illustrates the negative differential resistance with memory characteristic of a typical device. The negative differential resistance device with memory has two stable states. The first state resembles that of Fig. 2.4 (a). The second state is conductive, which is established at higher currents and remains without decay. The first state can be re-established by increasing the current above a certain value and by switching it off rapidly. The final I-V characteristics observed is shown in Fig. 2.4 (d). This characteristic represents switching with memory. This device is normally in its low conductivity or blocking state for voltages less than the threshold value. The current increase monotonically with applied voltage and this I-V relation depends on the material used and on the mode of operation (a c or d c). When the voltage exceeds the threshold value a transition occurs from the low conductivity state to the high conductivity state. The high conductivity state may be maintained for a period of months even though the applied

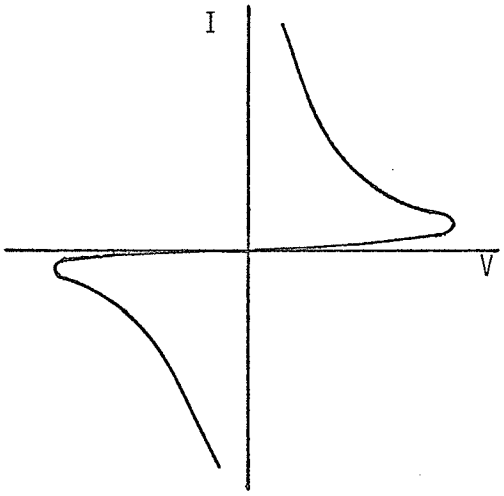

(a) Negative Resistance

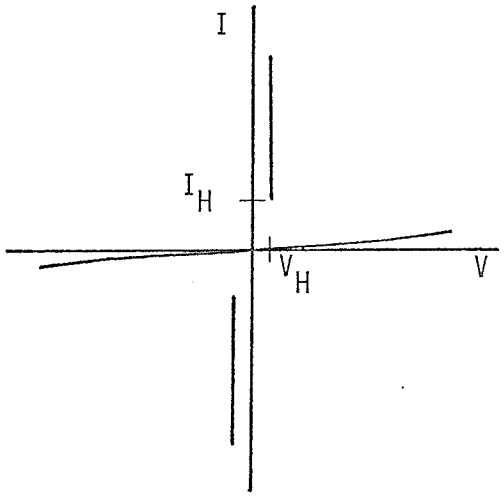

(b) Threshold Switching

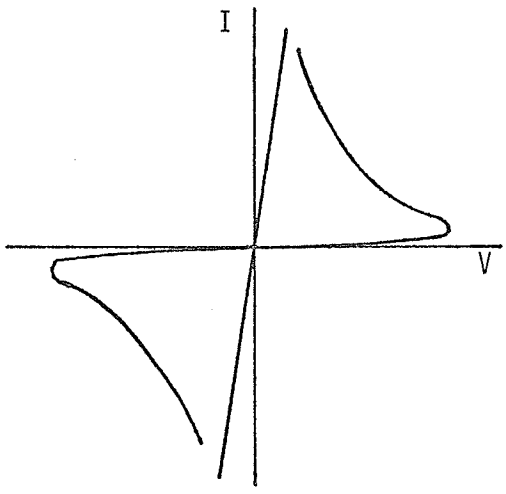

(c) Negative Resistance
With Memory

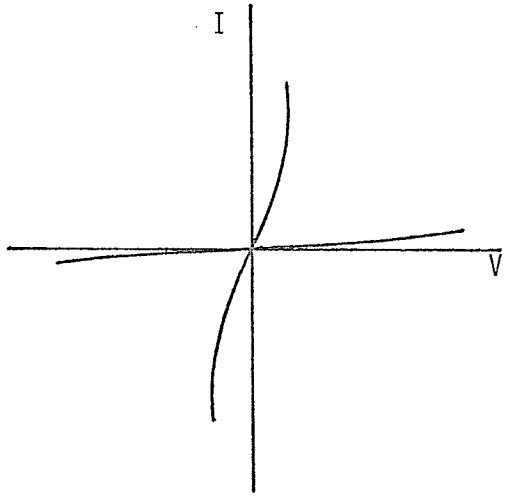

(d) Threshold Switching
With Memory

Fig. 2.4. Classification of current-controlled switching characteristics. (after Fritzsche and Ovshinsky 1970).

voltage is reduced or removed completely. To recover the original state of low conductivity, the device must be subjected to a sufficiently large a c or d c current, a temperature or pressure shock, radiation from an RF discharge, or an RF current. In the following section we shall discuss switching of the types illustrated in Fig. 2.4 (b) and (d) in more detail.

2.3.1 THE AMORPHOUS THRESHOLD SWITCH

The amorphous threshold switch is a device having two electrodes with the active switching amorphous material between them. It is characterized by a resistance ranging from several megohms to several hundred megohms in its blocking state, a very rapid transition time to the high conductivity state (less than 150 p sec in some devices), and a resistance ranging from several ohms to several hundred ohms in its conducting state. Fig. 2.5 shows the typical I-V characteristics of a particular threshold switch known as an OTS (ovonic threshold switch, after Ovshinsky 1965). The active amorphous material used in this device is an evaporated film of $Te_{48}\ As_{30}\ Si_{12}\ Ge_{10}$, of thickness 5×10^{-5} cm, between two carbon electrodes with a contact area of about 10^{-4} cm ^{2}. As the applied voltage across the device initially in a blocking state is increased, the leakage current increases in a somewhat nonlinear fashion described by an ohmic region near zero and an exponential region at higher voltages. When the applied voltage reaches a critical threshold voltage V_{TH}, corresponding to a threshold current I_{TH}, the device rapidly switches to the conducting state. The conducting state is characterized by an approximately constant conducting voltage V_c which is considerably smaller than the switching threshold volt-

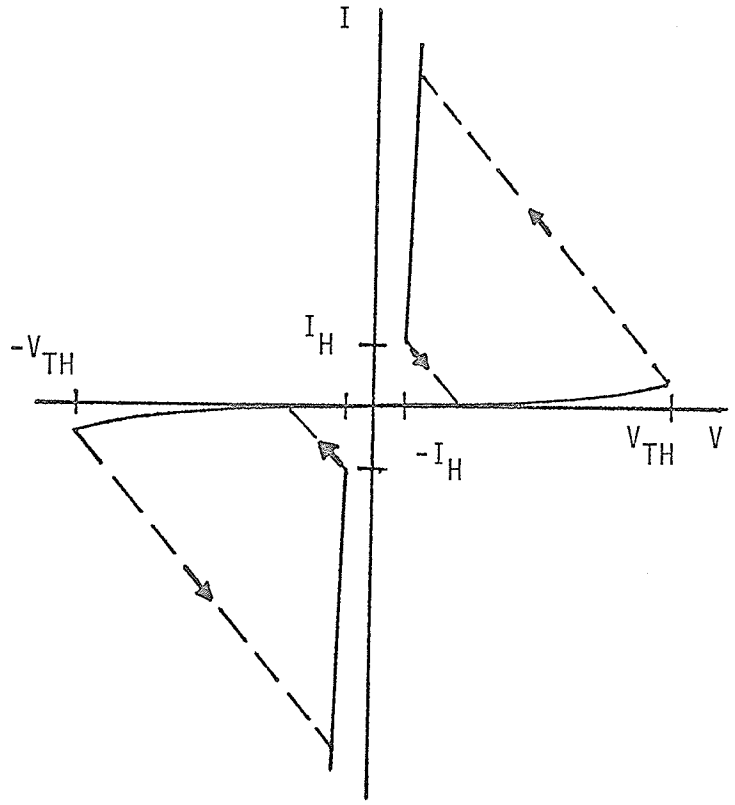

Fig. 2.5. Ovonic threshold switch I-V characteristics. (after Shanks 1970).

age V_{TH} and is determined by the resistance of the device in its conducting state. The conducting state will be retained as long as operating current remains above a critical holding value, I_H. When the current is reduced below I_H, which is usually between 0.3 and 0.7 mA, the device reverts back to the blocking state.

The capacitance of such a device is extremely small, (e.g. three picofarads or less). The OTS can be made to have conducting voltages as low as 0.5 volts and threshold voltages ranging from several to many hundreds of volts - depending on the choice of materials, electrodes, and sample thickness. In addition some samples have been operated to $8x10^{12}$ cycles without significant change in properties (Ovshinsky 1968).

There are switching delays for both the turn on and the turn off operations in amorphous threshold switches. That is, once a sufficiently high voltage to bring about switching is applied, the device does not immediately switch to the conducting state but rather a time increment exists between the occurrence of the leading edge of the applied pulse and a rapid transition from the blocking to the conducting state. This time increment is called the delay time t_D and decreases rapidly as the applied voltage exceeds the threshold value. It has been observed that at high voltage the delay time decreases with applied voltage following a simple exponential relation (Evans et al. 1970, Shanks 1970). One of the device parameters which has the greatest effect on delay time is the sample thickness, with increases in active material thickness resulting in increases in the delay time. For example, in a typical OTS device a film thickness of 0.8 μm results in a threshold voltage of about 15 volts and a delay time between 1 and 5 μ sec, while a thickness of 1.6 μm results in

a threshold voltage of about 25 volts and a delay time of 5 to 10 μ sec (Ovshinsky 1968). After the delay time t_D, the amorphous threshold switch undergoes a very rapid transition to the ON state. This transition time has been measured to be in the order of a fraction of a nanosecond which is considerably shorter than the delay time (Ovshinsky 1968).

When the operating current of a device in the conducting state is reduced below I_H, the amorphous threshold switch requires a short time period, termed the recovery time t_R, typically of the order of several μ sec, to regain its blocking state. Since the turn on process is characterized by two variables, voltage and delay time, and the recovery process is also time dependent, the recovery characteristics depend on the waveform of applied voltage.

2.3.2 THE AMORPHOUS MEMORY SWITCH

The main feature about amorphous memory switching which differs from ordinary threshold switching is that no energy is required to retain either the conducting or blocking state. Ideally, a memory switch should be small so that a maximum density of information storage can be achieved. Also, the memory action must be non-volatile; that is, the stored information should be unaffected either by interrogation or by loss of input power.

The amorphous memory switch, like the threshold switch, is basically a layer of suitable active amorphous material sandwiched between two electrodes. The process of memory switching, like ordinary threshold switching, involves a transition from a state of low conductivity to a state of high conductivity once a critical voltage is reach-

ed. Also, just like threshold switching, memory switching exhibits a time delay after the application of a voltage pulse, that varies inversely with the ratio of pulse voltage to threshold voltage and directly with the thickness of active material. It is postulated that the basic process of memory switching involves the reordering of the elements in the active amorphous material towards longer range order; that is, towards more crystalline structure (Ovshinsky 1968). As the bonding of atoms is changed to form another type of local order, the electrical characteristics are also changed because the band gap of the material has been altered. According to this argument, the active material used in a typical threshold switch should be chosen such that it would not undergo structural changes over a wide temperature range. However, for memory devices the active material should be chosen so that the cross link elements, which tend to shorten the polymeric chains and tie all the bonding sites, are partially removed to allow for some polymonic movement including bond rotation, chain shortening and lengthing, and very limited spatial diffusion of atoms. Thus, it is possible that ordinary threshold switching involves a temporary structural reordering along the switching path so that a minimum energy input is required to maintain the new structural arrangement. Memory switching, however, involves a permanent change in structure towards greater long range order so that even complete removal of applied voltage does not result in a transition back to the low conductivity state. The original state of disorder corresponding to the blocking state of the device can be reintroduced only if sufficient energy is made available to cause a transition from the conductingto the blocking state, by the application

of a sufficiently high current pulse, for example.

The above argument may indicate that although threshold switching without memory, and switching with memory seem to have some features in common, the basic mechanisms involved may be somewhat different (at least after switching has occurred).

2.4 MECHANISMS OF SWITCHING

2.4.1 SWITCHING DUE TO ELECTRONIC PROCESSES

Henisch et al. (1970) have presented a qualitative theory for the electrical switching processes in monostable amorphous structures based on the assumption that there are two overlapping regions of discontinuous energy level origination from the conduction and valence bands. The main point in this theory regarding switching is that the band levels correspond to electron and hole traps and by their very nature are present in equal numbers.

The effective low field resistivities of many amorphous semiconducting materials (e.g. Ge-As-Te and Ge-As-Te-Si of various composition) are generally between 10^5 and 10^8 ohm - cm at room temperature. Although the thermoelectric experiment indicates that these materials are p-type, the Hall effect measurement indicates that they are n-type; thus these materials are believed to be close to intrinsic semiconductors as far as carrier concentrations are concerned. As a result, the application of an external voltage between the electrodes of a typical device would produce symmetrical or almost symmetrical space charges, one negative due to the

tunnel-injection of electrons from the cathode, and the other positive due to the tunnel-injection of holes from the anode.

The basic features of the space charge model are illustrated in Fig. 2.6. It is postulated that the space charge results in a field distortion as shown in Fig. 2.6 (b) on the assumption that the diffusion length of both carriers are much smaller than the electrode separation. Although Schottky barriers exist at the contacts, it is assumed that they are very thin and therefore may be ignored in the present analysis (Tredgold 1965, Lampert 1962). The resulting space charge would most certainly result in an increased field at the center of the specimen and a diminution near the electrodes. In the absence of other processes, each space charge region will, in the course of time, build up a quasi-steady-state profile. The initial current would be due, at least in part, to the charge occommodated in the traps. This current would tend to gradually diminish to a steady value because the space charges inhibit the influx of additional charge carriers. The model thus predicts negative current creep at threshold and just below. Because the injection process depends on the field at the contacts, only a small space charge density would be required to stabilize the current at the lower level. The limiting situation occurs when the steady state current depends entirely on diffusion. Fig. 2.6. (b) illustrates this process even though the actual limit may not be reached. It should be noted that the amount of field distortion and the amount of negative creep actually obtained depends on several factors such as the injection ratios, and the temperature dependence of current. As a result, actual quantitative calculations for these factors have not yet been reported in the literature.

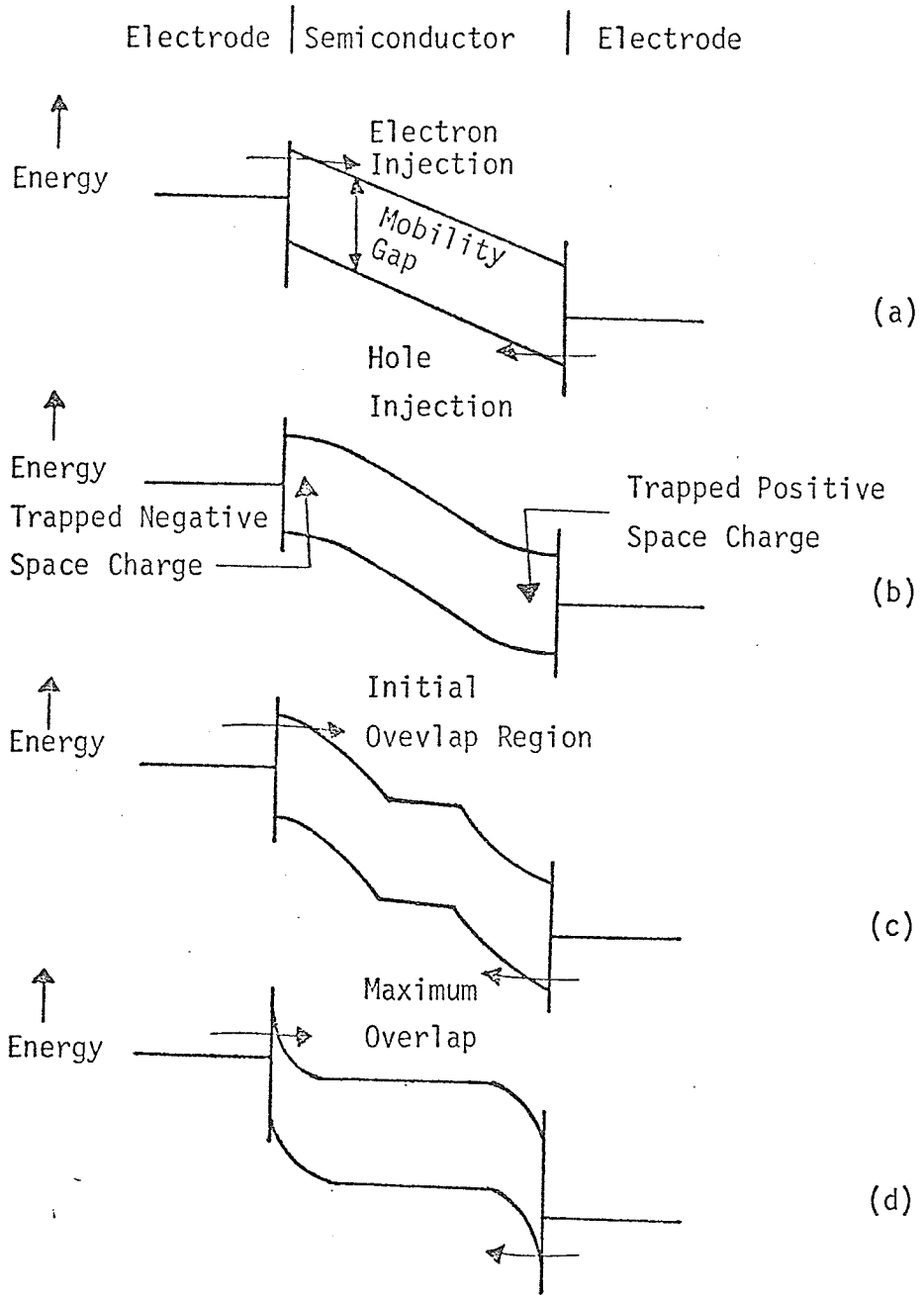

Fig. 2.6. Sequence of events during threshold switching.
(a) Voltage applied; instantaneous situation.
(b) Space charge established on opposite sides.
(c) Beginning of space charge overlap; unstable condition.
(d) Maximum space charge overlap. (after Henisch et al. 1970).

As the applied voltage is increased, the space charge regions will extend to the center and eventually the space charge regions will overlap. In the overlap region, electron traps would be completely filled with electrons, and hole traps completely filled with holes. As a result this region would be free of all space charge. Also, since additional incoming electrons and holes cannot be accomodated in the traps, they would remain free in the conduction and valence bands, respectively, where they would contribute to the conduction process. Therefore the overlap region would be a region of much lower resistivity than any other region in the system. Accordingly, the electric field would be distorted by the overlap region as shown in Fig. 2.6. (c), with the result that higher fields would appear within the space charge regions of the specimen near the electrodes. These, in turn, would lead to a greatly increased injection and to a further spread of the space charge, thereby widening the central high conductivity regions. Thus, the situation becomes inherently unstable and a rapid transition from low conductivity to high conductivity will result. When this occurs, the traps (or, at any rate, those which are effective at the temperature concerned) are completely filled and mutually neutralizing throughout most of the specimen. The system is then highly conducting, corresponding to the high-current (ON) state of a threshold switch. In the immediate vicinity of the contacts, residual space charges may persist. The potential profile in the high current state, which leads to a self-stabilizing post breakdown holding voltage, is illustrated in Fig. 2.6. (d). In terms of the present model, the observed delays before threshold switching are associated with the build-up of the space charge regions before the overlap takes place. This is further supported by

the fact that the number of carriers passing through a threshold device before the onset of switching is of the right order of magnitude to fill all the traps ($\sim 10^{18}$ cm^{-3}) which are believed to be present (Henisch et al. 1970).

The trap filled states must be maintained against the operative recombination mechanisms by a sufficiently high current density. In the low field zone, carrier transport is slow and thus the probability of recombination would be correspondingly high. When the current falls below a critical value, traps become empty and the potential configuration of Fig. 2.6. (a) is restored. These processes cannot normally occur in the common crystalline insulators because the electron and hole traps contained in them, due to the presence of impurities or structural defects or both, are not inherently present in equal concentrations.

2.4.2 SWITCHING DUE TO ELECTRICALLY INDUCED THERMAL PROCESSES

The basic postulate regarding electrically induced thermal switching is the formation of filamentary paths between electrodes whose conductivity is much higher than the rest of the semiconducting material. This process is believed to occur as a result of localized heating and subsequent phase transformation of the material between the electrodes, and is the result of current flow in the device.

If a large ac or dc voltage is applied across a sample which initially has a high resistance of several megohms, and if sufficient power is allowed to dissipate in the material to produce Joule heating, several events take place. The resistance begins to drop, a high

conductivity path between the electrodes begins to form, and the I - V characteristics start to display a current controlled negative differential resistance. Stocker (1970) has reported that the paths thus formed are in the fact devitrified, and X-ray analysis shows evidence of crystallites.

The most important features of this model (Stocker 1970) may be summarized as follows: 1) After the application of an electric field, the Joule heating produces local devitrification. Once the process has been initiated it proceeds extremely rapidly, possibly at the speed of sound, and soon a filamentary path of devitrified material is formed. 2) The current continues to increase until a limit is reached, determined either by the external circuit, or by the resistance of the structure itself. The result is the formation of a filamentary path consisting of molten material at high temperature. 3) Upon reduction of the current, the effect of cooling will result in a transformation of the molten filament back to the glassy state. The cooling rate must be fast enough to ensure that the molten state is transformed to a glassy state rather than to a state involving phase separation.

The experimental results obtained in several investigations (e.g. Feldman and Moorjane 1970, Uttecht 1970, Sliva et al. 1970) suggests that threshold switching due to thermal mechanisms can take place in a system which has at least two phases and therefore is not necessarily a bulk property of the semiconducting material. It may also be stated on the basis of the above model that the memory effect is probably due to the rearrangement or recrystallization of material along a filamentary path in a two phase system. Thus a series of pulses would alternately close or break

such a conducting path. The experiments in thin film devices indicate a great degree of similarity to the switching phenomenon in paths of devitrified material (Stocker 1970). That is, what is readily observable in bulk paths may also take place in thin film structures but on a much smaller scale.

2.5 SOME IMPORTANT EXPERIMENTAL RESULTS

2.5.1 CONDUCTIVITY AND I-V CHARACTERISTICS FOR THE Te-As-Si-Ge SYSTEM

The electrical conductivity and I-V characteristics for the Te-As-Si-Ge system have been investigated by Croitoru et al. (1970) at low and high electric fields and at temperatures between $77^{o}K$ and $350^{o}K$. Fig. 2.7 shows the conductivity as a function of temperature. At low fields only one activation energy, 0.47 eV appears, provided that the sample is not heated above the deposition temperature. A similar result has been reported by Fagan and Fritzsche (1970), and the value 0.47 eV agrees well with optical absorption measurements. At high fields and at low temperatures there is a slight decrease of the activation energy with decreasing field. Fig. 2.8 shows that at high fields the I-V characteristics follow the relation

$$I = I_{o} \exp \left(\beta V^{\frac{1}{2}} / K_{B}T \right) , \qquad (2.11)$$

where

$$\beta = \left(q^{3}/\varepsilon d \right)^{\frac{1}{2}} , \qquad (2.12)$$

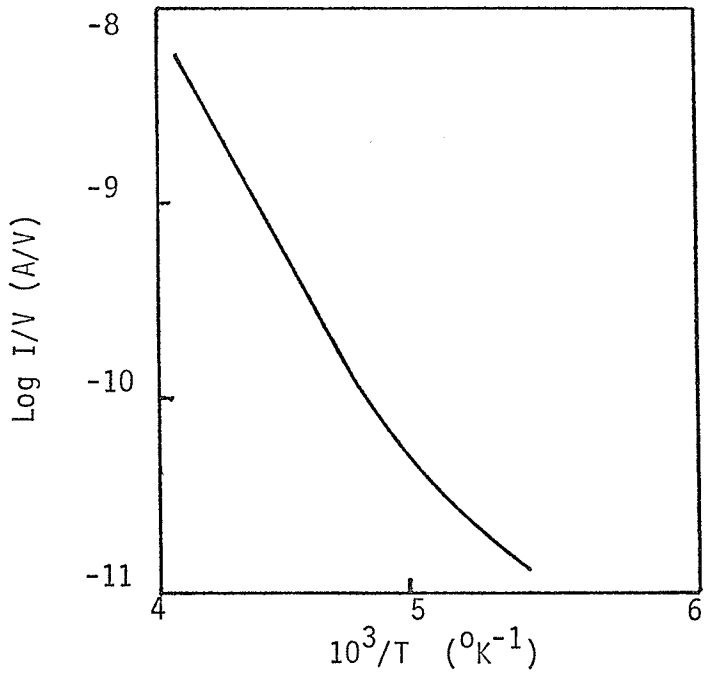

Fig. 2.7. Conductivity vs. T^{-1} for coplanar As-Te-Ge-Si structures at a voltage of 100 V. (after Croitoru et al. 1970).

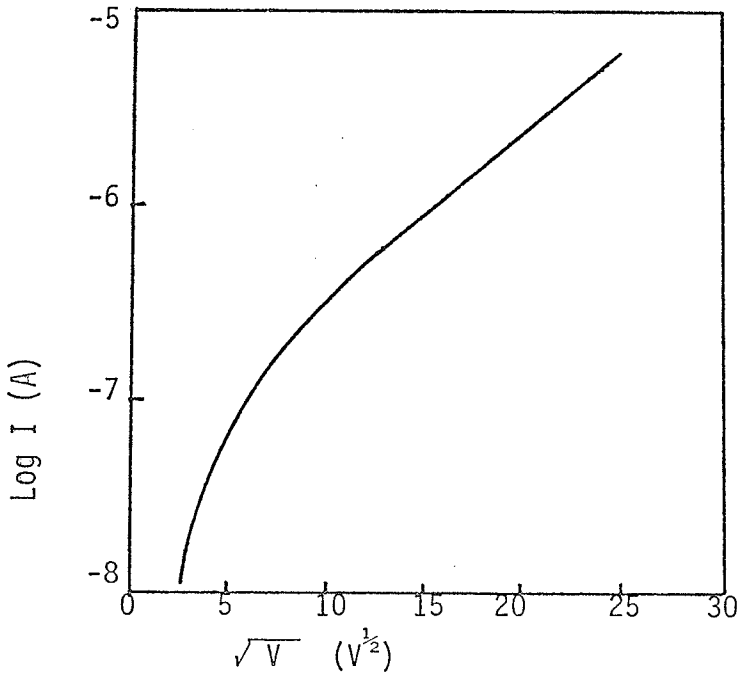

Fig. 2.8. Current v s. voltage for coplanar As-Te-Ge-Si structures for an active material thickness of 150 μm. (after Croitoru et al. 1970).

and d is the electrode separation. The variation of β with $d^{-\frac{1}{2}}$ has been verified experimentally by Croitoru et al. (1970) for electrode separations between 80 and 1000 μm.

All electrical measurements were performed at temperatures below the temperature of the substrate during the evaporation. Croitoru et al. (1970) have reported that under this experimental condition conductivity - temperature curves are highly reproducible. This implies that under such conditions no structural changes could occur which might influence the activation energy of the conductivity.

2.5.2 THE DEPENDENCE OF THRESHOLD VOLTAGE ON SAMPLE THICKNESS

The work reported thus far on the variation of threshold voltage with active material thickness has been restricted almost exclusively to thin film structures (i.e. less than 10 μm). Stocker et al. (1970) have investigated the thickness dependence of threshold voltage for a series of thin amorphous films of thickness from 0.1 to 8.5 μm. Their samples were prepared by the evaporation of an ingot of $Ge_{20}\ As_{30}\ Te_{50}$ onto polished Al substrates held at room temperature. It was found, however, that the evaporation process would result in considerable variation of composition from that of the bulk material. In particular, electron microprobe analysis revealed a reduction of As content by as much as 30%. The actual composition of two thin films was found to be $Ge_{23}\ As_{27}\ Te_{50}$ and $Ge_{19}\ As_{27}\ Te_{54}$ rather than the composition of $Ge_{20}\ As_{30}\ Te_{50}$ for the bulk material. In spite of these variations, carefully controlled evaporation conditions

resulted in films of good quality with reasonably reproducible composition.

The variation of threshold voltage with film thickness is shown in Fig. 2.9. It is quite clear that the threshold voltage increases steeply with thickness below 1 μm, and that above 1 μm the dependence becomes less sensitive. The curve in Fig. 2.9 has been adjusted to give the best fit to the data. It must be pointed out that due to the compositional variations brought about by film deposition, extrapolation of these results to bulk samples of the original material (large thickness) may not be justified.

2.5.3 THE DEPENDENCE OF THRESHOLD VOLTAGE ON TEMPERATURE

Deis et al. (1970) have investigated the temperature dependence of threshold voltage for the amorphous composition $Te_{65.5}$ $As_{24.3}$ $Ge_{7.3}$ $Si_{2.9}$. The sample used in their experiment was a bulk disk of thickness of .55 mm, and diameter of 1.9 mm. This sample was mounted in a standard microwave diode holder using silver paint to make contact on one side and a gold bellows on the other. The temperature dependence of the threshold voltage for temperatures between 0^{o} C and 200 ^{o}C is shown in Fig. 2.10. It can be seen that the threshold voltage approaches 0 V as the temperature approaches the softening temperature of the material (i.e. 300 ^{o}C). The disappearance of switching with increasing temperature has also been noted by Walsh et al. (1969).

Shanks (1970) has attempted to characterize the OTS (Ovonic threshold switch) and has reported some results concerning the temperature dependence of threshold voltage for these devices. The devices which were investigated were packaged in a DO-7 configuration incorporating pyrolytic

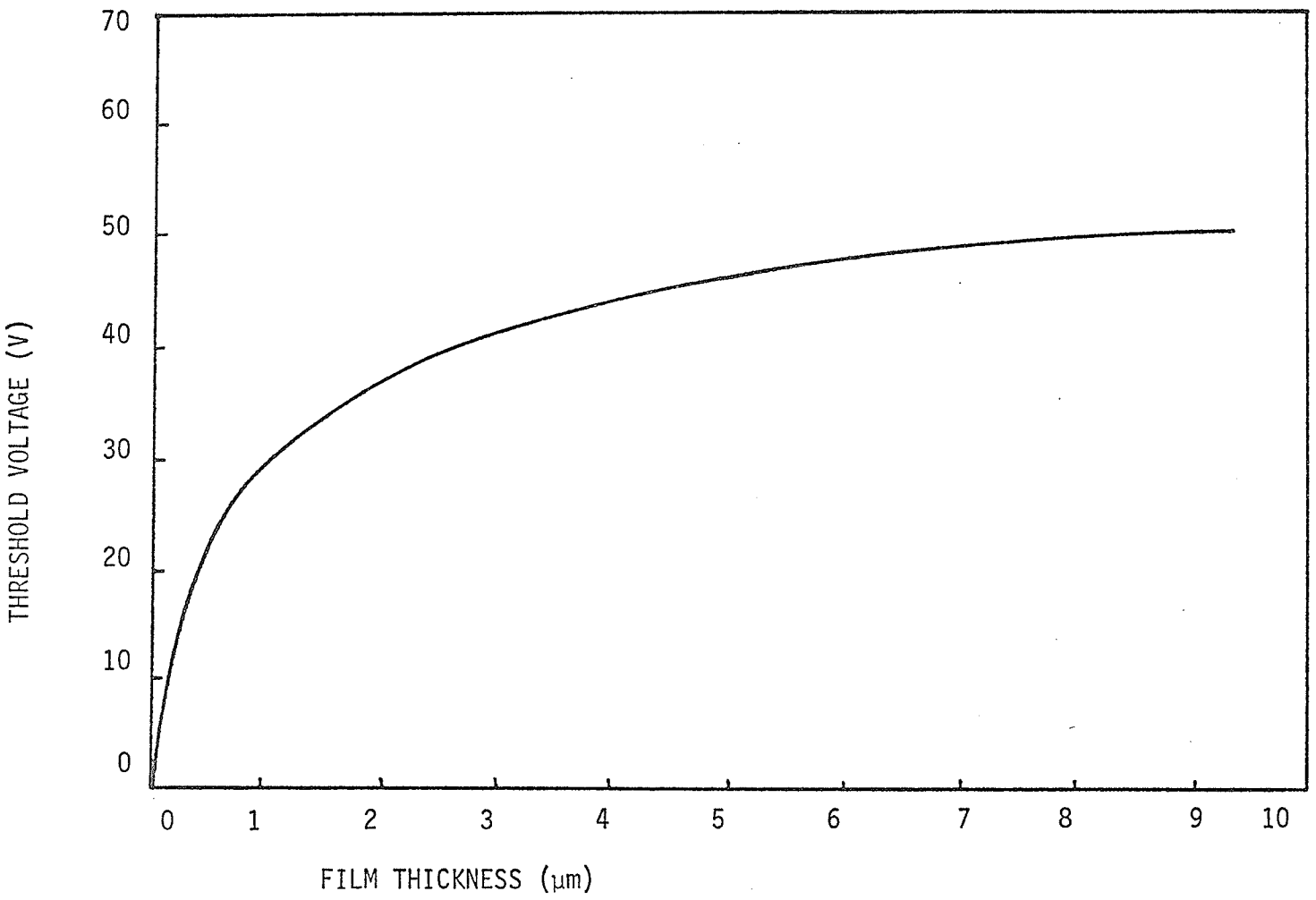

Fig. 2.9. The dependence of dc threshold voltage on thickness for thermally evaporated films of Ge_{20} As_{30} Te_{50}. (after Stocker et al 1970).

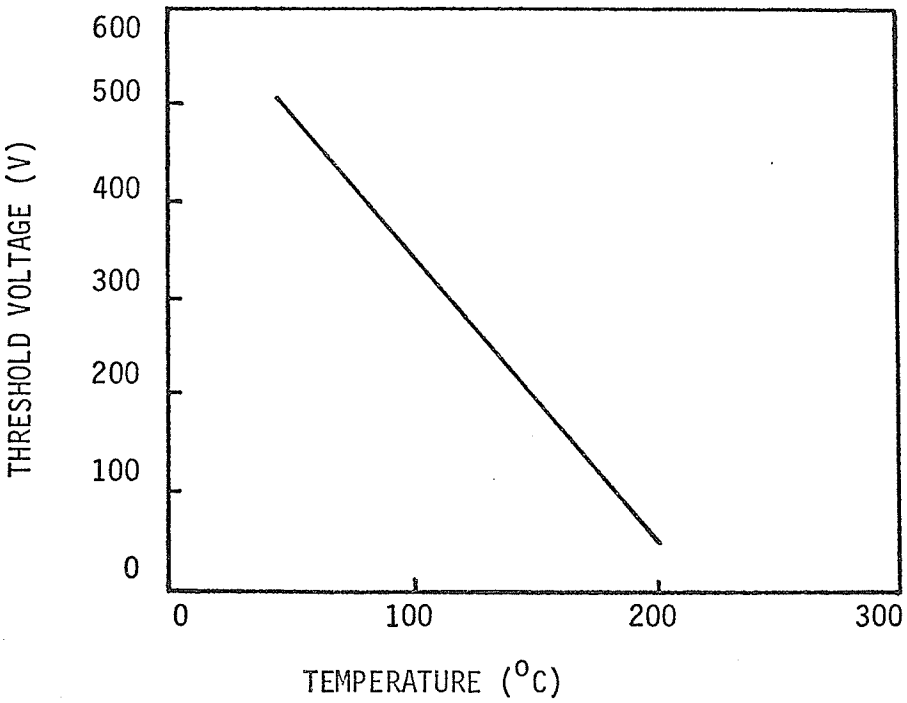

Fig. 2.10. Threshold voltage as a function of temperature for the composition $Te_{64.9}\ As_{23.9}\ Ge_{7.5}\ Si_{3.7}$. (after Deis et al. 1970).

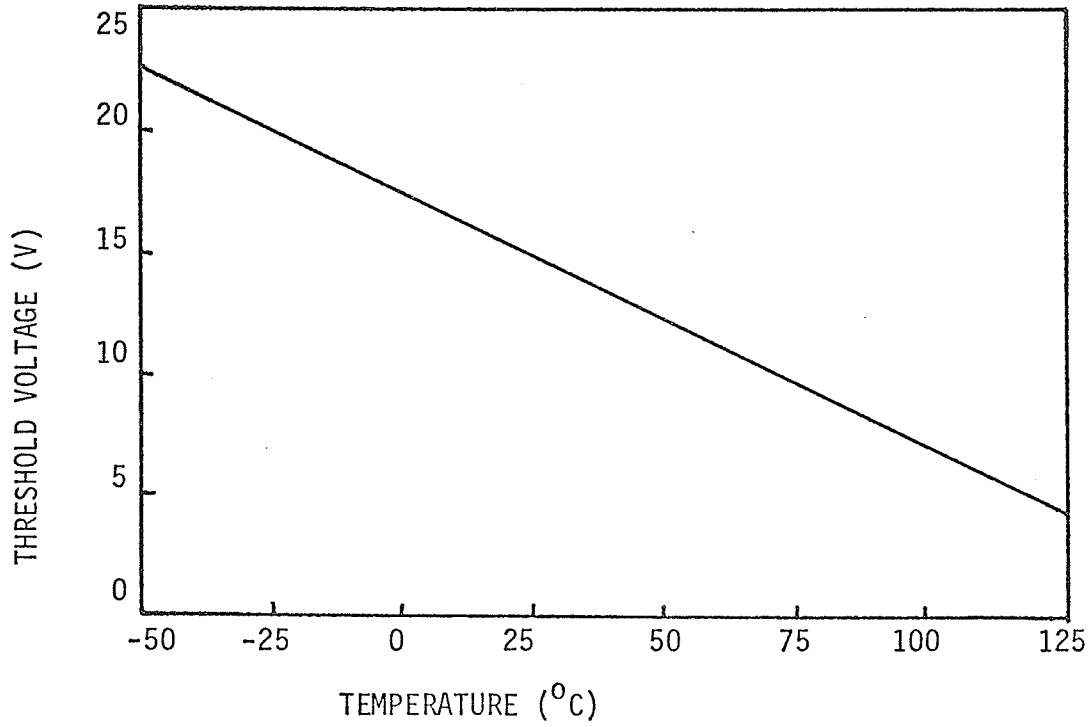

Fig. 2.11. Threshold voltage as a function of temperature for a 15 V OTS. (after Shanks 1970).

carbon electrodes with an active material thickness of approximately 1 μm. The active amorphous material was Te_{48} As_{30} Si_{12} Ge_{10} and the range of switching voltage was from 15 to 20 V. The threshold voltage measurements were made using a slow rise-time wave form such as a 60 Hz sine wave and the results are given in Fig. 2.11. The threshold voltage decreases linearly with increasing temperature at a rate of about 0.7 % per degree C. It is interesting to note that Fig. 2.10 is similar to Fig. 2.11 in the region of low threshold voltages. The trend is clearly approaching a more linear relationship for higher temperatures and lower threshold voltages. That there is some degree of correspondence between the two sets of results even though the materials used and the experimental conditions were not the same suggests that the basic physical processes involved in the switching action for these two materials are quite similar in nature.

2.5.4 THE DEPENDENCE OF SWITCHING DELAY TIME AND RECOVERY TIME ON APPLIED VOLTAGE

The basic concepts of switching delay and recovery time have been discussed in some detail in previous sections. It would be interesting to consider the factors which have the greatest influence on these quantities. For completeness, both the threshold switch without memory, and the threshold switch with memory will be considered.

Evan et al. (1970) used the material Ge_{15} Te_{81} P_4 in their amorphous memory devices. The devices were produced by depositing a film of this memory material of thickness between 1 and 10 μm onto graphite hemispheres having a radius of curvature of approximately 10 mm. The

hemishperes were spring-loaded against each other to form a conducting area of approximately 10^{-6} cm^2. Rectangular pulses were used to measure the switching delay time and the recovery time for these devices. The application of a rectangular pulse with amplitude greater than the d c threshold voltage to an amorphous memory switch does not bring about an immediate transition to the conducting state. There is always a delay time t_D for this transition. The delay time decreases with increasing pulse voltage as shown in Fig. 2.12. For the same percentage of overdrive, the delay time decreases rapidly as the thickness of the active film is reduced. Once the memory device has switched to the conducting state it will remain in this state until a suitable current pulse is used to drive the device back to the low conductivity state. The device recovery time t_R is the time interval between the initial application of the current pulse and the time at which the voltage across the device reaches one-half of its d c threshold value. Fig. 2.13 shows the normalized threshold voltage versus time after the application of a current pulse. It can be seen that it takes approximately 10 μ sec after the application of the current pulse for the voltage across the device to reach one-half of its dc threshold value.

Shanks (1970) has performed several experiments related to delay and recovery times for threshold switching devices (without memory). As with the memory structures already discussed, the delay time for these devices decreases rapidly as the applied voltage exceeds the threshold voltage. Fig. 2.14 shows the dependence of the delay time on the applied voltage for devices which have a threshold voltage of 15 V. It can be seen that at high voltages the delay time varies approximately exponentially with the applied voltage.

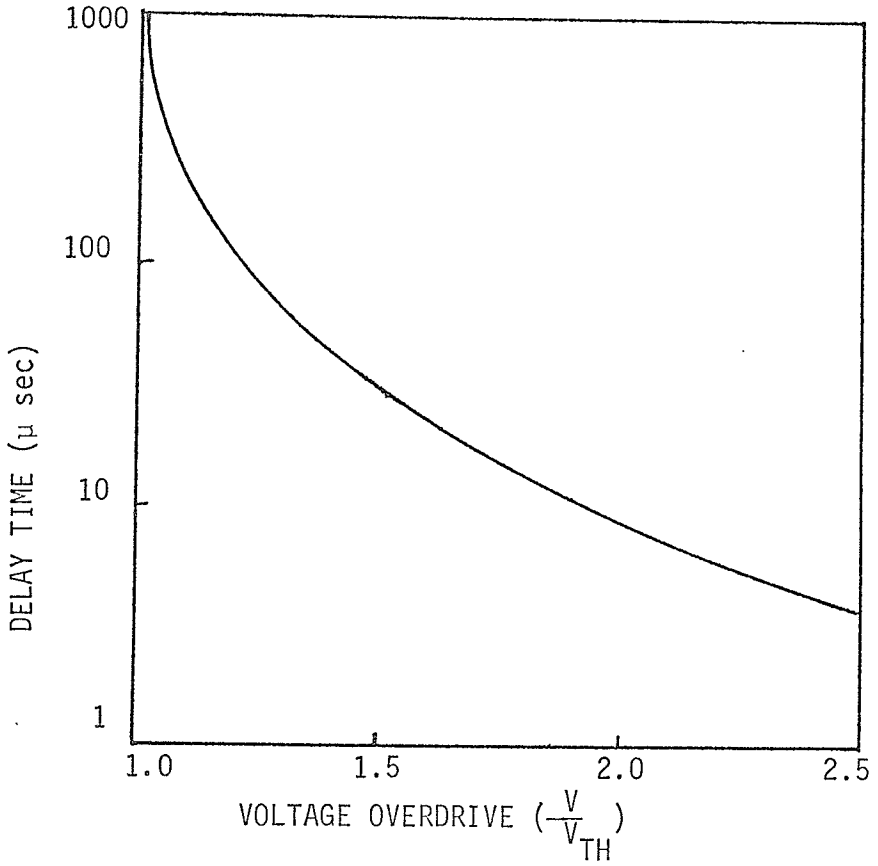

Fig. 2.12. Switching delay time as a function of voltage overdrive for a 10 μm memory device (after Evans et al. 1970).

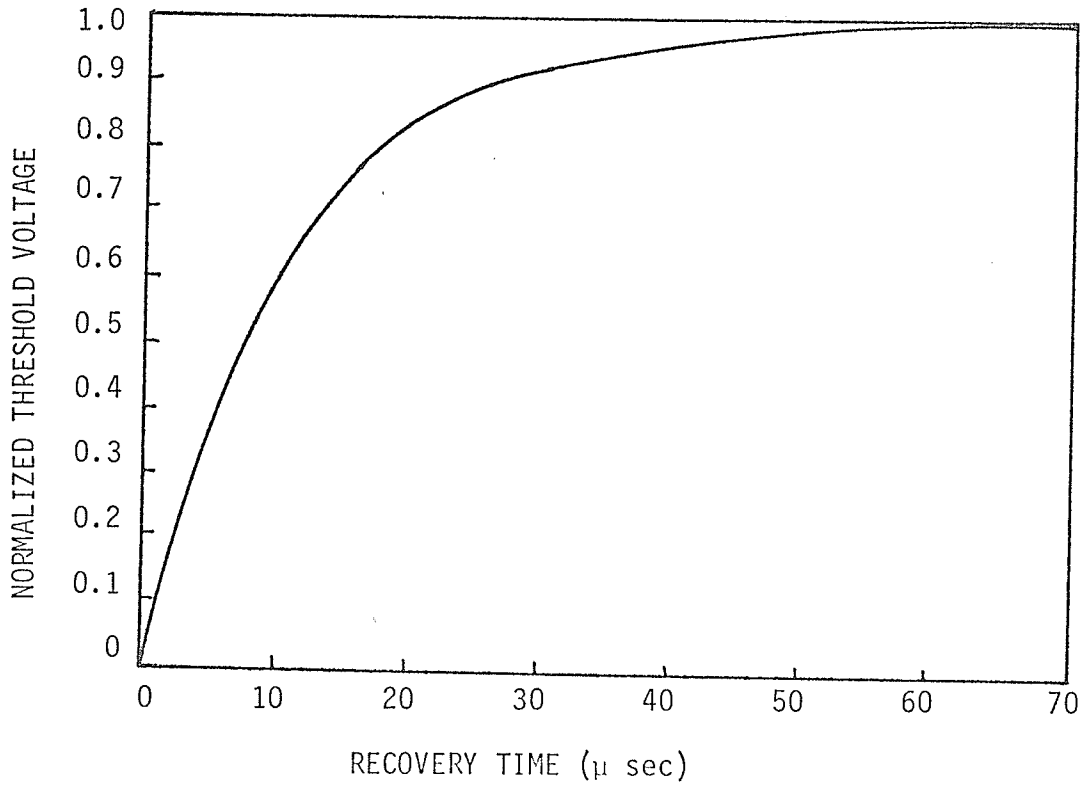

Fig. 2.13. Normalized threshold voltage as a function of recovery time for a 10 μm memory device. (after Evans et al. 1970).

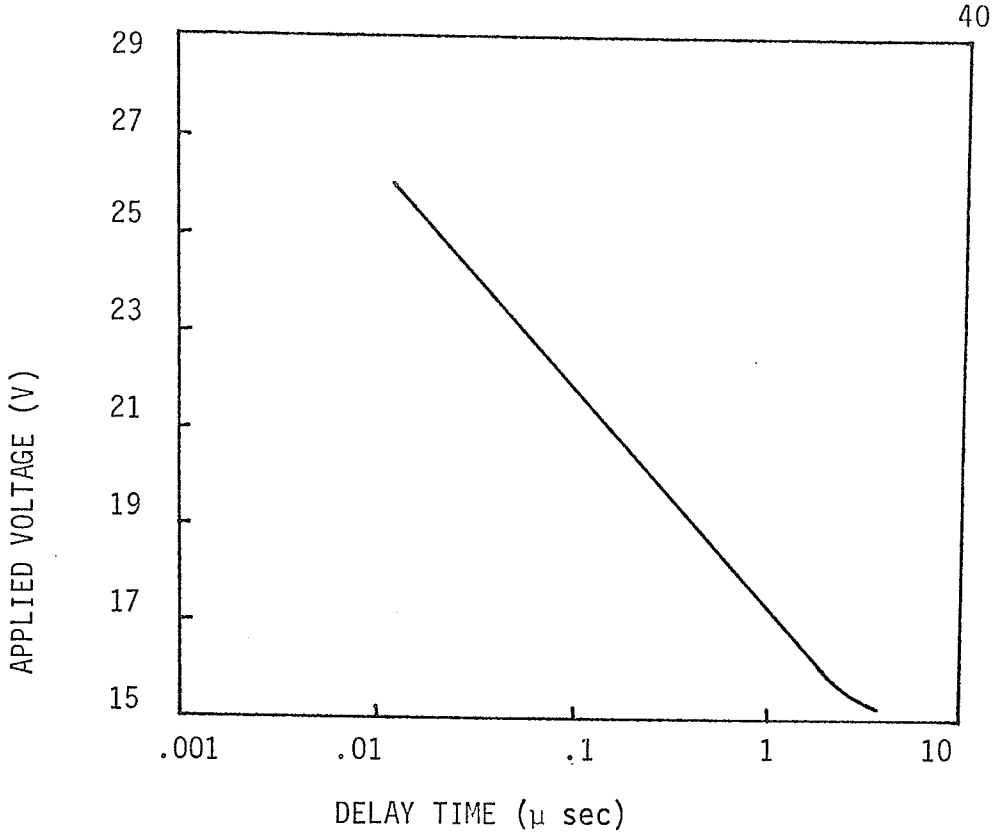

Fig. 2.14. The delay time as a function of applied voltage for a 15 V OTS. (after Shanks 1970).

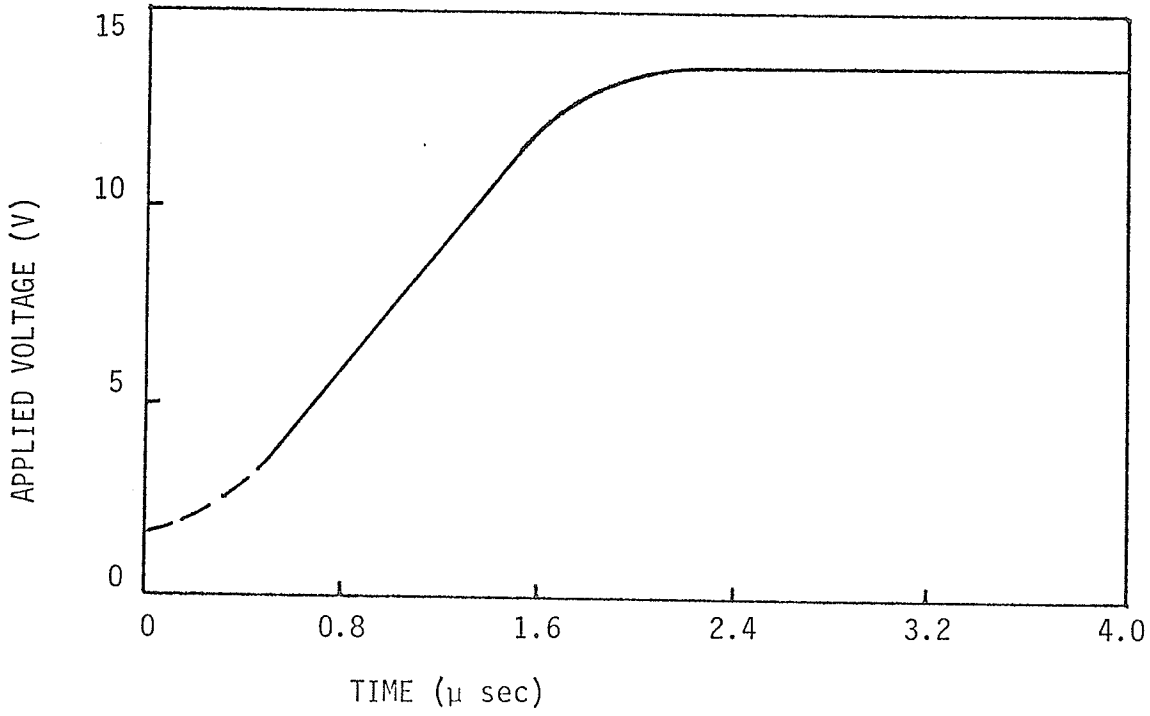

Fig. 2.15. Recovery time envelope developed with exponential waveforms. (after Shanks 1970).

As long as the current through a switching device in the ON state does not fall below the holding value I_H, the device will not revert back to the OFF state. However, when the current does fall below I_H the device requires a short time period, typically of the order of 1 to 2 μ sec, to regain its low conductivity state. If a voltage is applied to a device which is in the recovery period, switching may occur at voltages considerably less than the original threshold value. Fig. 2.15 shows the maximum time constant and amplitude allowable for an exponentially rising voltage applied to a typical device without causing switching. As long as the applied voltage does not exceed that shown on the curve, the device will not switch during the recovery period. Other waveforms may also be used to characterize the recovery time as in Fig. 2.15. For example, a step voltage, a rectangular pulse, and a sinusoidal waveform are all suitable. Since the switching of a device depends on both the amplitude and duration of applied voltage, the variation in waveform would, of course, result in a difference in the recovery envelope.

CHAPTER 3

THEORETICAL APPROACHES

Most of the research carried out in the field of amorphous semiconductors thus far has been experimental in nature, and much of the theoretical work has been restricted to qualitative models. Several authors (Mott 1967, Böer 1970, Mattis and Landoviz 1970, Klinger 1970, Dearnaley et al. 1970), however, have made significant contributions by means of theoretical approaches, towards a better understanding of some phenomena in disordered structures. The present chapter will discuss the theoretical approaches to the mechanisms responsible for some important properties of disordered semiconductors such as the conductivity, the I-V characteristics, the threshold voltage, the delay time, and the model of filament formation.

3.1. CARRIER MOBILITY AND CONDUCTIVITY IN DISORDERED STRUCTURES

In covalent amorphous semiconductors such as those of the Te-As-Si-Ge system, the energy close to the band edges no longer has band character but is localized due to the high degree of disorder. The density of states, however, remains the same order of magnitude as that in the crystalline structure, and within the energy gap it decreases with increasing distance from the band edges, presumably lacking a pronounced structure (Mott 1969, Stuke 1969, Cohen et al. 1969, Cohen 1970). Theoretically, carriers in each of these states can contribute to the total conductivity, although various conduction mechanisms may be involved.

In order to find the over all conductivity it is necessary to compare the magnitudes of the different contributions and to identify the

predominant transport mechanism for particular cases. Five different mechanisms of carrier transport will be considered and the relative contribution of each of these mechanisms to the over all conductivity will be analysed. For simplicity the analysis will be carried out for n-type conductivity only.

(1) Carrier Drift

This transport mechanism is mainly due to the carriers migrating within the conduction band of the semiconductor, in which the transport is relatively unimpeded and regular band conduction predominates. Because the mean free path λ is large compared to the interatomic distance a, the carriers encounter only occasional scattering. If the mean free path is larger than the De Broglie wavelength of the electrons such that the mobility μ is at least of the order of $100 cm^2/V$ sec, the mobility can be expressed in terms of λ, the effective electron mass m_n, and its thermal velocity v_t as (Ioffe and Regel 1960)

$$\mu_1 = \frac{q\lambda}{m_n v_t} = 1.51 \times 10^8 \sqrt{\left(\frac{m_o}{m_n}\right)} \sqrt{\left(\frac{300}{T}\right)} \lambda \, . \qquad (3.1)$$

For a typical effective electron mass, $m_n = .25\, m_o$, and at room temperature the above equation yields

$$\lambda \simeq \frac{1}{3} \mu_1 \, , \qquad (3.2)$$

where λ is expressed in $\mathring{A}$, and μ_1 is expressed in cm^2/V sec. In amorphous semiconductors the mean free path of electrons (within the conduction band) is probably determined by scattering at charged defects and depends on the kinetic energy of the carriers. Böer (1969) has estimated λ to be of the order of $60\mathring{A}$ for electrons having energy of 0.2 eV inside the conduction band and for a density of charged defects of 10^{19} cm^{-3}. This

gives rise to a microscopic carrier mobility of about 200 cm^2/V sec.

(2) Carrier Diffusion

This form of carrier transport takes place close to the edge of the conduction band where the energy states are probably localized and the electron motion is supposedly restricted to a diffusion from one atom to the next. The mean free path in this case is thus less than, or at most equal to the interatomic distance. The mobility due to diffusion follows the Einstein relation and may be expressed as

$$\mu_2 = \frac{qD}{K_B T} = \frac{1}{6}\left(\frac{q}{K_B T}\right) a^2 \nu_{el}, \qquad (3.3)$$

where D is the diffusion constant. At room temperature with $\nu_{el}=10^{15}$ sec^{-1} and $a \lesssim 3\text{Å}$ (typical values) the diffusion mobility is less than 1 cm^2/V sec. The usual range in mobility due to diffusion is $10^{-2} < \mu_2 < 1$ cm/V sec.

(3) Carrier Hopping

Carrier hopping means the tunneling of carriers from one defect level to another defect level, the energy difference between the two levels being within $K_B T$. If defect levels of about equal energy lie close enough to allow for marked tunneling, carrier migration takes place through these levels.

Using Einstein's relation and a reduced frequency factor for tunneling of an electron to a nearby unoccupied trap, the carrier mobility due to hopping is given by (Böer 1970)

$$\mu_3 = \frac{1}{6}\left(\frac{q}{K_B T}\right) R^2 \nu_{ph} \exp(-2\alpha R), \qquad (3.4)$$

where the effective phonon frequency ν_{ph} is of the order of 10^{12} sec^{-1},

and the characteristic tunneling length α^{-1} for neutral traps is approximately 10Å. By assuming a total trap density $N_t \simeq 10^{20}$ cm^{-3} and a band gap $E_g \simeq 0.5$ eV, which corresponds to a trap density $N_t(K_BT) \simeq 5 \times 10^{18}$ cm^{-3} with energy difference between traps within K_BT, the upper limit of the hopping mobility is estimated to be approximately 10^{-5} cm^2/V sec. From Equations (3.3) and (3.4) the ratio of the mobility due to hopping to that due to diffusion μ_3/μ_2 is given by

$$\frac{\mu_3}{\mu_2} \simeq 10^{-3} \left(\frac{R}{a}\right)^2 \exp(-2\alpha R) \cdot \tag{3.5}$$

Thus, it can be seen that the maximum contribution of hopping to the total conductivity occurs at $\alpha R_m = 1$, that is, when the characteristic tunneling length $1/\alpha$ is equal to the average distance between trapping centers. If we assume that $\mu_3 \lesssim 10^{-1}\, \mu_2(R_m) \simeq 10^{-3}$ dm^2/V sec as an upper limit for traps very close to the conduction band edge and that the decrease in α is proportional to $(E_c - E)^{\frac{1}{2}}$, then we can use a simple model of tunneling through a square barrier to estimate the energy dependence of μ_3 for a homogeneous trap distribution. Thus,

$$\mu_3(E) \lesssim 10^{-3} \frac{K_BT}{E_c - E} \exp\left[-\gamma \frac{(E_c - E)^{\frac{1}{2}}}{K_BT}\right], \tag{3.6}$$

where γ has the dimensions of $E^{\frac{1}{2}}$.

(4) Thermally Activated Carrier Hopping

Lattice relaxation near an occupied trap and consequently the lowering of the trap level make it difficult to maintain the hopping process without thermal activation. As a result, an electron will lose energy while traveling and finally end up at the Fermi-level where it will find few

unoccupied traps. For thermally activated hopping the mobility may be expressed as (Böer 1970)

$$\mu_4 = \mu_3(E') \exp(-E'/K_B T) , \tag{3.7}$$

where E' is the energy of an excited state of the occupied trap. It should be noted that an electric field would not be effective in supplying the necessary energy to compensate for lattice relaxation unless the field $F > \eta\, \delta E/Re$, where $\eta\, \delta E$ is the average energy loss by lattice relaxation for a hop of average distance R. With $\eta \simeq 1$ and $\delta E \simeq 0.1$ eV a field of at least 100 kV/cm is necessary to keep the hopping process going, if there is no thermal activation.

(5) Carrier Hopping Activated By Potential Fluctuation

This transport process involves the tunneling of carriers from defect level to defect level of different energy, activated by potential fluctuation. Potential fluctuation due to fluctuation of space charges provides another means of shifting energy levels relative to each other, giving an opportunity for level matching and hence for carrier tunneling.

If the semiconductor is divided into volume elements A^3 with a diameter equal to the Debye screening length, then each volume element may be expressed as

$$A^3 = (K_B T\, \varepsilon\varepsilon_o/q\, N_t)^{3/2} . \tag{3.8}$$

The number of charges in volume element A^3 is given by $A^3/R_o{}^3$ where $R_o \simeq (N_t'\, N_t)^{-1/3}$ and N_t' is the fraction of charged traps. The mean deviation of the space charge can be expressed as

$$\delta\rho \simeq (A\, R_o)^{-3/2} , \tag{3.9}$$

the field fluctuation over a Debye length is

$$\delta F \simeq (q/\varepsilon\varepsilon_o)\ A^{-1/2}\ R_o^{-3/2}\ , \tag{3.10}$$

and the potential fluctuation from trap to trap is

$$\delta V \simeq (q/\varepsilon\varepsilon_o)\ (A\ R_o)^{-\frac{1}{2}}\ . \tag{3.11}$$

This fluctuation has a frequency factor $\nu_\sigma \simeq \sigma/\varepsilon\varepsilon_o$, and the mobility caused by this process may consequently be written as

$$\mu_s = \frac{1}{6}\ (q/K_B T)\ R_f^{\,2}\ \nu_\sigma\ \exp\ (-2\alpha\ R_f)\ \ , \tag{3.12}$$

where $R_f \simeq (E_g/q\ \delta\ V\ N_t)^{1/3}$. For highly disordered structures the potential fluctuation lies in the order of 1V and therefore makes practically all levels available for mutual tunneling. This implies that $\exp(-2\alpha\ R_f) \simeq 1$, and, thus the resulting mobility is (Böer 1970)

$$\mu_5 \simeq \frac{1}{6}(q/K_B T)\ R_f^{\,2}\ \nu_\sigma\ \ , \tag{3.13}$$

which can contribute considerably to carrier transport provided that the carrier density is high enough.

Each of the transport mechanisms described above contributes to the total conductivity in the disordered semiconductor. The conductivity in an amorphous semiconductor can be written as

$$\sigma = \sum_{i=1}^{5} \sigma_i = q \sum_{i=1}^{5} \int_{E_F}^{\infty} \mu_i(E)\ N(E)\ f(E)\ dE\ \ , \tag{3.14}$$

where $N(E)$ is the density of states at energy level E, $f(E)$ is the Fermi-Dirac function, and E_F is the energy of the Fermi-level. For simplicity the five integrals in Equation (3.14) can be evaluated at their

maximum value for an energy interval of about $K_B T$ and the different contributions can be compared.

For carrier drift within the conduction band at $\chi = 0.2$ eV above E_c, Equation (3.14) yields

$$\sigma_1(E_c + \chi) = qN_c(E_c + \chi)\mu_1(E_c + \chi)\, f(E_c + \chi - E_F), \tag{3.15}$$

where $N_c(\chi)$ is the effective density of states and is given by (Spenke 1965)

$$N_c(\chi) \simeq 2(m_n K_B T/2\pi h^2)^{3/2} (\chi/K_B T)^{3/2} . \tag{3.16}$$

At room temperature with $m_n = 0.25\, m_o$, $\mu_1 \simeq 10^2$ cm^2/V sec, and for scattering at a density of charged defects of 10^{19} cm^{-3} and $E_c + \chi - E_F = 0.47$eV Equation (3.15) yields

$$\sigma_1(E_c + \chi - E_F) \simeq 2 \times 10^3 \exp(-0.47/K_B T) \simeq 5 \times 10^{-6}\ \Omega^{-1}\ \text{cm}^{-1} .$$

Turning next to the conductivity due to diffusion Equation (3.14) yields

$$\sigma_2 \simeq qN_c\, \mu_2(E_c)\, f(E_c - E_F) . \tag{3.17}$$

With $N_c = N_c(K_B T)$, i.e., the density of energy levels within $\pm K_B T$ of E_c and by setting $E_c - E_F$ equal to 0.47 eV, Equation (3.16) gives

$$\sigma_2(E_c) \simeq 10^{-9}\ \Omega^{-1}\ \text{cm}^{-1}.$$

Now considering the conductivity σ_3 due to tunneling from defect level to defect level (within $K_B T$ of each other) and using Equation (3.6) as an upper limit, the highest conductivity would occur at an energy level a little more than $K_B T$ above the Fermi-level (in order to have enough neighbouring defects unoccupied so as to allow for electron migration).

With $N_t(E_c - E_F + K_BT) \simeq 5 \times 10^{18}$ cm^{-3} and setting $(E_o - E) = 0.47$ eV, we obtain from Equation (3.6)

$$\sigma_3(E_c - E_F + K_BT) \leq qN_t(K_BT)\,\mu_3 \exp[-\gamma \frac{(E_c - E_F + K_BT)^{\frac{1}{2}}}{K_BT}$$

$$\simeq 10^{-10}\ \Omega^{-1}\ \text{cm}^{-1}\ .$$

For carrier hopping enhanced by thermal activation an additional integration over excited states has also to be taken into account. The energy density of these states is not known, however, and only an upper limit can be estimated by assuming that most of the electrons in the deeper traps can have a finite probability to tunnel through excited states with a smaller barrier height, so that the exponential term in Equation (3.6) can be dropped. Using this assumption and setting $E_c - E_F \simeq 0.47$ eV, we obtain

$$\sigma_4 \leq qN_t \chi\, 10^3 \exp\,[-(E_c - E_F)/K_BT\,] \leq 10^{-11}\ \Omega^{-1}\ \text{cm}^{-1},$$

where N_t, the total density of traps, is of the order of 10^{20} cm^{-3}.

We now turn to the final contribution to the conductivity, namely, hopping activated by potential fluctuation. For a potential fluctuation of the order of 1 eV and a frequency factor $\nu_\sigma \simeq 5 \times 10^6$ sec^{-1} (obtained from the measured conductivity), we obtain from Equations (3.13) and (3.14)

$$\sigma_5 \simeq qN_t \frac{1}{6} \frac{e}{K_BT} R_f^2 \frac{\sigma_o}{\varepsilon\varepsilon_o} \exp(-\frac{\Delta E}{K_BT}) \simeq 10^3 \exp\,(-\frac{\Delta E}{K_BT}) \simeq 10^{-6}\ \Omega^{-1}\ \text{cm}^{-1}.$$

In comparing the different quantitative contributions given above, it appears that only carrier drift with occasional scattering and carrier hopping activated by potential fluctuation contribute appreciably to the overall conductivity of disordered semiconductors. Thus, we can write the total

conductivity as

$$\sigma_T = \sum_{i=1}^{5} \sigma_i \simeq \sigma_1 + \sigma_5 = 2 \times 10^3 \exp(-\Delta E/K_B T) + 10^3 \exp(-\Delta E/K_B T)$$

$$\simeq \sigma_o \exp(-\Delta E/K_B T) \ . \qquad (3.18)$$

This equation agrees well with experimental results for most covalent amorphous semiconductors with σ_o between 10^3 and 10^4 Ω^{-1} cm^{-1} (Böer 1970).

3.2. THE CURRENT VOLTAGE (I - V) CHARACTERISTICS FOR COVALENT AMORPHOUS SEMICONDUCTORS

Consider an amorphous semiconductor sample subject to a slowly increasing dc voltage. Increased power input results in uniform internal heating of the sample. The current can be expressed as (Croitoru et al 1970).

$$I = I_o(V) \exp(\Delta T \ \Delta E/K_B T^2) \ , \qquad (3.19)$$

where ΔT denotes incremental temperature rises which are assumed to be much less than the ambient temperature T. Under steady state conditions the temperature rise due to Joule heating can be assumed proportional to the power input. Thus,

$$\Delta T = R_T \ V \ I \ , \qquad (3.20)$$

where R_T is the thermal resistance of the sample. Using Equation (3.20) and setting $\Delta E/K_B T^2 = \phi_T$, Equation (3.19) becomes

$$I = I_o(V) \exp(\phi_T \ R_T \ V \ I) \ , \qquad (3.21)$$

and after rearranging terms, we have

$$\frac{V}{V_I} = \frac{q \ \ell n[I/I_o(V)]}{I/I_o(V)} \tag{3.22}$$

in which,

$$V_T = [\phi_T \ R_T \ qI_o(V)] \ . \tag{3.23}$$

By introducing a transient thermal resistance into Equation (3.20), the pulse Joule heating energy, rather than Joule heating due to a slowly increasing applied voltage as treated above, can be expressed in the form

$$\Delta T(t) = P \ R_T(t) \ , \tag{3.24}$$

where the temperature increase ΔT and the thermal resistance R_T now depend on the pulse width. If the power input P = const., $R_T(0) = 0$, and $R_T(\infty) = R_T$ then the current depends on the duration of the applied voltage pulse V. Thus,

$$I(t) = I_o \exp \ [\phi_T \ V(R_T(t) + \int_o^t \frac{dI}{d\tau} \ R_T(t - \tau) \ d\tau)] \ . \tag{3.25}$$

Fig. 3.1(a) gives some results based on the numerical solution of Equation (3.21) and Equation (3.24) - curve A, based on Equation (3.21) corresponding to uniform selfheating, and curve B based on Equation (3.25) corresponding to pulse selfheating (Croitoru et al 1970). In curve A a thermal turnover occurs at a certain voltage V which corresponds to the switching threshold voltage of the sample. Curve B is for a pulse length of 6 msec, and it can be seen that beyond a certain voltage (corresponding to the threshold voltage) the current begins to increase very rapidly.

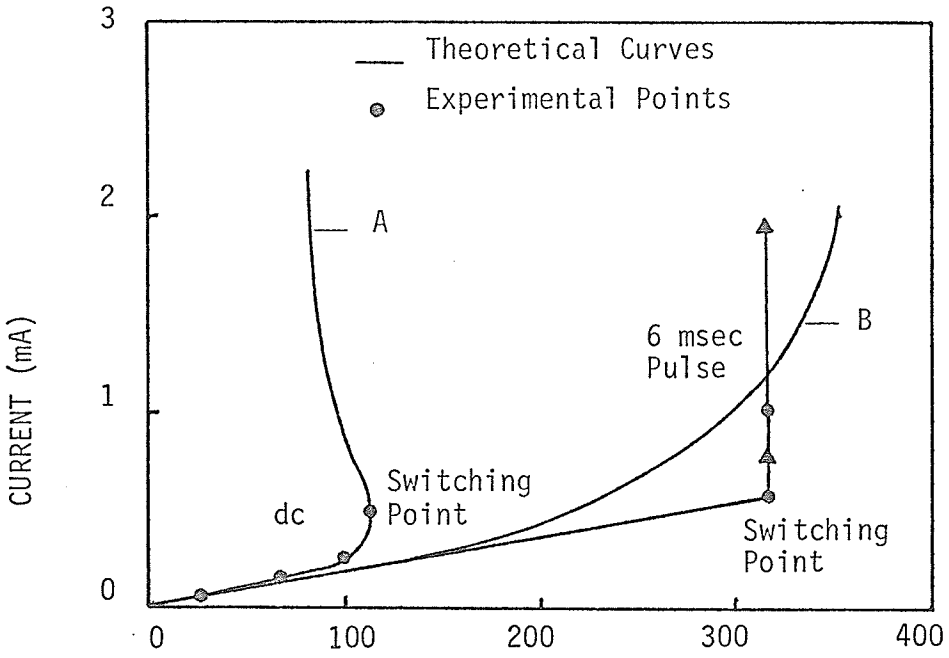

Fig. 3.1 (a). Current-voltage characteristics et al. for a coplanar Te-As-Si-Ge structure. (after Croitoru et al. 1970).

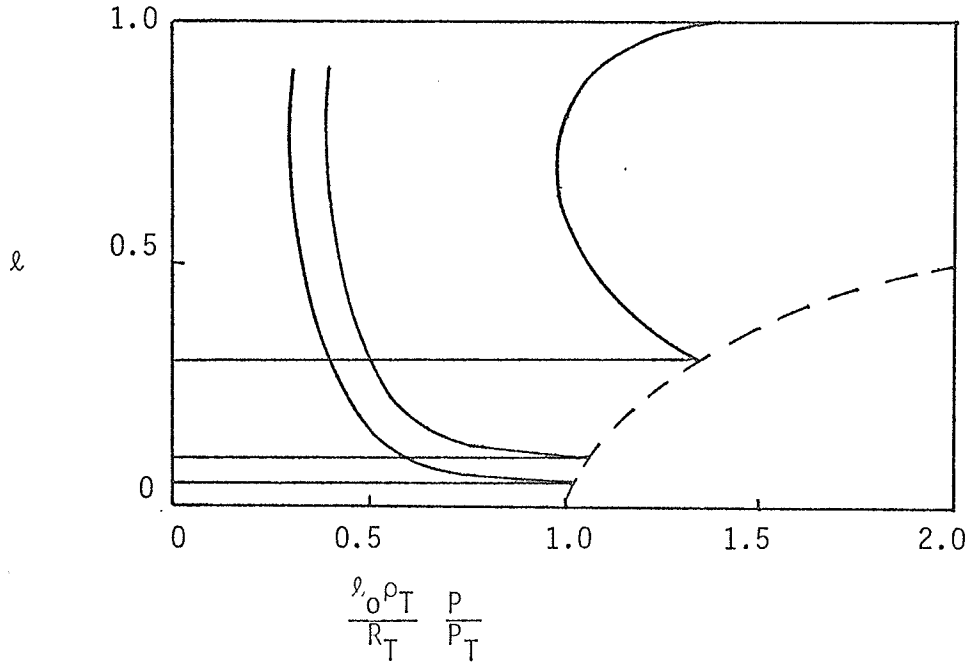

Fig. 3.1 (b). The power dependence of the current distribution factor. (after Croitoru et al. 1970).

Although the theoretical curves represent the general I - V characteristics of amorphous switching devices, there is considerable deviation in the region of transition from the "OFF" to the "ON" state from the experimental results. More specifically, the theoretical curves show a somewhat gradual increase in current beyond the threshold voltage, whereas in the experimental I - V characteristic of a typical device there is a decrease in the voltage, and a very rapid increase in current when the threshold voltage is reached. The above analysis therefore, does not accurately describe the switching process and as a result some modifications are necessary.

The discrepancy may be attributed to the thermal inhomogeneity appearing during or shortly before switching. To take this inhomogeneity into account, it is assumed that a thin region or filament can achieve a temperature θ greater than the average temperature of the surrounding material. The steady state balance equation for an ambient temperature T_a can be expressed as

$$\theta = T_a[\rho_T \ell + R_T(1 + \ell)] \text{ VI}, \tag{3.26}$$

where ρ_T is the thermal resistance of the filament, R_T is the thermal resistance of the rest of the sample, I is the total current (through filament and surrounding region), and ℓ is the ratio of filament current to total current. If $\theta - T_a << T_a$, the electrical resistance of the sample surrounding the filament, and the electrical resistance of the filament itself can be expressed respectively as

$$R = R_o \exp [- \phi_T(T - T_a)] \ , \tag{3.27}$$

and

$$\rho = \rho_o \exp\,[-\phi_T(\theta - T_a)] \quad , \tag{3.28}$$

where T is the temperature of the bulk sample. From Equations (3.26), (3.27) and (3.28) it is possible to obtain a relation between ℓ and P which is given by (Croitoru et al 1970)

$$\frac{\ell_o\,\rho_T}{R_T}\,\frac{P}{P_T} = \frac{\ell_o}{\ell - \ell_o}\,\ell n\,\left(\frac{1/\ell_o - 1}{1/\ell - 1}\right) \quad , \tag{3.29}$$

where $P = VI$, and ℓ_o is value of ℓ when $\theta = T$ which corresponds to the situation prior to switching when no thermal inhomogeneity exists. Equation (3.29) is solved numerically and plotted in Figure 3.1(b) which shows the relation between the current distribution factor ℓ and the power input to the device (which is a function of the applied voltage) for various values of ℓ. Above a critical input, corresponding to the onset of switching, the current distribution factor and therefore the current through the conducting filament increases abruptly as observed experimentally.

3.3. CALCULATION OF THE THRESHOLD VOLTAGE AND THE DELAY TIME BASED ON THERMAL SWITCHING

After the application of a critical voltage $(\geq V_{TH})$, the temperature in the amorphous material rises and after a delay time t_D a critical temperature is reached. Once this critical temperature is exceeded, no stable uniform temperature distribution is possible, and any small local fluctuation in temperature would increase in time leading to the formation of a thermal filament. This causes a current controlled negative differential

resistance in the I - V characteristics. The temperature in the filament rises extremely rapidly until an upper bound is reached caused by the external resistance in the circuit. Upon reduction of the current, the temperature is reduced and the structure returns to its original low conductivity state.

In the analysis which follows, it is assumed that the lateral extension of the contact electrodes is much larger than the thickness of active material, and that the contact electrodes are held at a constant temperature T_o which is reasonable provided that the contacting material has a sufficiently large thermal conductivity, thickness, and heat capacity. Then thesteady state heat conduction equation for the plane parallel geometry is given by (Stocker et al 1970)

$$\sigma_T \frac{\partial^2 T}{\partial x^2} = - \sigma (T,F) F^2 \quad , \tag{3.30}$$

where σ_T is the thermal conductivity, T is the local temperature, F is the electric field strength, and $\sigma(T,F)$ is the electrical conductivity which is given by

$$\sigma(T) = \sigma_o \exp [\gamma(T - T_a)] \quad , \tag{3.31}$$

in which

$$\gamma = \frac{A}{T_a^2} \quad , \tag{3.32}$$

where A is the activation energy expressed in temperature units. Furthermore, the electric field can be assumed to be constant. This assumption introduces only a small error if the thickness of active material is greater than about 1μm (Stocker et al 1970). By introducing dimesionless parameters

$$\tau = A(T - T_a) / T_a^2 = \gamma(T - T_a), \tag{3.33}$$

and

$$\xi = 2x/d \quad , \tag{3.34}$$

Equation (3.30) can be written in the form

$$\frac{\partial^2 \tau}{\partial \xi^2} + \lambda e^{\tau} = 0, \tag{3.35}$$

where

$$\lambda = \frac{\gamma \sigma_o F^2 (d/2)^2}{\sigma_T} \quad . \tag{3.36}$$

Integration of Equation (3.35) gives

$$\left(\frac{\partial \tau}{\partial \xi}\right)^2 = 2\lambda(e^{\tau_m} - e^{\tau}) \quad , \tag{3.37}$$

where τ_m is the maximum value of τ, which by symmetry, is obtained at $\xi = 0$. Integrating Equation (3.37) from $\xi = 0$, $\tau = \tau_m$ to $\tau = 0$, we obtain the following transcedental equation:

$$\exp(-\tfrac{1}{2}\tau_m) \cosh^{-1}[\exp(\tfrac{1}{2}\tau_m)] = (\tfrac{1}{2}\lambda)^{\frac{1}{2}} \, . \tag{3.38}$$

The solutions of Equation (3.38) for τ_m are plotted versus λ in Figure 3.2(a). The basic results of the above analysis are quite similar to those described in the previous section (i.e., section 3.2). In Figure 3.2(a) only the lower portion of the curve, of positive slope, corresponds to a stable temperature distribution. For $\lambda > \lambda_{cr} = 0.88$ no solution exists. As far as physical implications are concerned, this means that if the applied

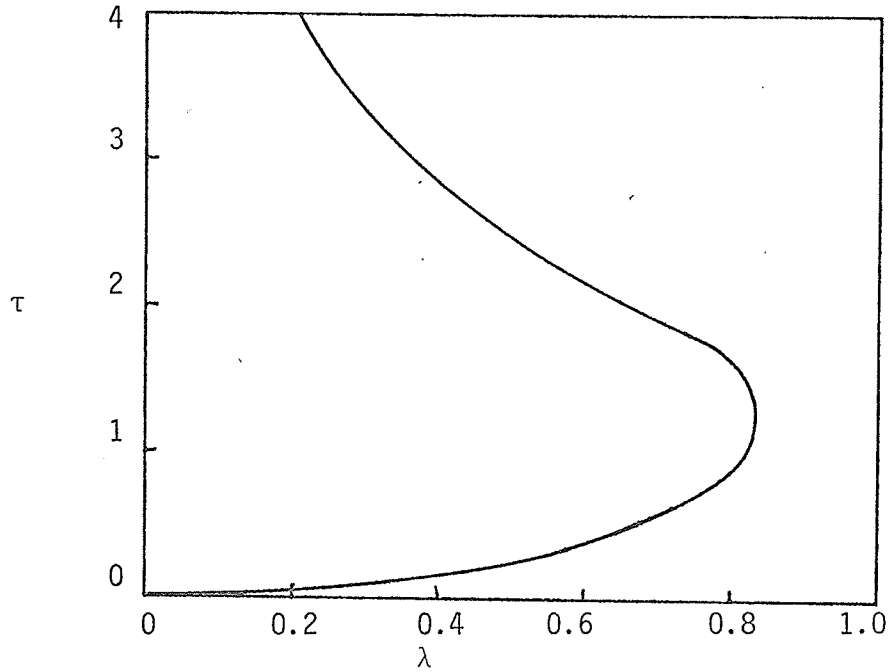

Fig. 3.2 (a). Maximum temperature vs. parameter λ according to Eqn. (3.38) for plane paralled geometry. (after Stocker et al. 1970).

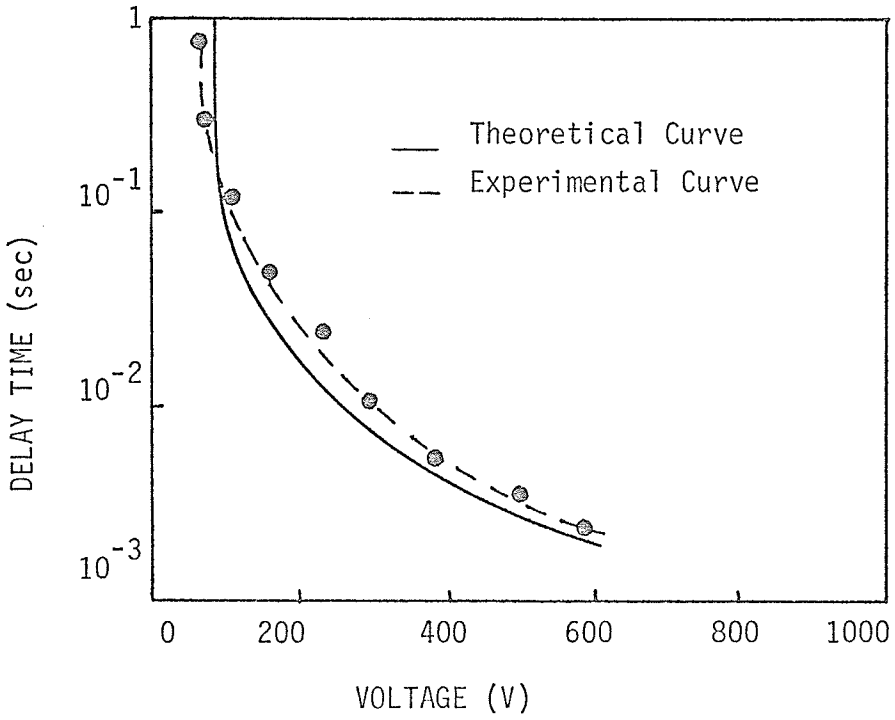

Fig. 3.2 (b). Delay time vs. voltage for a 115 μm piece of bulk $Si_{10}\ Ge_7\ As_{43}\ Te_{37}\ P_3$ glass. The solid line is the function F (V/V_{er}) calculated from Eqn. (3.44) multiplied by $\tau_o = 5X10^{-2}$ sec. (after Stocker et al. 1970).

voltage exceeds a critical value, the temperature will increase indefinitely resulting in a current controlled negative differential resistance, and filament formation.

The value of τ_m corresponding to $\lambda = \lambda_{cr}$ is $\tau_{m,cr} = 1.2$. It is now possible to write down two basic equations for the critical or threshold field F_{cr}, and the critical temperature T_{cr}:

$$F_{cr} = \frac{0.94(\sigma_T/A\ \sigma_s)^{\frac{1}{2}}\ T_a}{d/2}\ , \tag{3.39}$$

and

$$T_{cr} = 1.2\ T_a^{\,2}/A + T_a\ . \tag{3.40}$$

From these two equations several features may be deduced. It can be seen from Equation (3.39) that the critical field is proportional to $\sqrt{\sigma_T}$, therefore, switching due to thermal mechanisms can be achieved more easily in materials having a lower thermal conductivity. Also, the critical field depends on the ambient temperature following approximately the relation

$$F_{cr} \sim T_a \exp\ (-A/2T_a)\ . \tag{3.41}$$

From Equation (3.40) we can estimate that the critical temperature T_{cr} at the threshold voltage is only of the order of 18°C for a material of activation energy of 0.5eV.

Now, if we define the delay time t_D as the time it takes to raise the temperature in the active switching material from T_a to T_{cr}, it is possible to calculate t_D from the simplified heat conduction equation

$$C\,\frac{\partial T}{\partial t} = -\frac{\pi}{2(d/2)^2}\,(T - T_a) + \sigma_o \exp(\gamma T)\ F^2\ , \tag{3.42}$$

where C is the heat capacity per unit volume. Integrating Equation (3.42) from T_a to T_{cr} gives

$$t_D = t_o \, F(V/V_{cr}) \quad , \tag{3.43}$$

where

$$t_o = \frac{4CT_o^{\,2}(d/2)^2}{\sigma_o \, A \, V_{cr}^{\,2}} \simeq \frac{1.73C(d/2)^2}{\sigma_T} \quad , \tag{3.44}$$

and

$$F(V/V_{cr}) = \int_0^1 [(V/V_{cr})^2 \, e^{x} - ex]^{-1} \, dx \quad . \tag{3.45}$$

The function $F(V/V_{cr})$ is a steeply falling function of V/V_{cr} for small overvoltages and then decreases as $(V/V_{cr})^{-2}$ for larger overvoltages. The constant t_o depends on the square of the thickness of active material. Figure 3.2(b) gives the experimental and theoretical delay times as a function of applied voltage for Si_{10} Ge_7 As_{43} Te_{37} P_3 of thickness 115 μm (Stocker et al. 1970).

3.4 SWITCHING DUE TO ELECTRONIC PROCESSES - AVALANCHE IONIZATION

The previous two sections have dealt with the possible thermal processes involved in the switching phenomenon. In this section we shall consider the production of electron-hole pairs by hot electrons (or holes), leading to an avalanche multiplication of carriers. In the hot-electron problem, it is necessary to balance the rate of energy gain by electrons

from an applied field, with the rate of their energy loss by inelastic scattering. The energy loss processes in an amorphous covalent alloy are basically the same as those in a crystal (Hindley 1972). At low energies the most important process is energy loss to phonons.

The following analysis is based on the Shockley model which assumes that the electron distribution is Maxwellian, with a temperature T_e higher than the lattice temperature T. Thus, the Maxwell distribution function is given by

$$f(E) = f_o(E,T_e) = \exp\,[-(E - E_F)/K_B T_e] \quad . \tag{3.46}$$

It should be noted that there is in general no reason why the distribution should be Maxwellian. However, there is at present no other method for treating the hot-electron problem in materials with a relatively short mean free path, for which the Boltzmann transport equation is not valid. Also, the present analysis is primarily intended to give a first estimate of avalanche ionization phenomenon and in that respect it is quite useful.

The electron temperature T_e can be calculated by balancing the rate of energy gain and energy loss. The rate of energy gain from the applied field is given by (Hindley 1970)

$$\left(\frac{dE}{dt}\right)_F = q\mu(T_e)\, F^2 \quad . \tag{3.47}$$

In order to simplify the calculations only polar optical phonons are considered. The rate of energy loss due to electron-phonon scattering is

$$\left(\frac{dE}{dt}\right)_{ph} = -\frac{56\pi\, q^2\, \hbar\, a^2}{n} \left\{ \frac{\exp[\frac{\hbar\nu_{ph}}{K_B}](\frac{1}{T} - \frac{1}{T_e})] - 1}{\exp\,(\frac{\hbar\nu_{ph}}{K_B T}) - 1} \right\} N(E_c) \quad , \tag{3.48}$$

where $N(E_c)$ is the density of states at the mobility edge, and

$$\frac{1}{\eta} = \frac{\nu_{ph}}{4\pi}\left(\frac{1}{\varepsilon_\infty} - \frac{1}{\varepsilon_s}\right) \quad , \tag{3.49}$$

where ε_∞, and ε_s are the dielectric constants at infinite and zero frequencies, respectively. The value of η can be deduced from infrared reflectivity measurements in the lattice absorption region. If Equations (3.47) and (3.48) are combined, it is possible to express T_e as a function of the field. Thus,

$$\frac{\exp\left[\frac{\hbar\nu_{ph}}{K_B}\right]\left(\frac{1}{T} - \frac{1}{T_e}\right)] - 1}{\hbar\nu_{ph}/K_B T_e} = \frac{F^2}{F_{cr}^2} \quad , \tag{3.50}$$

where the critical field F_{cr} is about 10^5 V/cm in many amorphous materials.

Now we turn to consider the process of producing electron-hole pairs. It can be assumed that above a threshold energy E_o, pair production contributes considerably to energy loss. Thus, the electron distribution will drop off sharply above E_o and the following assumptions may be made:

$$\begin{aligned} f(E) &= B_1\, f_o(E, T_e) \quad , \quad (E < E_o) \\ f(E) &= B_2\, f_o(E, T_e') \quad , \quad (E > E_o) \end{aligned} \tag{3.51}$$

with

$$B_1 f_o(E_o, T_e) = B_2 f_o(E_o, T_e') \quad . \tag{3.52}$$

In crystals both energy and crystal momentum must be conserved so that if the electron and hole effective masses are equal, the threshold energy E_o is $3/2\ E_g$, where E_g is the energy band gap. In amorphous materials, however, there is essentially no momentum conservation requirements so that the final state of electrons and the final state of holes are close to the

mobility edge. The threshold E_0, measured from the mobility edge, is therefore equal to E_g.

If we consider the transition from a state with one electron in the state $|K_i>$ of energy E_{K_i}, to a state with two electrons in states $|K_1>$, $|K_2>$ and a hole in state $|K_3>$, the transition probability is (Hindley 1970)

$$P_t = \frac{2\pi}{h} \sum_{K_1K_2K_3} |<K_3K_i| \; U \; |K_1K_2>|^2 \; f_{K_i} f_{K_3} \; (1 - F_{K_1})(1 - f_{K_2}) \; x$$

$$x \; \delta(E_{K_i} - E_{K_1} - E_{K_2} - E_{K_3} - E_g) \; . \qquad (3.53)$$

In this equation we can put $f_{K_3} = 1$ and $f_{K_1} = f_{K_2} = 0$ since we are primarily concerned with electron-hole transistions. For the random phase model (Hindley 1970) in which the states $|K>$ are expressed in a set of localized states, and the phases of the coefficients at different atomic sites are assumed to be random, the matrix element is simply a constant, and Equation (3.53) can be written as

$$P_t = \frac{2\pi \; a^2}{h \; V^3} \; U^2 \; f_{K_i} \sum_{K_1K_2K_3} \delta(E_{K_1} + E_{K_2} + E_{K_3} + E_g - E_{K_i}), \qquad (3.54)$$

where U is a constant with the dimensions of energy. If the sums are now converted into integrals over the density of states, the expression for the transition probability becomes:

$$P_t = \frac{f_{K_i}}{\tau_{pp}} \left(\frac{E_{K_i}}{E_g} - 1\right)^2 \quad , \qquad (3.55)$$

where τ_{pp} is a time constant for electron-hole pair production which may be written as

$$\frac{1}{\tau_{pp}} = \left(\frac{\pi}{\hbar}\right) a^9 \; U^2 \; N(E_v) \; N^2(E_c) \; E_g^2 \quad . \tag{3.56}$$

The rate of energy loss is

$$\left(\frac{dE_{K_i}}{dt}\right)_{pp} = - \frac{2\pi \; a^9}{\hbar \; V^3} \; U^2 \; f_{K_i} \sum_{K_1 K_1 K_3} (E_{K_i} - E_{K_1}) \; \delta(E_{K_1} + E_{K_2} + E_{K_3} + E_g + E_{K_i}) \tag{3.57}$$

$$= - \frac{1}{\tau_{pp}} \left(\frac{E_{K_i}}{E_g} - 1\right)^2 \; \frac{1}{3} E_g \left(1 + \frac{2E_{K_i}}{E_g}\right) f_{K_i} \quad . \tag{3.58}$$

This may be averaged over the distribution assumed in Equation (3.51), and the result can be written as

$$\left(\frac{dE}{dt}\right)_{pp} = - \frac{4E_g}{\tau_{pp}} \left(\frac{K_B \; T_e'}{E_g}\right)^2 N(E_g) \; K_B \; T_e \left(1 + \frac{2K_B \; T_e'}{E_g}\right) B \; x$$

$$x \; \exp\left(- \frac{E_g - E_F}{K_B \; T_e'}\right) \quad . \tag{3.59}$$

Using Equation (3.47) the rate of energy gain from the field for electrons with $E > E_o$ is

$$\left(\frac{dE}{dt}\right)_F = B \; \sigma_o \; F^2 \; \frac{N^2(E_g)}{N^2(E_c)} \; \exp\left(- \frac{E_g - E_F}{K_B \; T_e'}\right) \quad . \tag{3.60}$$

If pair production is the dominant energy loss process, and for $E > E_g$,

Equations (3.59) and (3.60) yield

$$\left(\frac{K_B T_e'}{E_g}\right)^3 \left(1 + \frac{2K_B T_e'}{E_g}\right) = \sigma_o F^2 \left(\frac{N^2(E_g)}{N^2(E_c)}\right) \frac{\tau_{pp}}{4E_g^2 N(E_g)} \quad , \qquad (3.61)$$

where the term $\frac{2K_B T_e'}{E_g} << 1$ and can be neglected.

The average rate of pair production per unit volume is given by

$$R_{pp} = 2 \int P_t N(E) \, dE \quad , \qquad (3.62)$$

which can also be expressed as:

$$R_{pp} = n n' v_d = 2n'F \int_o^\infty \mu(E,T_e) N(E) f(E) \, dE \quad , \qquad (3.63)$$

where n is the number of electrons per unit volume, n' is the number of electron-hole pairs produced by a single particle travelling a unit distance in the direction of the field, and v_d is the drift velocity. By combining Equations (3.51), (3.52), (3.55), (3.61), and (3.63), n' can be written as

$$n' = \frac{qF}{E_g} \frac{N^2(E_g)}{N^2(E_c)} \exp\left(-\frac{E_g}{K_B T_3}\right), \qquad (3.64)$$

or,

$$n' = n_o' \left(\frac{F}{F_{cr}}\right) \exp\left[-(E_g/\hbar \nu_{ph}) \frac{\hbar \nu_{ph}}{K_B T_e}\right] \quad , \qquad (3.65)$$

in which

$$n_o' = \frac{q F_{cr}}{E_g} \frac{N^2(E_g)}{N^2(E_c)} \quad . \qquad (3.66)$$

For a density of states ratio of 1 (the density of states ratio $N(E_g)/N(E_c)$ is actually greater than 1), and E_g = 1eV, then $n_o' = 10^5$ pairs/cm for $F_{cr} = 10^5$ V/cm. In order to obtain n' as a function of the applied field, Equation (3.50) must be solved. If $h\nu_{ph}/K_B T_e$ is small, so that $F >> F_{cr}$, we can obtain an approximate solution of Equation (3.50) in the form:

$$\frac{\hbar \nu_{ph}}{K_B T_e} = \left[\exp\left(\frac{\hbar \nu_{ph}}{K_B T}\right) - 1\right] \frac{F_{cr}^2}{F^2} \tag{3.67}$$

so that

$$n' \simeq \exp\left[-G \frac{F_{cr}^2}{F^2}\right] , \tag{3.68}$$

where

$$G = \left[\exp\left(\frac{\hbar \nu_{ph}}{K_B T}\right) - 1\right] \left(\frac{E_g}{\hbar \nu_{ph}}\right) . \tag{3.69}$$

For an energy band gap of 1 eV, and a reasonable value of phonon frequency (i.e., $\nu_{ph} \simeq 10^{12}$ sec^{-1}), $G \simeq 50$. It can be seen that n' increases very rapidly with field for $F^2 << GF_{cr}^2$, but the increase becomes linear for $F^2 >> GF_{cr}^2$.

Closely related to the avalanche ionization treated above is the process of avalanche injection studied by Gunn (1957). The process of avalanche injection occurs when the potential distribution is controlled by the space charge of the carriers. The high field region, in which the avalanche occurs, is confined to a region near the electrodes, and this region injects large numbers of electrons into the rest of the sample. As the current increases, the thickness of the high-field region, and the voltage across it, decrease thus giving rise to negative differential

resistance.

Although avalanche ionization may help to explain several experimental results such as the statistical variations in the delay time, it does not explain the non-ohmic current-voltage characteristics in the low conductivity state which sets in before avalanche ionization can occur. This indicates that there may be several mechanisms simultaneously operative in amorphous semiconductors and that these mechanisms probably involve both thermal and electronic processes.

CHAPTER 4

EXPERIMENTAL TECHNIQUES

4.1 SAMPLE PREPARATION

The material used in the experimental work is a concentrated amorphous alloy containing the elements Te, As, Si, Ge, in proportions 48 wt % Te, 30 wt % As, 12 wt % Si, and 10 wt % Ge (Te_{48} As_{30} Si_{12} Ge_{10}). This amorphous semiconductor was supplied by Malven Radar Research Laboratories in England, and was received in the form of an ingot approximately 3 cm in length and 1 cm in diameter. The basic steps in producing good switching devices from the bulk material are outlined as follows:

(1) The ingot was cut into wafers with a precision diamond wheel cutter, each wafer being approximately 0.5 mm in thickness. It was found that wafers with thickness less than 0.5 mm broke easily during cutting. A diamond edge cutter was used to cut the wafers into individual squares, each square sample being approximately 4 mm X 4 mm in size.

(2) To facilitate polishing, each square sample was mounted on a brass block using wax as the adhesive. Care had to be taken at this point not to subject the sample to excessive heat for this could result in localized regions of recrystallization. The brass block was heated to the melting temperature of the wax, and once the sample had been placed into position the entire assembly was quickly cooled to room temperature. After one surface had been polished the sample was removed and remounted on the brass block so that the other surface could be polished. The final polishing step involved not only polishing, but also reducing the sample thickness to

the desired value. The sample thickness used for all the experimental work was 100 μm, and it was measured using a precision micrometer accurate to ± 1 μm. The uniformity in thickness is important since each square sample contains a number of individual devices and the switching threshold voltage of each device is dependent on the thickness of active material.

(3) Once the desired thickness had been achieved the sample was removed from the brass block and placed in warm trichloroethylene to remove wax, fingerprints, dust, and other foreign material from the surfaces. Since trichloroethylene is a strong cleaning agent and tends to react chemically with other substances, the sample was not subjected to trichloroethylene cleaning for more than five or ten minutes. After this process the sample was cleaned in petroleum ether for about 30 minutes and then transferred to methanol. Since methanol is a mild cleaning agent, and does not tend to react chemically with other substances, the sample was left in this solution until the vacuum system was ready for electrode deposition. As long as the sample is immersed in methanol oxidation of the polished surfaces can be avoided. It should be mentioned that this amorphous material is extremely brittle. For thicknesses of 100 μm or less, ultrasonic cleaning usually resulted in sample breakage. Thus, special care had to be taken in handling the polished samples.

(4) After the cleaning sequence had been completed the sample was transferred to the vacuum system which was then pumped down to $2X10^{-6}$ mm Hg pressure. A stainless steel mesh was used to produce about 70 Ag electrodes per cm^2, the area of each individual electrode being approximately .6 mm X .6 mm. The opposite surface of the sample was completely

coated with In. For the size of samples (4 mm X 4 mm) and the size of Ag electrodes (.6 mm X .6 mm) used it was possible to obtain about 8 to 12 electrodes on each square sample. Each individual Ag electrode constitutes a switching device in itself, so that a total of 8 to 12 devices were made from each square sample. After deposition was completed the samples (and tungsten boat) were allowed to cool to room temperature before they were removed from the system. This was necessary to prevent oxidation of the evaporated electrodes, particularly the In electrodes. (5) The final procedure is to mount the sample on a conducting base and to make contacts to the individual Ag electrodes. The sample holder arrangement is illustrated in Fig. 4.1. Conducting silver paint was used to adhere the sample to the copper base (Ag electrodes being on the outer surface). Approximately 30 minutes was allowed for the silver paint to dry. Once the sample was securely mounted fine copper wire was soldered to the pins on the base of the sample holder and the other end of these wires were attached to each Ag electrode with silver paint. The entire procedure was carried out using a microscope of magnification X20.

4.2 EXPERIMENTAL PROCEDURES

4.2.1 SWITCHING INSTABILITIES IN NEW DEVICES

The initial switching behaviour of new devices has been found to be erratic and unstable over the first few switching cycles, after which the threshold voltage for the onset of switching becomes almost

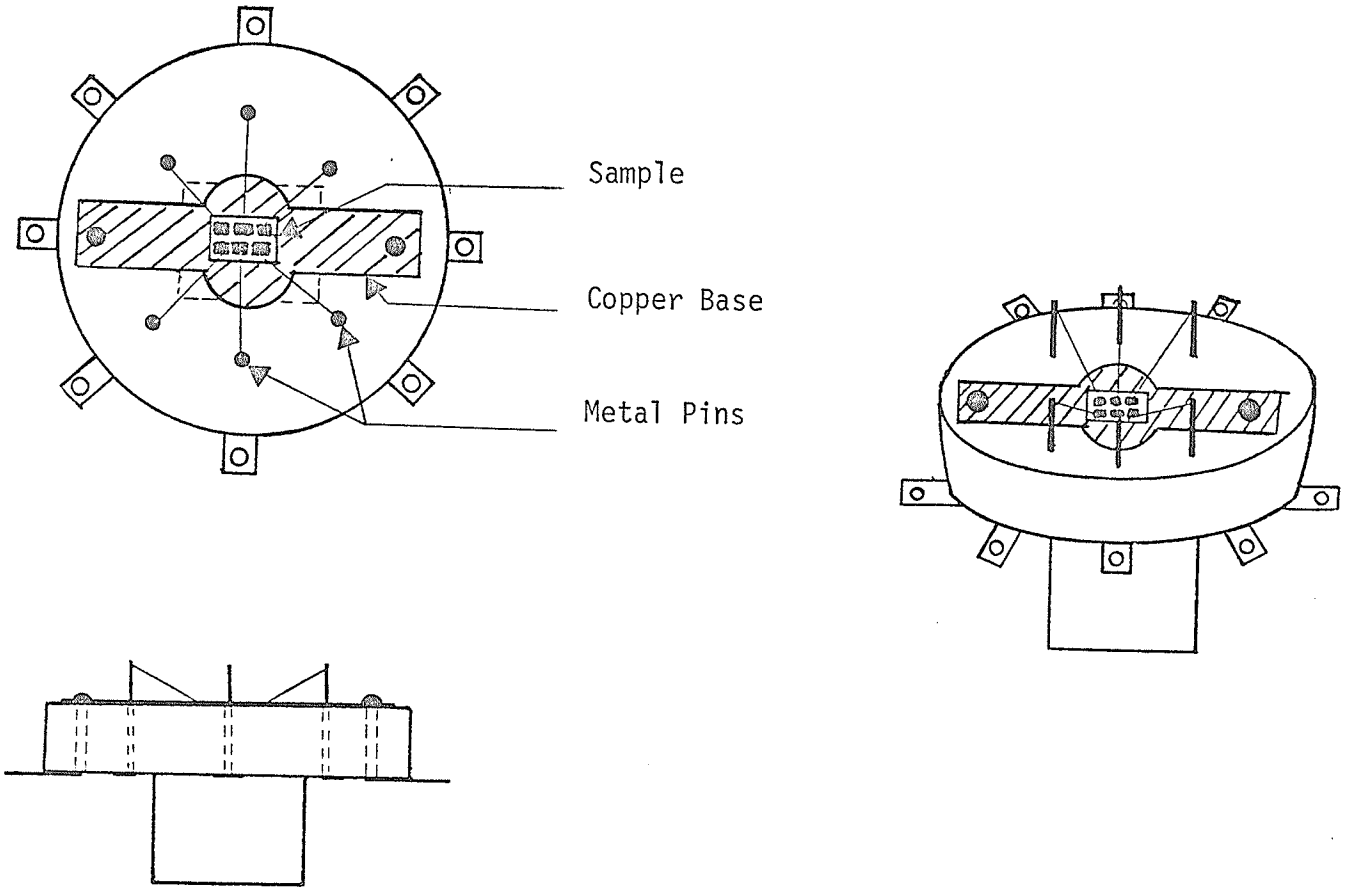

Fig. 4.1. Illustrated is the sample holder with a sample having six devices. The six metal pins provide contacts to the top of the sample and the copper base plate provides the other contact. (Drawn to actual size)

constant. Several aspects of this "breaking in" behaviour of new devices seem to depend on a number of factors. The purpose of this experimental investigation is to determine the effect of various current levels, and the effect of switching cycle rate on the unstable switching behaviour of new devices.

A schematic illustration of the testing circuit used for this experiment is given in Fig. 4.2. Switch S is initially in the closed position so that the voltage across the capacitor (C = 20 μf) and the device is zero. When S is opened the capacitor begins to be charged through R_1 which has a value of 150 kΩ. Thus we have a slowly rising voltage across the device. At the instant that V_{TH} is reached the amorphous device switches to the conducting state and switch S is then manually closed. Since the device is now in the high conductivity state, and S is in the closed position, the capacitor discharges through the paralled combination of R_2 and R_3. Thus, the peak current through the device is determined by R_3, and the rate of decay of this current is determined by the parallel combination of R_2 and R_3. When the current falls below I_H the device reverts back to the low conductivity state and the entire procedure can be repeated. The current-voltage characteristics were recorded using a Honeywell Model 193 pen recorder. The rise time of the voltage output is determined by the time constant R_1C which is 3 sec and is kept constant throughout the experiment. Similarly, the fall time of the current passing through a device in the "ON" state is determined by the time constant associated with R_2, R_3, and C, which is arbitrarily chosen to be 1 sec. The fall time of the current is therefore three times faster than the rise time of the voltage waveform. It

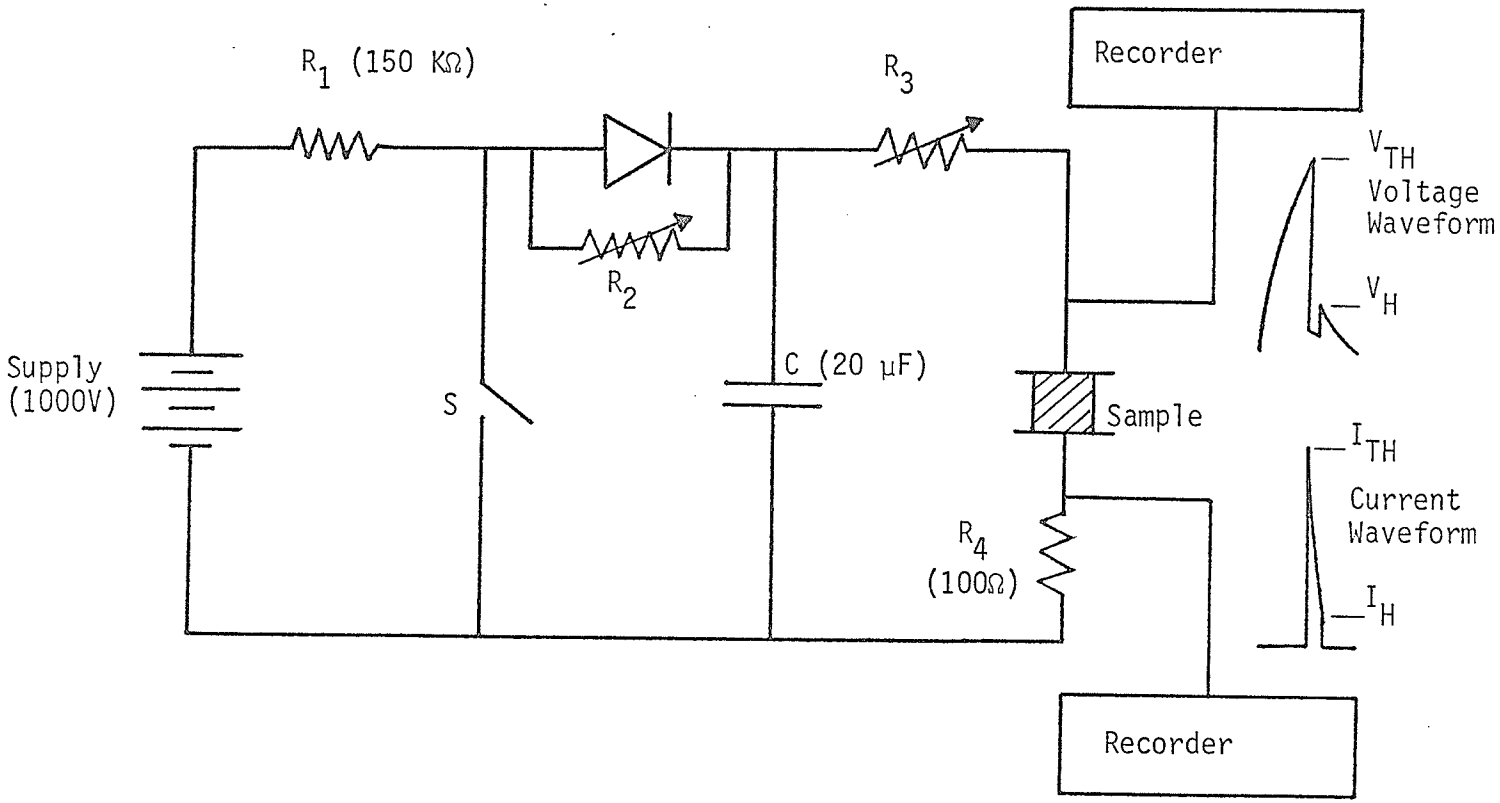

Fig. 4.2. Schematic illustration of the circuit and measuring arrangement used in the investigation of initial switching properties of new devices.

should be mentioned that the voltage rise time and the current fall time chosen are quite arbitrary. Once these parameters had been selected, however, they were kept constant throughout the experiment.

The investigation was carried out under four sets of experimental conditions which are summarized in table 4.1. With a current limiting resistance of 500 KΩ the peak current corresponding to a switching voltage of 750 V for example, would be 1.5 mA. The actual peak current would of course be determined by the value of the switching voltage as well as the resistance R_3. A repetition rate of 2 cycles /min would cause a switching cycle to occur (by opening and closing switch S) at intervals of 30 sec. Since R_3 has been fixed at 500 KΩ and [R_2 R_3 C/ (R_2 + R_3) ≃1], R_2 must be 55 KΩ. The first device is tested with the above conditions until a stable value of threshold voltage is reached. The threshold voltage was considered to be stable when approximately 25 or 30 consecutive switching cycles gave the same value of V_{TH} (within about 5% variation). In the second set of experimental conditions R_3 is changed to 250 KΩ while the repetition rate is maintained at 2 cycles/min. With R_3 set at 250 KΩ the peak current corresponding to a given value of V_{TH} is about twice the value obtained under the first set of conditions. Also, since R_3 has been changed and it is desired to have the same time constant for the fall time of the current [R_2 R_3 C/ (R_2+R_3) ≃ 1 sec] , R_2 must be adjusted to a value of 62.5 KΩ from its previous value of 55 KΩ. The final two sets of experimental conditions are similar to the ones described above except that the repetition rate was 4 cycles/min rather than 2 cycles/min.

TABLE 4.1

The various experimental conditions for the investigation of initial switching behaviour of new devices.

Experimental Arrangement	Current Limiting Resistance (KΩ)	Switching Rate (Cycles/min)
A	500	2
B	250	2
C	500	4
D	250	4

Four devices were used in the investigation, one for each of the four sets of conditions listed in table 4.1. The devices had no switching history prior to the experiment, and so it was possible to obtain the initail switching behaviour of each device under these conditions. Furthermore, all of the devices were from the same sample, and they were all adjacent to each other so that the possible effects of non-uniformity in sample thickness or stoichiometric variations in material composition could be minimized.

4.2.2 THE EFFECT OF LONG-TERM CONTINUOUS CYCLING ON THE PROPERTIES OF THRESHOLD SWITCHES

Although a stable value of threshold voltage is reached in most devices after a certain number of switching cycles (usually less than one hundred), this does not guarantee that V_{TH} will remain constant after a very large number of switching cycles. It is possible that the stability may persist only for several hundred cycles and then give way to a new region of stability having a different characteristic V_{TH}, or possibly a region of unstable switching as observed in new devices. The circuit illustrated in Fig. 4.3 was used to examine the long-term effects of continuous cycling on the properties of threshold switches. This circuit is basically similar to that shown in Fig. 4.2. The rise time of voltage output, the fall time of current through a device in the "ON" condition, and the peak current allowed to flow at the point of switching can all be adjusted by varying the values of components within the circuit. The capacitance and resistance values are chosen to

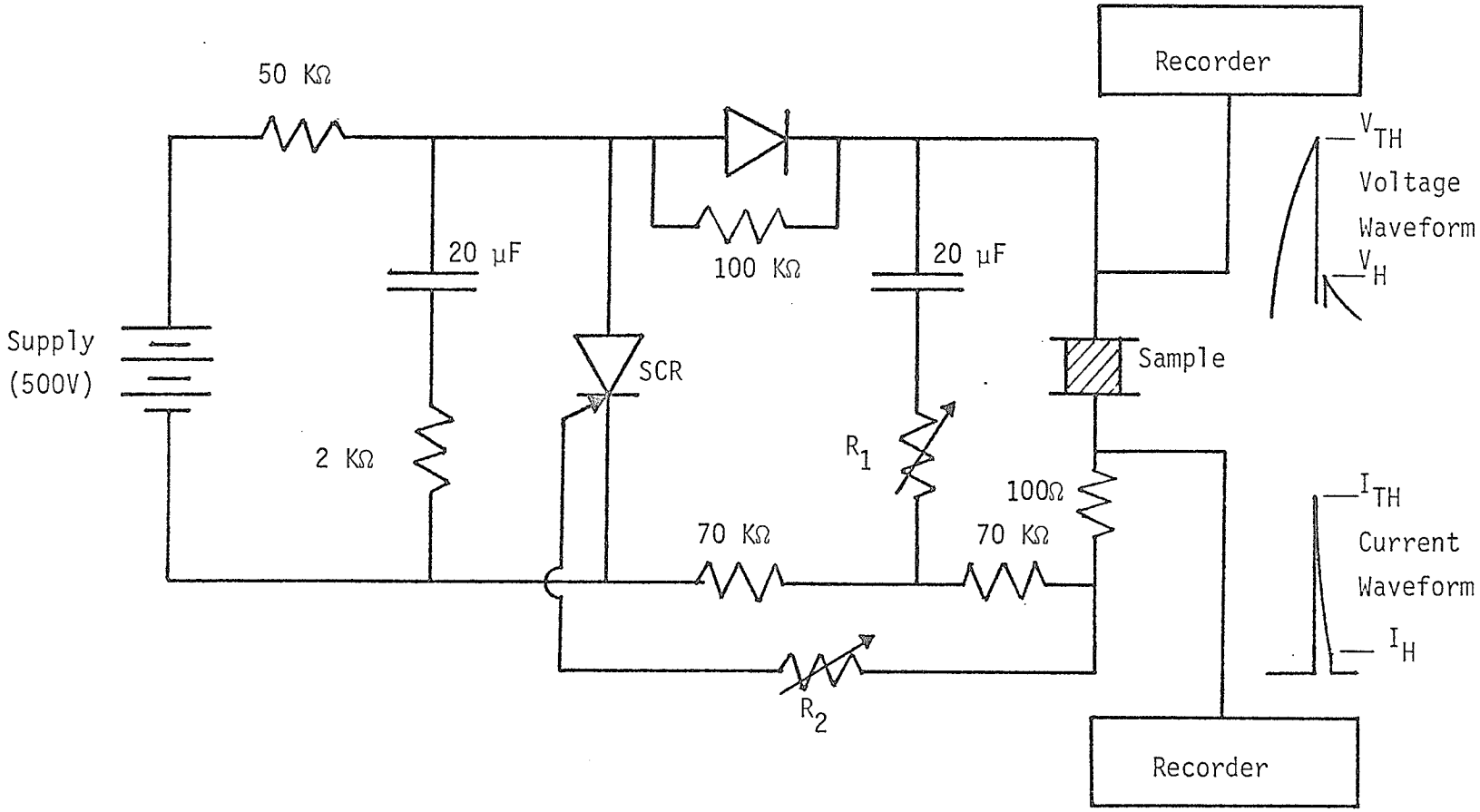

Fig. 4.3. Schematic illustration of the circuit and measuring arrangement used in the investigation of long-term continuous cycling effects on the properties of threshold devices. R_1 is the current limiting resistor (0-500 KΩ), and R_2 controls the triggering of the SCR.

give a voltage rise time of approximately 100 V/sec, and a current fall time of .5 ma/sec. The SCR acts as an automatic switch which is triggered by the switching of the amorphous device and essentially is used to isolate the 500 V supply from the rest of the circuit. This allows the current flowing through the device to decay below the holding value I_H so that a transition back to the "OFF" state can occur. Since the gate current to the SCR is now negligible, it also switches off because the original current through the SCR is not sufficient to "lock it in". Thus, the capacitors start to be charged again and a slowly increasing voltage is again applied to the device under investigation. This entire procedure is automatically controlled by the SCR and will continue regardless of the value of V_{TH} of the amorphous device (within the limits of the supply). Using this circuit it is possible to determine the effect of many thousands of switching cycles on the stabiltiy of amorphous switching devices.

Several devices were studied using various values of current limiting resistance (i.e. peak current) in an attempt to determine the expected lifetime of amorphous switches when subjected to continuous operation at various current levels.

4.3.2 THE EFFECT OF PEAK CURRENT ON THE DURABILITY OF AMORPHOUS THRESHOLD SWITCHES

Subjecting a switching device to a very large number of switching cycles may not be sufficient to determine the lifetime and durability of the device. It is also important to know how long a device will display stable characteristics when it is switched at consecutively higher

values of peak current, and at what current levels a significant change in characteristics may occur. The circuit illustrated in Fig. 4.2 was used to study the effect of peak current on the durability of amorphous threshold switches. The peak current allowed to flow through a device at the instant of switching was increased in discrete steps from one switching cycle to the next. As described previously this circuit requires manual control (by altering the position of switch S).

Three devices were used, each having a stable threshold voltage of 400 V to 500 V. The first device, which had a threshold voltage of 400 V (at room temperature) was switched, only once, with a current limiting resistance R_3 of 400 KΩ corresponding to a peak current of 1 mA at the instant of switching. The value of R_3 was then reduced to 200 KΩ corresponding to a peak current of 2 mA, (provided of course that V_{TH} is still 400 V) and the device was once again cycled. Similarly after the second switching had been completed R_3 was further reduced and the operation was repeated. The value of R_3 needed for a given peak current was determined by the threshold voltage of the previous switching cycle. The device was switched only once for each value of desired current, and a period of several minutes was allowed to elapse between switching events in order to eliminate the possibility of residual effects from the previous switching. The procedure was carried out until significant changes in characteristics occurred,or until actual destruction of the device took place. The two parameters which were recorded at each switching cycle were the threshold voltage V_{TH}, and the holding current I_H. To ensure consistency in results, the experiment was repeated three times using three different devices.

4.2.4 MEMORY BEHAVIOUR OF THRESHOLD DEVICES IN THE Te-As-Si-Ge SYSTEM

The memory behaviour of amorphous devices using Te_{48} As_{30} Si_{12} Ge_{10} as the active switching material has been the subject of considerable investigation in recent years, but many published results are still contradictory. For example, the memory state for devices using this composition has been observed by Bagley and Bair (1970), but Ovshinsky (1968) who worked with the same composition reported that there is no memory behaviour for this material.

It has been found in the present experimental investigation that a memory state for the composition Te_{48} As_{30} Si_{12} Ge_{10} is possible, provided that a sufficiently high current having a minimum duration time, is applied to a device when it is in its conducting state. It has also been found that the memory condition may be erased if a current pulse of sufficient magnitude and perferably of opposite polarity is passed through the device. To determine the relation between current magnitude and current duration required to obtain memory in these devices, a square current pulse of variable amplitude and duration was used. The magnitude and the duration of the current were adjusted until the correct combination of these two parameters resulted in the memory state. With the appropriate current limiting resistor a typical device was switched and maintained in the conducting state for a specified period of time, and then checked to see if memory had been induced. If memory had not been induced and the characteristics of the device had not changed appreciably due to the previous switching, the operation was repeated

using a longer current pulse duration. This was continued until memory was observed to take place. If, during this trial and error procedure, the characteristics of the threshold switch changed from what they were originally, then it became necessary to use a different device or to bring back the original characteristics of the same device (by passing a large current pulse through it, for example) before continuing to the next combination of current strength and current duration.

In general, for low current magnitudes relatively large duration times were required to induce memory, and vice versa. For this reason it became impractical to use a manually controlled switch to apply current for the case of large currents and consequently short duration times. For duration times less than 5 sec the circuit shown in Fig. 4.4 was used. This circuit is capable of producing single square current pulses of accurate amplitude and duration for pulse durations as short as several m sec. With switch S in position 1 capacitor C is charged to voltage V. The SCR however, provides an open circuit since there is no gate current. As a result, no voltage is applied to the device. Placing S in position 2, however, provides the SCR with sufficient current through its gate to cause triggering. The supply is now connected to the device which rapidly switches to the "ON" state. The current allowed to flow is determined by R_2. Also, since capacitor C discharges through the gate of the SCR and through R_1, the gate current soon falls below the holding value required to keep the SCR conducting. At this point the SCR switches off and current flow to the device is terminated. Thus, the current magnitude can be controlled by R_2, and the current pulse duration is determined by the value of V, C, and R_1. The output wave-

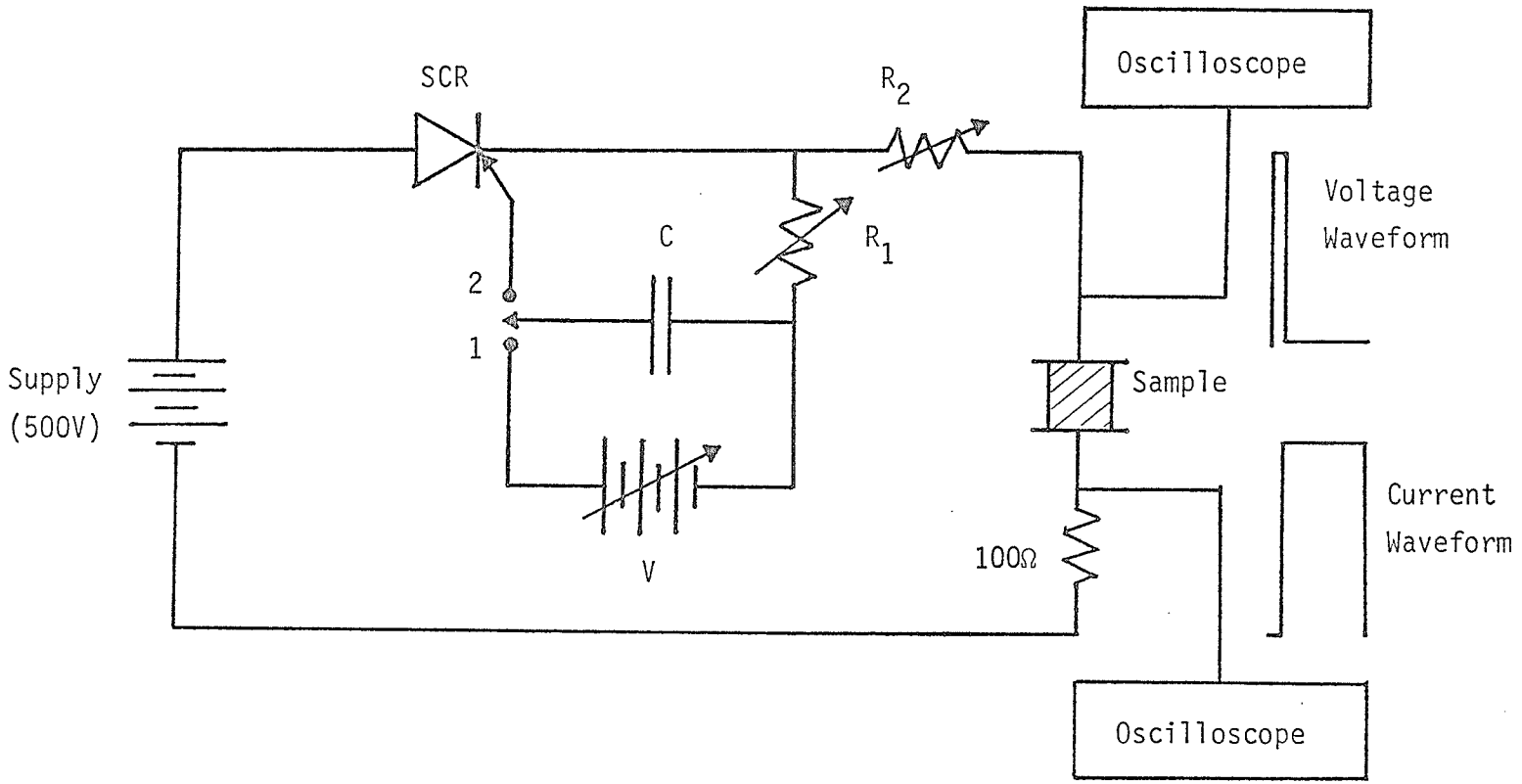

Fig. 4.4. Schematic illustration of the circuit and measuring arrangement used in the investigation of the memory properties of amorphous threshold devices.

form was in each case displayed on an oscilloscope so that the various components in the circuit could be adjusted to produce the desired current amplitude and pulse duration. Using this circuit it was possible to determine the dependence of current strength on duration time required to obtain memory.

4.2.5 THE EFFECT OF TEMPERATURE ON THE SWITCHING VOLTAGE AND SWITCHING TIME

The experimental arrangement is shown in Fig. 4.5. The temperature range considered was from 100^{o}C to -50^{o}C. Switching devices used for this experiment had a stable threshold voltage of 400 V at room temperature (i.e. 20 ^{o}C). The circuit shown in Fig. 4.2 with a current limiting resistor of 400 KΩ was used, so that at room temperature with a threshold voltage of 400 V, the peak current allowed to flow through a given device would be 1 mA. Threshold voltage V_{TH}, holding current I_H, and switching time were measured at 25^{o} C intervals starting from 100^{o} C down to -50^{o} C, using a Tektronix Model 549 storage oscilloscope and a Honeywell Model 193 chart recorder, and oscillograms were also taken at each temperature for analysis purposes.

CHAPTER 5

EXPERIMENTAL RESULTS AND DISCUSSION

5.1 GENERAL SWITCHING AND MEMORY CHARACTERISTICS

Before proceeding to the presentation of specific and systematic experimental results, it is desirable to present first some of the switching characteristics for the devices used in the experimental work, such as the current-voltage characteristics, the switching time properties, and the memory behaviour. These are discussed separately as follows:

5.1.1 THE CURRENT-VOLTAGE CHARACTERISTICS

Fig. 5.1 shows an oscillogram of the current-voltage characteristics of a typical threshold switch. The threshold voltage for this device is approximately 400 V. The value of current limiting resistance used in this particular case was 400 KΩ so that the device was switched at the 1 mA level. A further increase of voltage after the onset of switching results only in an increase of the current through the device. It can be seen that for low voltages the current increases very slowly until the threshold voltage is approached. Once the threshold value is reached the transition from the low conductivity state to the high conductivity state is very rapid - in fact the transition is so rapid that the scope is unable to trace the entire switch-on curve. If the supply voltage is slowly decreased when the device is in the conducting state the current will de-

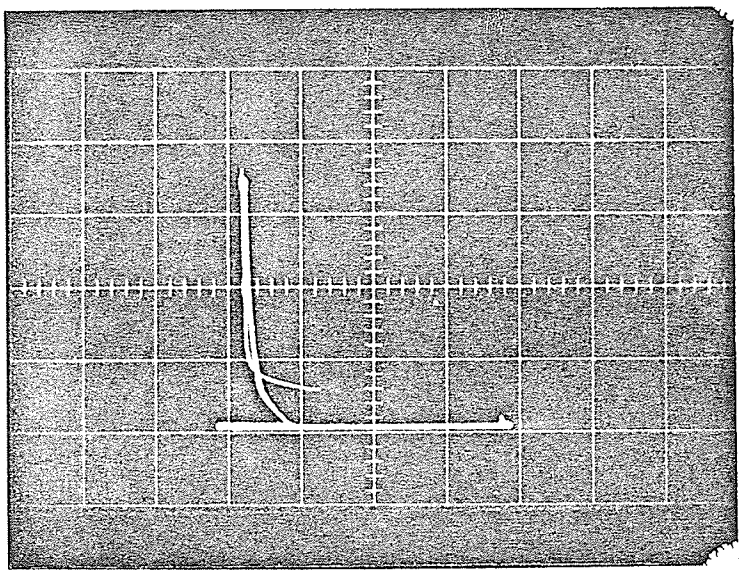

Fig. 5.1. Current-voltage characteristics of a typical threshold switch. Scale: horiz. 100 V/div; vert. 1 mA/div.

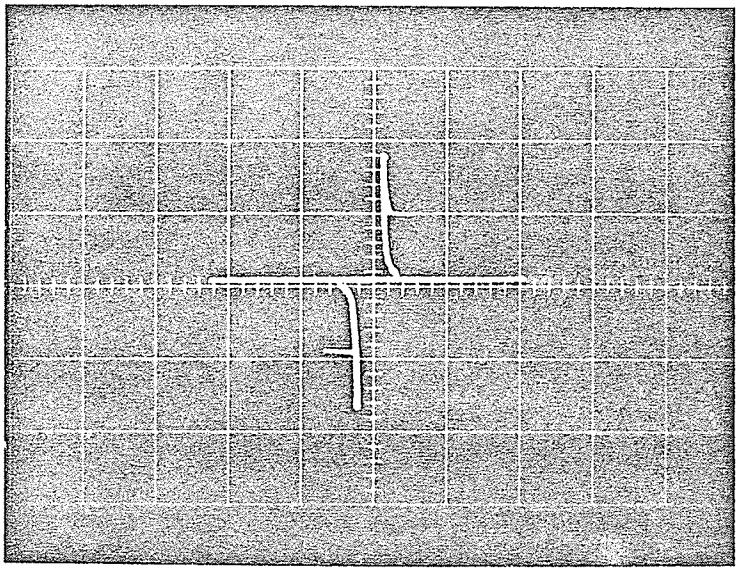

Fig. 5.2. The current-voltage characteristics of a typical threshold switch illustrating the bistable nature of the switching action. Scale: horiz 200 V/div; vert. 1 mA/div.

crease along the switch-off curve. As soon as the current falls below the holding value I_H, which in this case is approximately 0.25 mA and corresponds to a holding voltage V_H of 100 V, the device reverts back to the low conductivity state. A typical value of the blocking resistance of the devices used throughout the experimental work was $50X10^6$ Ω, and the "ON" state resistance was as low as several hundred ohms in some cases. Therefore, the transition from the "OFF" state to the "ON" state sometimes involved a change of resistance of the order of 10^5 Ω.

Fig. 5.2 illustrates the bistable nature of the amorphous devices; that is, the I-V characteristic is independent of the polarity of applied voltage. It was found, however, that the reversal of polarity sometimes resulted in a less stable device. This may be due to the fact that the electrode materials used on the opposite surfaces of the amorphous device were different.

5.1.2 THE SWITCHING TIME

The switching time observed in most of the devices typically range between 90 n sec and 120 n sec for a slowly increasing applied voltage at room temperature. As described previously, the total switching time is made up of a delay time t_D, and an actual switching time which is usually much less than t_D.

Fig. 5.3 shows an oscillogram of the switching time for a typical device. It can be seen that the total switching time is approximately 100 n sec, of which 80 n sec is the delay time, and only 20 n sec the actual switching time. The switching time depends strongly on thick-

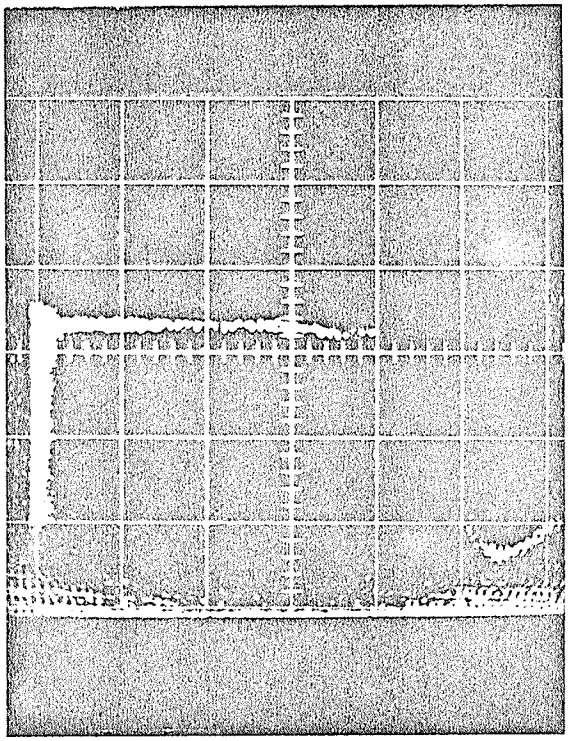

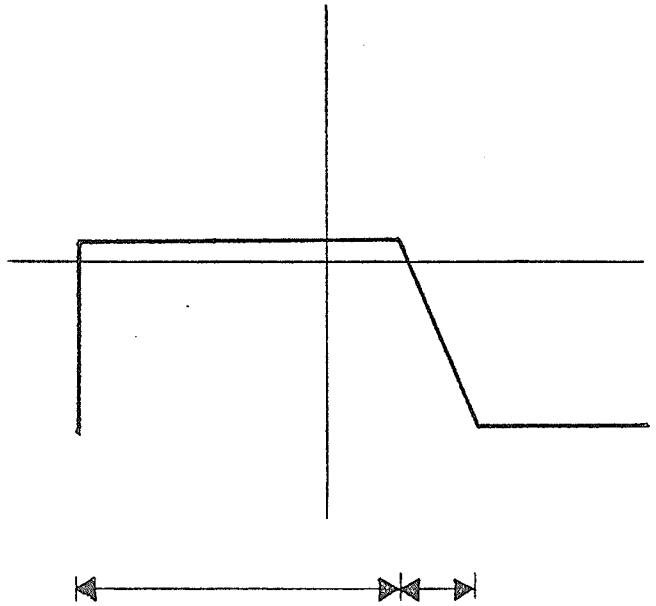

Fig. 5.3. Oscillogram and corresponding schematic equivalent of the switching time. Oscillogram Scale: horiz. 20 nsec/div; vert 200 V/div.

ness of active amorphous material, and on overvoltage applied to the device. For example, film devices having an active material thickness down to a fraction of a μm will typically have a switching time in the p sec range, whereas devices using bulk samples of many μm thickness have a switching time as high as several hundred μ sec. Also, for a given device the switching time decreases rapidly with overvoltage (voltage over the threshold value). On the other hand, the switching time seems to be independent of the voltage rise time. For example, a voltage rise time of 50 V/sec and 2000 V/sec gave approximately the same switching time.

5.1.3 THE MEMORY PHENOMENON

Fig. 5.4 shows the current-voltage characteristics of a device with memory behaviour. The turn-on characteristics are similar to those of an ordinary threshold switch. However, when the voltage is slowly reduced to zero the curve does not follow a switch-off pattern, but rather approaches zero directly. The memory behaviour could be set in by keeping the device in the conducting state at the 2 mA level for approximately 10 sec, which apparantly was sufficient to lock it into memory. A subsequent increase of voltage of either polarity results only in driving the device up and down the memory curve. It can be seen, however, that when a current pulse of sufficient magnitude and of opposite polarity is passed through the device, a transition back to the low conductivity state occurs, as illustrated by the switch-off curve of Fig. 5.4. After this transition, the device becomes an ordinary switch again and will display memory only if current magnitude and duration exceed the required critical values.

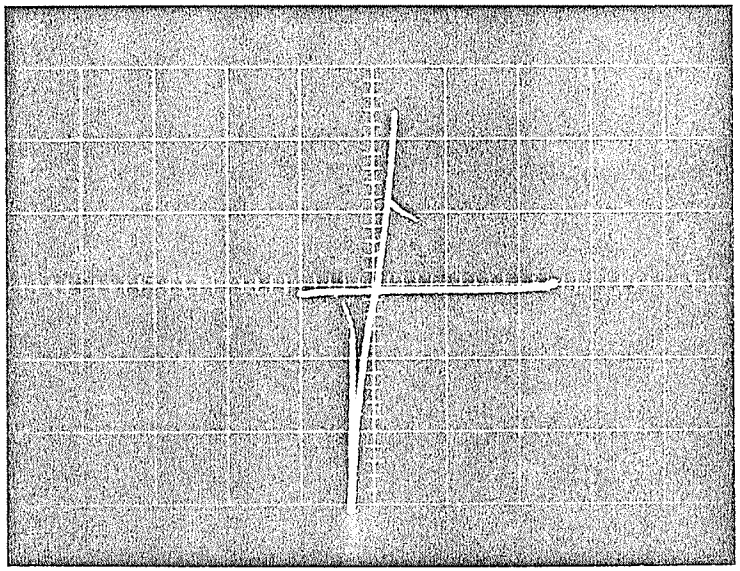

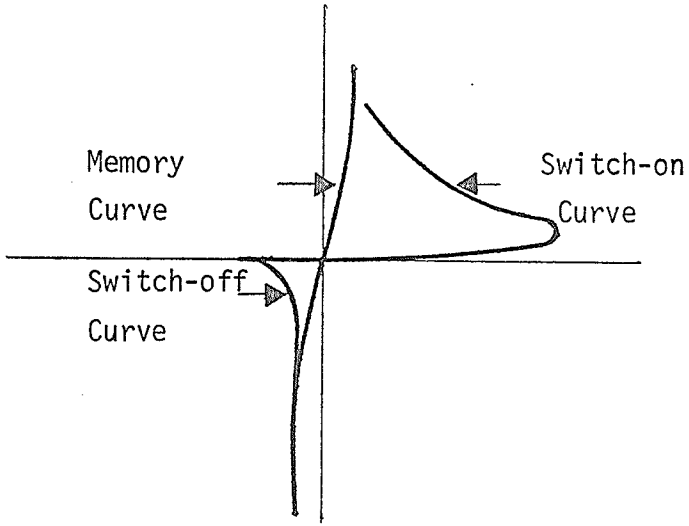

Fig. 5.4. Oscillogram and corresponding schematic equivalent of the memory characteristics. Oscillogram Scale: horiz. 200 V/div; vert. 1 mA/div.

For this particular device memory resulted when a current magnitude of 2 mA, and a duration of 10 sec was used. If this minimum energy required for memory was not reached then the I-V curve would show only ordinary switching characteristics and the removal of the applied voltage would result in a regular switch-off behaviour as shown in Fig. 5.1. It will be seen later in this chapter that the current of 2 mA and its duration of 10 sec is one of many possible combinations of current magnitude and duration for the onset of memory in these devices.

5.2 THE INITIAL SWITCHING BEHAVIOUR OF NEW DEVICES

Fig. 5.5 and Fig. 5.6 show the threshold voltage, and the holding current for the first seventy switching cycles of two new devices which had no previous switching history. The switching rate was 2 cycles/min, and the applied voltage was a slowly increasing d c voltage.

In both cases the threshold voltages for the first few cycles are considerably higher than the subsequent threshold voltages measured after twenty or thirty cycles. This was observed for all of the devices investigated and appears to be a general property of new devices. After about fifty switching cycles the threshold voltage became quite stable and remained practically constant at 420 V. It will be shown in the next section that this region of stability, which may persist for several hundred cycles, is in fact the first of several possible stability regions, each having a lower characteristic threshold voltage than the previous region.

It can be seen from Figs. 5.5 and 5.6 that the fluctuations in

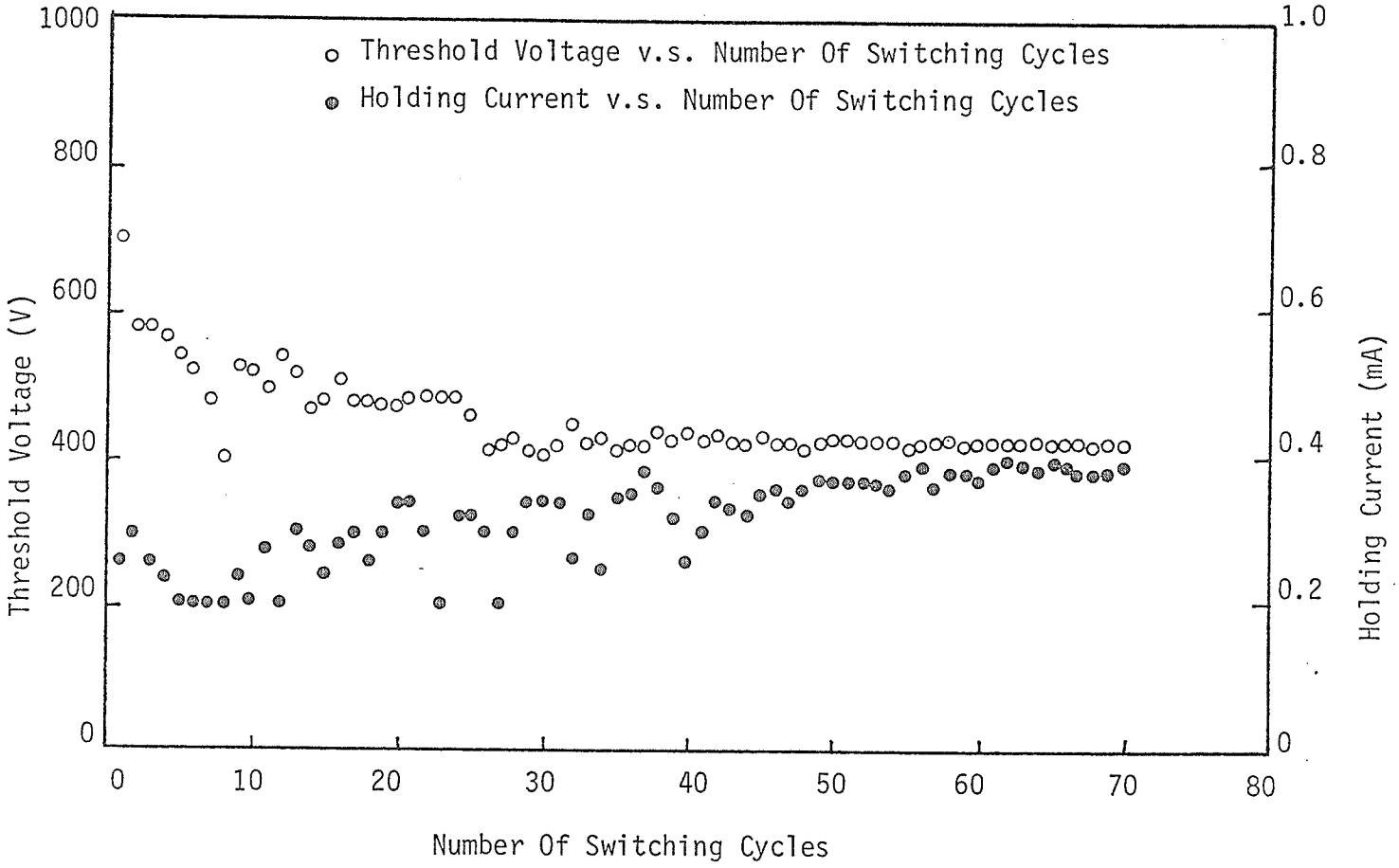

Fig. 5.5. The switching threshold voltage and holding current as functions of the number of switching cycles with a switching repetition rate of 2 cycles/min and a current limiting resistance of 500 KΩ.

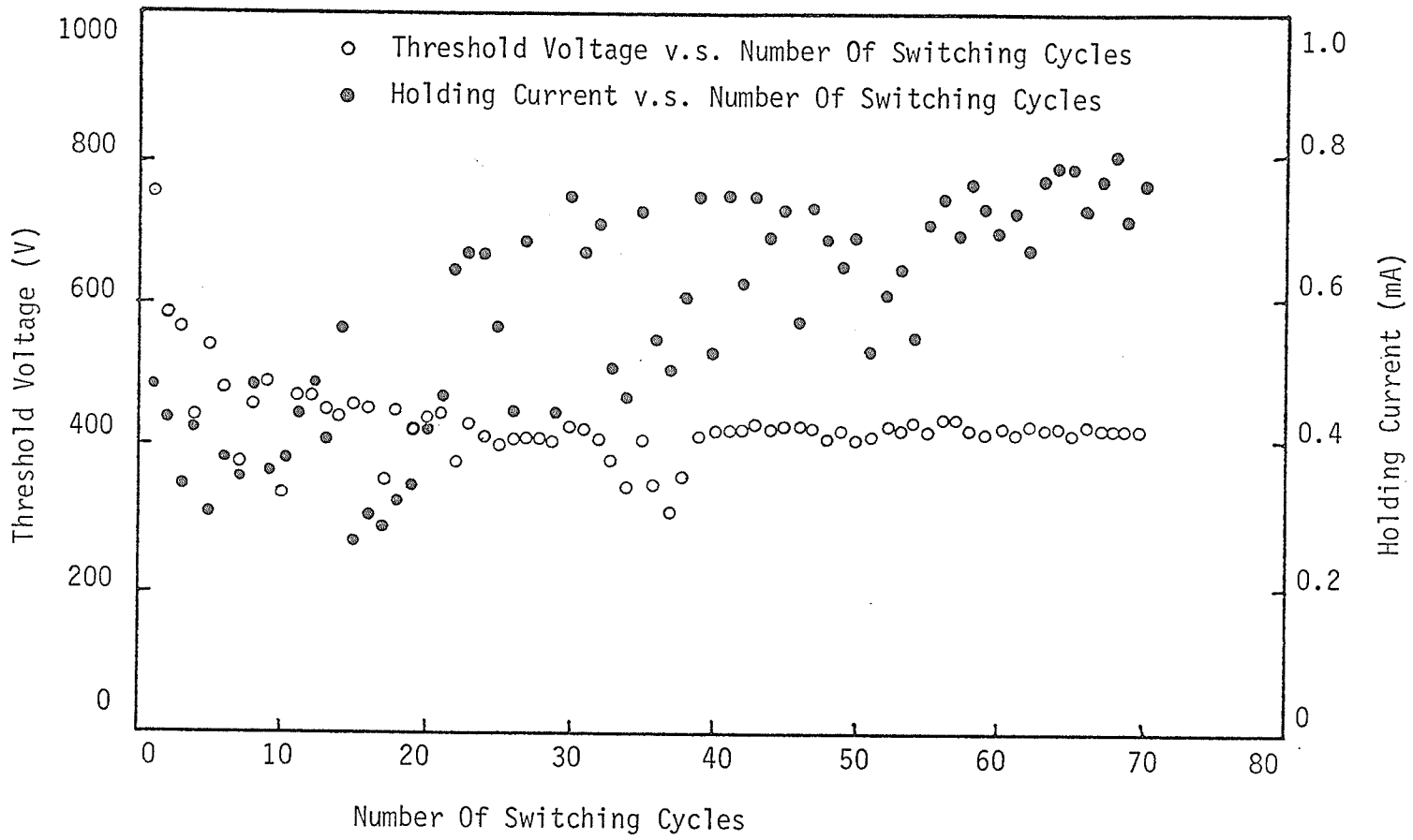

Fig. 5.6. The switching threshold voltage and holding current as functions of the number of switching cycles with a switching rate of 2 cycles/min and a current limiting resistance of 250 KΩ.

V_{TH} and I_H for the case with a current limiting resistance of 250 KΩ are far more pronounced and persist over a greater range that those with a current limiting resistance of 500 KΩ. This implies that the lower the peak current, the more stable is the initial switching behaviour. The general trend, however, seems to be the same in both cases; that is, the initial switching voltages, which are relatively high at first, eventually give way to lower and more stable values. It can also be seen that after approximately sixty switching cycles V_{TH} has only about 2 or 3 percent fluctuation for the low current case (Fig. 5.5), whereas for the high current case (Fig. 5.6) the fluctuation in V_{TH} approaches about 6 percent of the average value of 420 V. Furthermore, the holding currents for the lower current case are considerably less than that for the high current case. In both cases, however, the region having consistent V_{TH} is always associated with the highest average value of I_H. This is a significant observation and will be further discussed shortly.

Figs. 5.7 and 5.8 are similar to Figs. 5.5 and 5.6 but correspond to a switching rate of 4 cycles/min. Again the initial threshold voltage during the first few switching cycles is higher than the threshold voltage measured after a number of cycles. Also, the fluctuations in V_{TH} and I_H are much more dramatic for the case of higher currents than those for lower currents. The most stable region of switching occurs after approximately forty or fifty switching cycles, and this is associated with the highest average holding currents.

The above results indicate that a field induced thermal mechanism may be the principal cause of switching for the amorphous material used. It has been speculated that the applied field initiates a localized

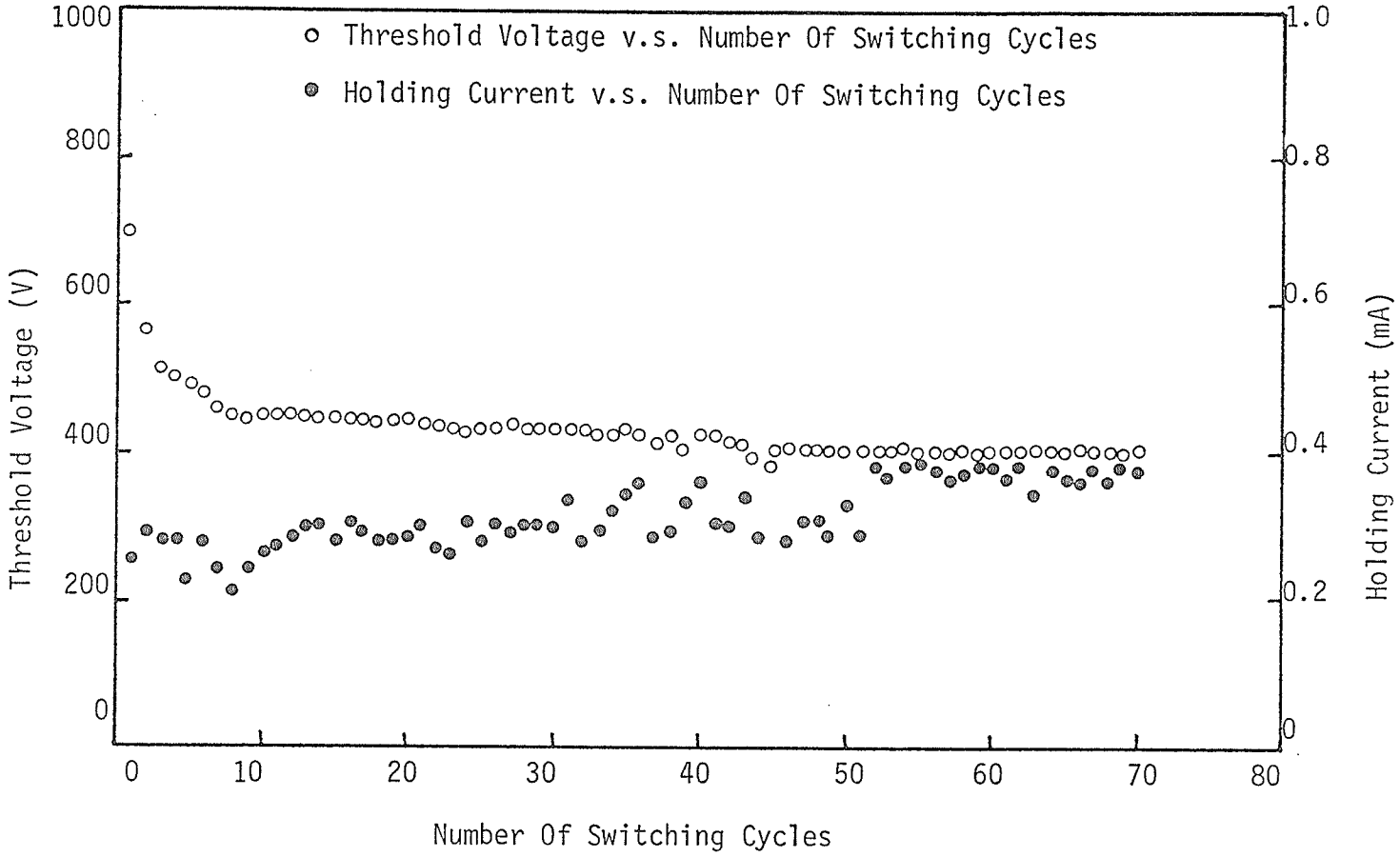

Fig. 5.7. The switching threshold voltage and holding current as functions of the number of switching cycles with a switching rate of 4 cycles/min and a current limiting resistance of 500 KΩ.

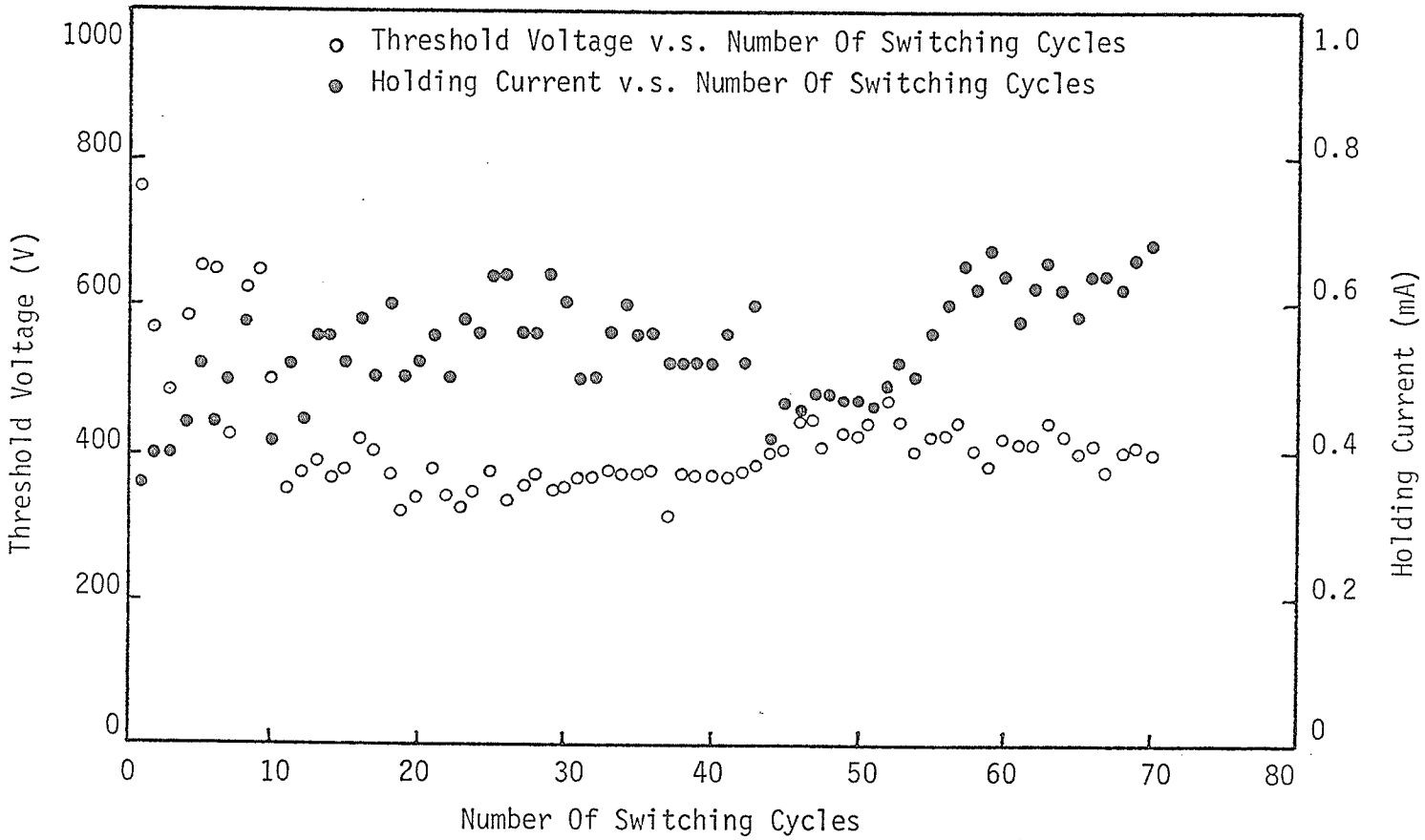

Fig. 5.8. The threshold voltage and holding current as functions of the number of switching cycles with a switching cycle rate of 4 cycles/min and a current limiting resistance of 250 KΩ.

filamentary region of high conductivity between the two electrodes, and in fact, such filaments have been observed by several investigators (Dearnaley et al. 1970, Stocker et al. 1970, Pearson and Miller 1969). Once a high conductivity filament has advanced from one electrode to the opposite electrode the low conductivity blocking state of the device collapses and current breakthrough occurs. In ordinary threshold switching the filament is maintained provided that the operating current is above I_H. Once the operating current falls below I_H the filament is removed and the blocking or low conductivity state returns. The mechanisms of filament formation and removal will be discussed in subsequent sections.

Based on the model of filament formation it is likely that the initial high values of threshold voltage correspond to the initial formation of filamentary paths between electrodes, and that the instability in V_{TH} is due to the formation of separate and distinct filamentary paths for the first few switching cycles, as well as the continuous cross-sectional growth of filaments when switching occurs along the same paths. Eventually, however, after a number of switching cycles, filamentary paths would tend to become fairly well established and subsequent switching would take place only along these paths. Also, cross sectional growth of filaments would eventually reach a steady state limiting condition which is possibly governed by the composition of the amorphous material, and the heat dissipation of the device. Thus, the random variations in V_{TH} are due to the random production of different filamentary paths, and the gradual stabilization of V_{TH} coincides with the ultimate tendency of filaments to grow along the same paths and the limiting constraints placed on the cross-sectional growth of filaments.

It is possible that higher current is more effective in initiating a greater number of conduction paths, and each new path has a somewhat different threshold voltage, thus resulting in a greater degree of instability. Furthermore, higher current may be more effective in disrupting or reorganizing already existing stable paths, and may also tend to accelerate cross-sectional filament growth which acts to offset, at least to some degree, the other causes of greater instability. All these processes would result in a gradual change towards more stable switching.

It has been noted that the most stable region of threshold voltage coincides with the region of highest holding current. As already mentioned the stable region of V_{TH} is due to the formation of well established switching paths within the amorphous material. These switching paths would have the maximum permissible cross-sectional diameter, depending on material composition, device configuration, and maximum current levels. As a result, a current higher than a certain critical value is required to maintain the filaments in the stable region. On the other hand, filaments which are not well defined and have a very small cross-sectional area, corresponding to unstable switching, would not require much energy to maintain them and would therefore have smaller holding currents.

5.3 THE EFFECTS OF LONG-TERM CONTINUOUS SWITCHING ON THE PROPERTIES OF THRESHOLD DEVICES

Fig. 5.9 shows the general tendency of V_{TH} towards lower values when the number of switching cycles is increased. Curve A corresponds to the results obtained for a device which was switched at a peak current of 1mA

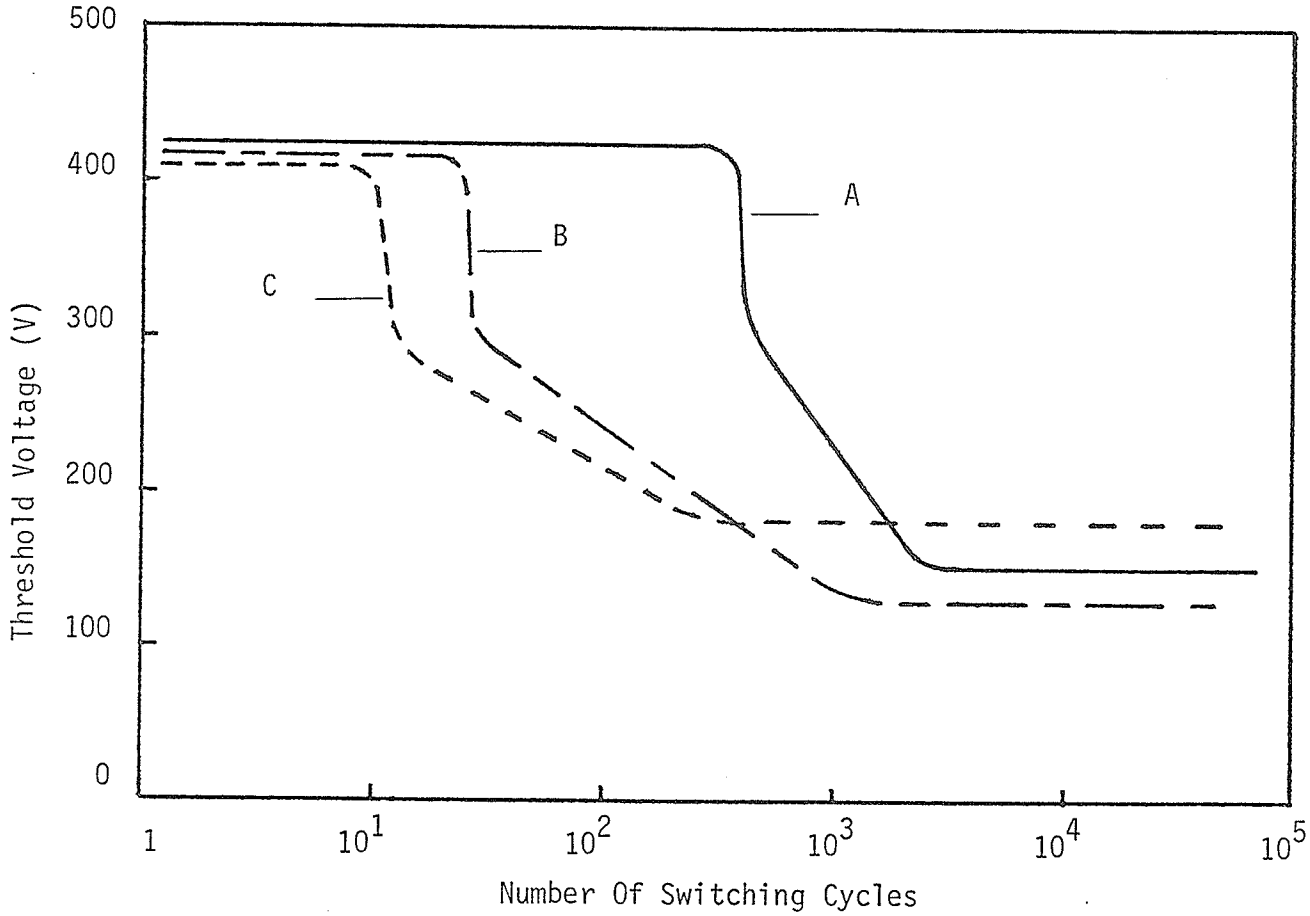

Fig. 5.9. The effect of long-term continuous switching on the threshold voltage for three amorphous devices. Curve A corresponds to a maximum current of 1 mA at V_{TH} = 425 V, curve B corresponds to a maximum current of 5 mA at V_{TH} = 416 V, and curve C corresponds to a maximum current of 10 mA at V_{TH} = 410 V.

for an initial stable threshold voltage of 425 V; curve B corresponds to the results obtained for a device which was switched at a peak current of 5 mA at its initial stable threshold voltage of 416 V; and curve C is for a device operated at 10 mA peak current for an initial stable threshold voltage of 410 V. All three devices gave similar results. The initial region of stability persists for a larger number of switching cycles when lower operating currents are used. For example, with a peak current of 1 mA at V_{TH} = 425 V (curve A) the initial stabilized threshold voltage persisted for about 400 cycles. On the other hand, with a peak current of 10 mA at V_{TH} = 410 V (curve C) the initial stable threshold voltage persisted for only the first 10 cycles, after which a transition towards lower V_{TH} commenced. The actual regions of decreasing V_{TH} seemed to vary in a somewhat random fashion. However, it seems likely that the actual transition towards lower V_{TH} occurs more rapidly when higher currents are used.

The three curves in Fig. 5.9 show only the general trend of V_{TH} with the number of switching cycles, but give no indication of variations in V_{TH} in the various intervals. The general tendency is towards greater variations in V_{TH} for higher peak currents. This is seen not only in the regions of decreasing V_{TH}, but also after many thousands of cycles when the general decreasing trend of V_{TH} has ceased. Fig. 5.10 shows the final switching behaviour of two devices after approximately 10,000 switching cycles. Each line represents an actual switching cycle and the maximum height of any given line gives the value of V_{TH} for that cycle. Fig. 5.10 (a) is for the device operated at low current levels (1 mA at V_{TH} = 425 V), and Fig. 5.10 (b) is for the device operated at higher current levels (10 mA at V_{TH} = 410 V).

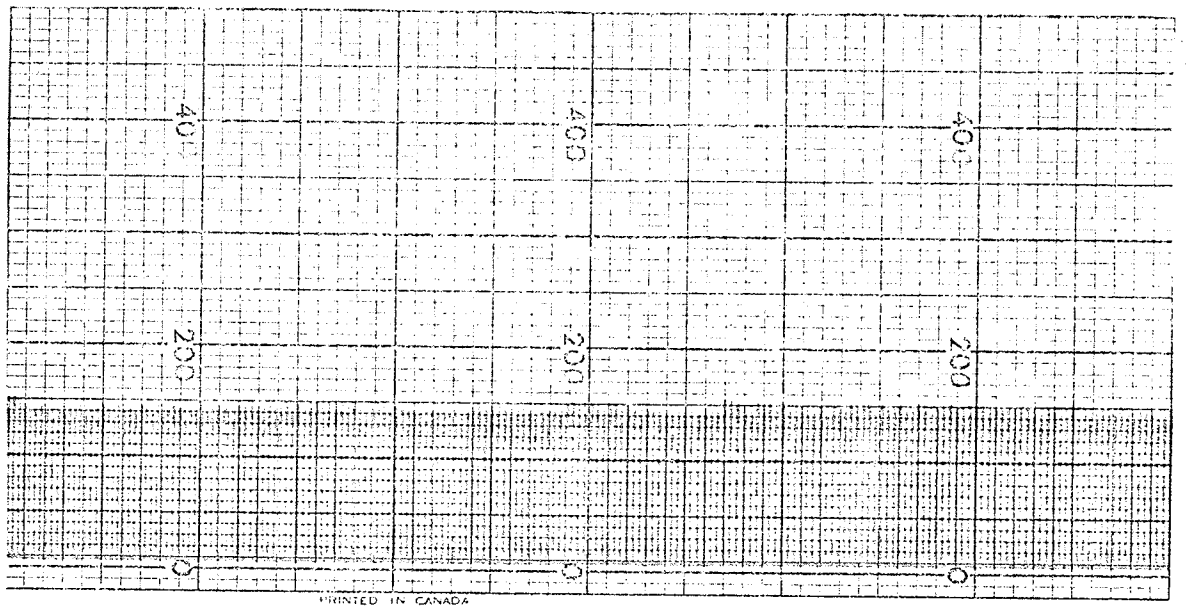

(a)

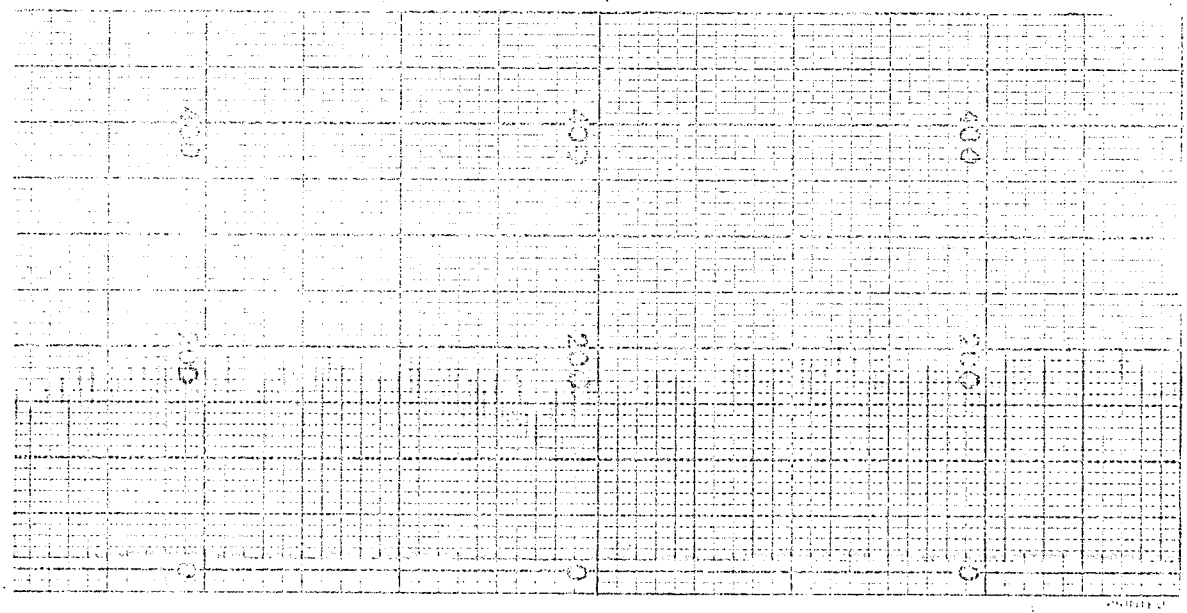

(b)

Fig. 5.10. The switching behaviour of two devices after approximately 10,000 switching cycles with a switching rate of 15 cycles/min.
(a) Low current case (1 mA at V_{TH} = 425 V).
(b) High current case (10 mA at V_{TH} = 410 V).
Scale: horiz. 2 min/in; vert. 10 V/div.

In general the lower the current used, the higher is the degree of stabiltiy.

In most cases the variations in V_{TH} are less than about 5% of its average value. However, if high current is used variations in V_{TH} approaching 50% are not uncommon.

5.4 THE EFFECT OF PEAK CURRENT ON THE DURABILITY OF THRESHOLD SWITCHES

The main objective here is to determine the maximum permissible current level which can be used without causing appreciable variations in the threshold voltage. The effects of peak operating current on V_{TH} and I_H are given in Figs. 5.11 and 5.12, respectively. Three devices having an initial stable threshold voltage of 450 V, 425 V, and 400 V were used in the investigations. Each point on the various curves corresponds to an individual switching cycle at a predetermined value of peak current, determined by the previous value of V_{TH}.

Fig. 5.11 gives the variation of V_{TH} with increasing peak current. In all three devicesthere is little change in V_{TH} until a peak current of 18 mA is reached. If the current is allowed to increase above the 18 mA level the threshold voltage decreases and eventually the device becomes completely deteriorated. For the results given in Figs. 5.11 and 5.12 each device was switched only once for each of the current values indicated. It should be pointed out, however, that the device could also become deteriorated if it is switched continuously at a current approaching, but not exceeding 18 mA.

Fig. 5.12 shows the variation of holding current, I_H, with peak operating current. There is a general increase in I_H with peak current until

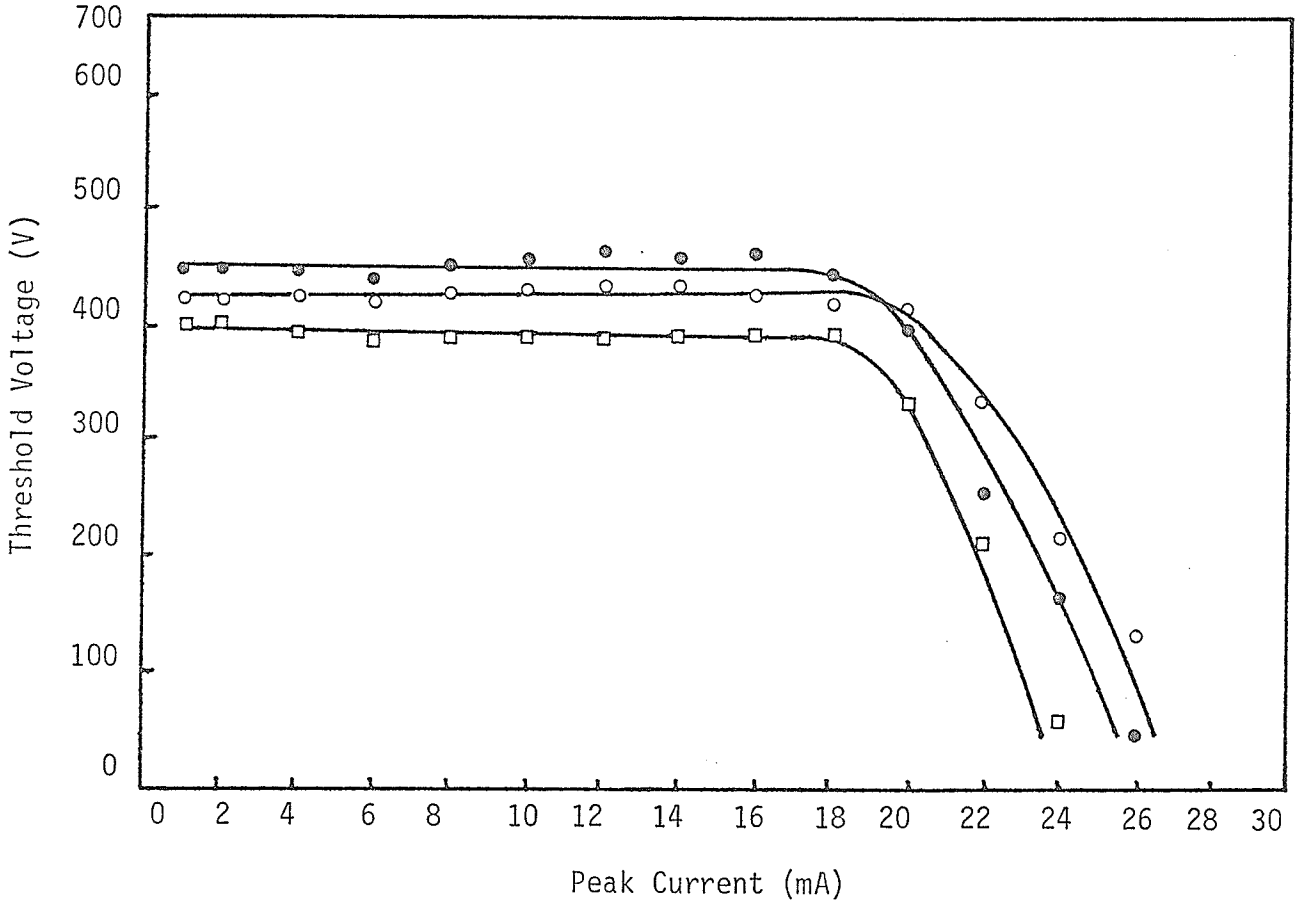

Fig. 5.11. The effect of peak current on the threshold voltage for three devices. Each point corresponds to a new switching cycle with an appropiate value of current limiting resistance determined by the previous value of V_{TH}.

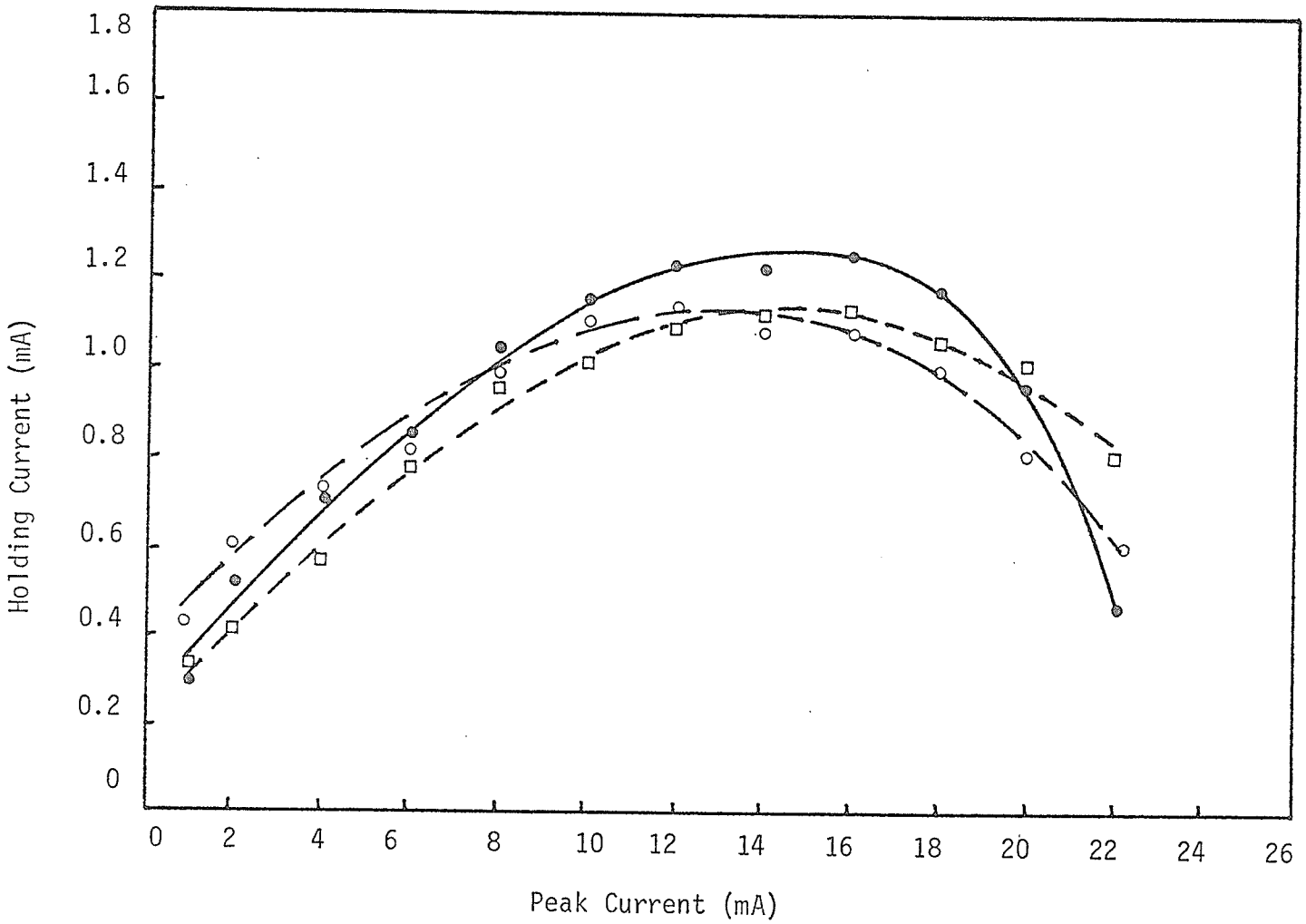

Fig. 5.12. The effect of peak current on the holding current.

a peak current of about 15 mA is approached, beyond which the dependence begins to diminish. A steep decrease in the holding current occurs for operating currents in excess of 18 mA, and this can be taken as the onset of device deterioration. It can also be seen that at peak operating currents of 12 or 14 mA a holding current of over 1 mA is required, which is considerably higher than the normal values between 0.3 mA and 0.7 mA.

These results seem to be consistent with the model of filament growth leading to switching as discussed previously. In particular, a single switching cycle at a peak current in excess of approximately 18 mA seems to be sufficient to alter the stable conditions of filament formation created after the first period of unstable switching. It has been postulated in previous sections of this chapter that stable switching corresponds to switching along a single preferred path, and also to the limiting conditions of cross-sectional filament growth. A peak current of 18 mA with a decay time of about 18 mA/sec (as determined from circuit parameters) could possibly result in a sequence of transformations in the filamentary conduction path and therefore cause appreciable variations in V_{TH} as seen in Fig. 5.11. For example a current of 18 mA may be sufficient to change the limiting conditions imposed on cross-sectional expansion of the conducting region. Also, it is quite conceivable that at sufficiently high current levels even a very short current duration may be sufficient to impart enough energy to the filament path to cause permanent structural rearrangement of component atoms towards a greater degree of order (or crystalline structure) along the filament path. This would invariably lead to a reduced switching voltage, and ultimately the switching property itself would be completely deteriorated.

5.5 MEMORY BEHAVIOUR OF THRESHOLD DEVICES IN THE Te-As-Si-Ge SYSTEM

The memory phenomenon has been attributed to the formation of a high conductivity material filament between electrodes (Ovshinsky 1967, Uttecht et al. 1970). This filament represents a stable and permanent reordering of component atoms along the filament path, whereas the filaments which cause ordinary threshold switching are temporary and can be disrupted by allowing the current to fall below I_H. Based on this important difference between memory filaments and ordinary switching filaments, it is reasonable to predict that amorphous compositions which are capable of undergoing structural transitions towards a greater long range order, and finally a crystalline structure, are more suitable for memory devices. The composition $Te_{48}\ As_{30}\ Si_{12}\ Ge_{10}$ has been investigated by Bagley and Bair (1970) in an attempt to correlate structural transformations with thermal energy. The results of differential scanning calorimetry clearly indicate that the transitions towards a crystalline structure do not occur for this composition even for temperatures as high as 490^{o} C. This indicates that this composition is ideal for threshold devices but not suitable for memory devices.

Although it is believed that memory based on the formation of permanent high conductivity filaments would not occur in $Te_{48}\ As_{30}\ Si_{12}\ Ge_{10}$, Phillips et al. (1970) have reported that a permanent state of high conductivity can be achieved for this composition at temperatures of about 300^{o} C. Furthermore Bagley and Bair (1970) have actually observed the memory behaviour in this amorphous material even though their analysis indicate that crystallization does not take place up to a temperature of 490^{o} C.

It has been found from the present investigation that a memory state for this composition is possible if sufficient energy is supplied to initiate a permanent memory filament. The results presented in Fig. 5.13 show the current magnitude and current duration required to obtain the memory state for devices having holding currents of .3 mA and .5 mA at the operating current of 1 mA. These curves actually show minimum energy required to induce the memory state which may be estimated from the simple relation

$$E = I^2 R_{ON} \tau \ , \qquad (5\text{-}1)$$

where I is the current, τ is the current duration, and R_{ON} is the resistance of the device in the "ON" state. From the curves of Fig. 5.13, and using a typical value of 10^3 Ω for the resistance in the "ON" state (the normal range is between 10^2 Ω and 10^3 Ω), the required energy appears to be of the order of 0.03 Joules. Variations from this value may be attributed to the different values in R_{ON} for different operating currents. These results indicate that memory may be achieved over a range of currents and duration times, lower currents requiring longer current duration and vice versa. All three curves tend to approach the holding current levels very slowly , in a somewhat asymptotic fashion. A number of devices were maintained in their conducting state at their I_H value for a period of several hours and did not exhibit memory. Thus, if finite current durations are used, then current levels considerably higher than I_H are necessary to obtain memory. This may be due to the fact that at lower current levels the minimum energy requirements for memory to occur can not be easily reached because of constant energy losses to the surrounding medium.

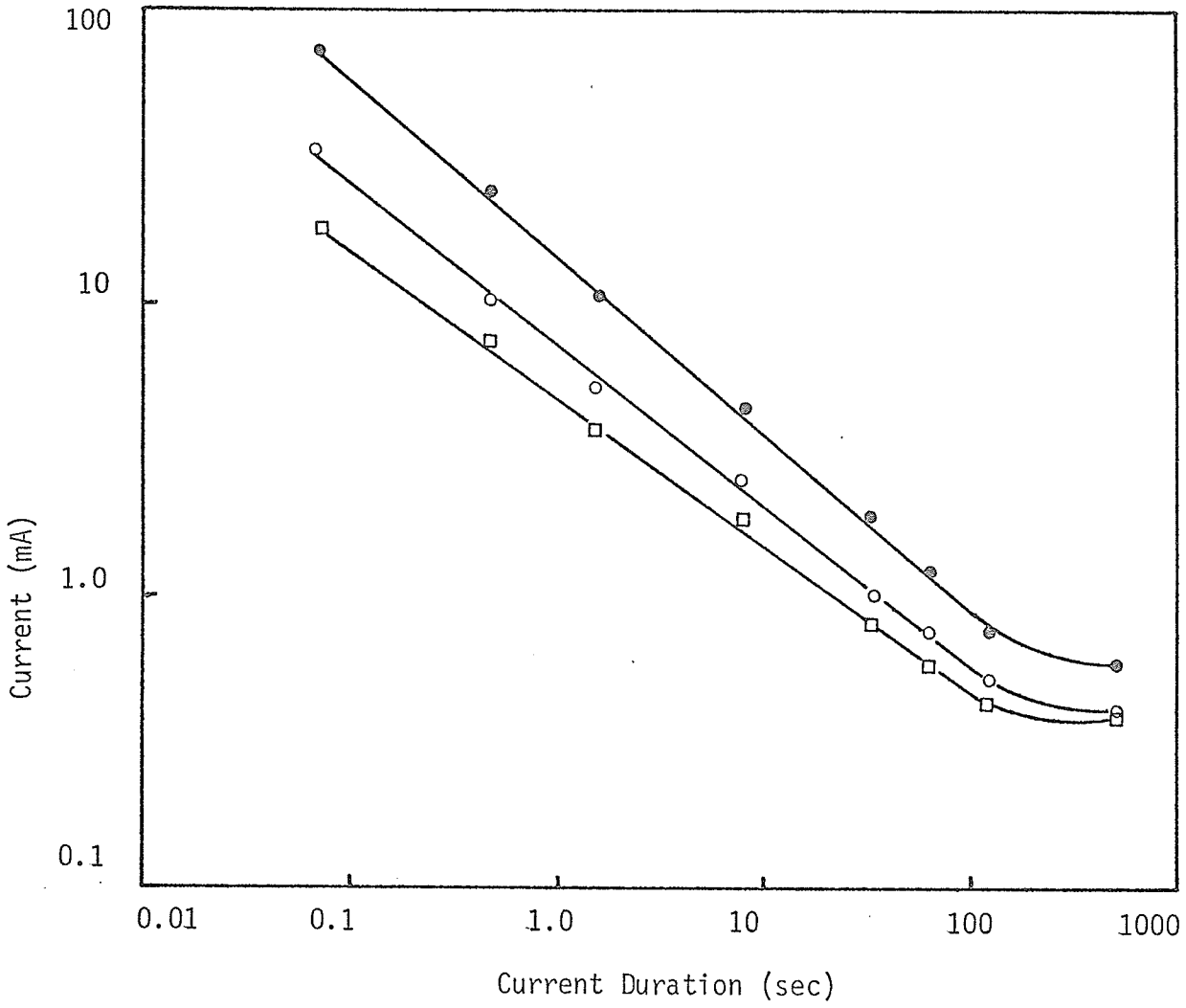

Fig. 5.13. Current as a function of current duration required to induce memory in three devices. The two lower curves correspond to devices with a holding current of .3 mA and the upper curve corresponds to a device with a holding current of .5 mA (at threshold voltage with a peak current of approximately 1 mA).

On the basis of the experimental results which have been presented, the model of filamentary transitions in amorphous semiconductors, and in particular the composition Te_{48} As_{30} Si_{12} Ge_{10}, may have to be modified. In particular, if this composition is highly stable in its amorphous state, and if a temperature in excess of 500^{o} C is required to introduce a reordering towards crystallinity, then ordinary threshold switching, as well as memory switching, would not be possible, since, in both cases, the present model assumes a reordering of component atoms along the filament path. A possible explanation for the observed switching and memory characteristics for this composition could, however, be formulated within the framework of the filamentary model. It is possible that the localized electric field and high-temperature region which exist as a result of the applied voltage, may cause a general diffusion of certain constituent atoms away from the high-field and high-temperature region, and other atoms towards this region. The result would be the formation of a filament which consists of atoms in concentration considerably different from the original bulk material. The implication is that the new concentration of constituent atoms along the filament tends to favour structural changes towards a crystalline structure whereas the original compostion may not. Another important possibliity, which is based on the above argument, is that both threshold switching and memory switching for this material involve the same basic processes of filamentary formation, the difference being only in the degree of changes in component concentrations and the physical extent of the filamentary region. This explains why it is possible to obtain both threshold switching and memory switching in the same material.

A number of papers which have appeared in recent literature tend to give strong support to the theory describe above. Deneufville (1972) has investigated the structural properties of the ternary system Te-As-Si and has concluded that most of these glasses are very stable, showing little tendency to crystallize when heated to temperatures in excess of their glass transition point. The work of Savage (1972) has shown that ternary systems of the type Te-As-X, in which X may be B, Al, P, Ga, In, Tl, or Ge, would exhibit single metastable crystallization with transition temperatures of less than 200^{o} C, but the Te-As-Si system shows no tendency towards crystallization for temperatures as high as 500^{o} C, in agreement with the results of Deneufville (1972). In particular, the Te-As-Si system constitutes a highly stable structure in the amorphous form, whereas the Te-As-Ge system tends to revert back to the crystalline structure much more readily. It is therefore highly possible that both switching and memory in $Te_{48}\ As_{30}\ Si_{12}\ Ge_{10}$ involve the diffusion of Si atoms away from the filamentary region thus leaving a filament of composition which favours the crystalline structure, the necessary transition being brought about by Joule heating along the filament path resulting from energy dissipation due to the applied field.

5.6 THE EFFECTS OF TEMPERATURE ON ELECTRICAL SWITCHING PROPERTIES

The switching characteristics of several devices were studied for a temperature range from 100^{o} C to -50^{o} C to determine the effect of temperature on the switching threshold voltage. The results are shown in Fig. 5.14. V_{TH} is highly sensitive to ambient temperature below 0^{o} C,

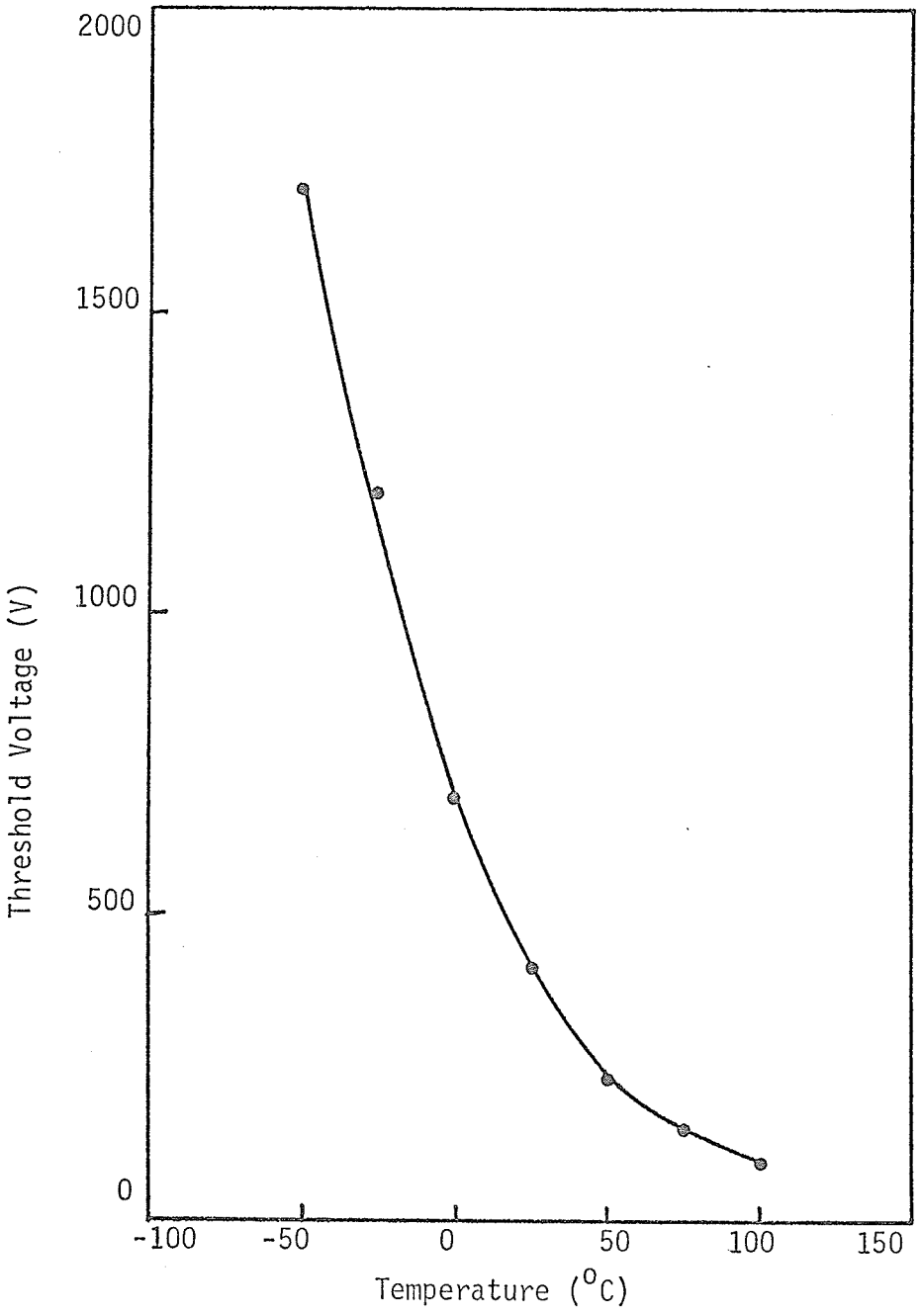

Fig. 5.14. Variation of switching threshold voltage with temperature.

with a decrease of 1^{o} C resulting in an increase in V_{TH} of approximately 20 V in this temperature region. The temperature dependence decreases for temperatures in excess of about 50^{o} C however, where an increase of 1^{o} C results in a decrease in V_{TH} of about 3 V. These results support the model that filament formation is due to Joule heating along discrete paths between electrodes. It would seem reasonable to expect that variations in ambient temperature should have a direct and pronounced effect on the production of high conductivity filaments. In particular, higher temperatures tend to favour the processes of reorganization of constituent atoms towards a greater long range order. This explains why higher temperatures result in lower values of switching threshold voltage.

CHAPTER 6

CONCLUSIONS

On the basis of the results given in chapter 5, the following conclusions are drawn:

6.1 SWITCHING PROPERTIES

(a) Electrical switching in the amorphous covalent alloy $Te_{48}\ As_{30}\ Si_{12}\ Ge_{10}$ involves a transition from a state of low conductivity to a state of high conductivity with a difference in conductivity as high as 10^5 υ between the two states.

(b) The transition from a state of low conductivity to a state of high conductivity in devices having 100 μm of active switching material occurs in about 100 n sec and is independent of voltage rise time.

(c) The initial switching behaviour of new devices is characterized by high threshold voltages which are unstable and somewhat unpredictable for the first forty or fifty switching cycles.

(d) The instability in threshold voltage is due to the initial formation of unstable conducting filaments, and the stabilization of the threshold voltage can be considered to correspond to switching along established paths, and the approach of steady state limitations for filament cross-sectional growth.

(e) Higher operating currents result in a greater degree of

instability in the threshold voltage, both initially and after many thousands of switching cycles, whereas lower operating currents result in very stable switching voltages.

(f) The regions of most stable threshold voltages is associated with highest average holding current.

(g) Devices operated for many thousands of switching cycles may display more than one region of stable switching, each subsequent stable region having a lower characteristic threshold voltage.

(h) Higher operating currents are more effective in producing stable filaments, but they are also more effective in disrupting filaments which have attained stability.

(i) The durability of threshold switches depends on the peak operating current; low current results in stable operation for many thousands of switching cycles whereas higher currents result in rapid deterioration of the device.

(j) The switching threshold voltage is strongly dependent on ambient temperature, an increase in temperature resulting in a decrease in V_{TH}. This phenomenon favours the thermal mechanism for switching.

6.2 MEMORY PROPERTIES

(a) The amorphous composition $Te_{48}\ As_{30}\ Si_{12}\ Ge_{10}$ displays memory behaviour if the input energy from the applied field exceeds a certain minimum value. The energy required to induce memory for the devices under investigation is about .03 Joules.

(b) The fact that both switching and memory behaviour is possible in the same material suggests that both properties involve the same basic mechanisms of filament formation, the only difference being the degree of stability of the conducting filaments. That is, memory will result provided the filament produced by the initial switching action is stable enough to persist even with complete removal of the applied voltage.

(c) In order for memory to occur the conducting filament must have a certain minimum cross-sectional area not only at the central regions of the active amorphous material, but also at the two semiconductor-electrode contacts.

(d) Both switching and memory in $Te_{48}\ As_{30}\ Si_{12}\ Ge_{10}$ are due to the diffusion of certain atoms away from the filament and certain other atoms towards the filament. Based on the fact that certain amorphous compositions require less energy to recrystallize than other compositions, it is likely that switching and in particular memory for the composition $Te_{48}\ As_{30}\ Si_{12}\ Ge_{10}$ involves the active transport of Si atoms away from the filamentary region, and the transport of the other constituents into the filamentary region. Thus, the major composition of the conducting filament consists of Te-As-Ge, and Si contributes a very minor proportion of the total concentration in this filament.

The major outcome of the work presented in this thesis has been the formulation of several new ideas which further clarify the theory of the switching behaviour of amorphous semiconductors. The most promising area of research in this field, both from the scientific and technological points of view, lies in the systematic analysis of the physical and chemical nature of the conducting filaments which are believed to be re-

sponsible for the switching and memory phenomena. With this in mind it is suggested that experiments involving electron-microscopy and X-ray diffraction could provide further information about the nature of conducting filaments. To understand the mechanisms responsible for all phenomena observed in amorphous materials is of great importance to the technical development of this field.

REFERENCES

Adler, D., Franz, J.M., Hewes, C.R., Kraemer, B.P., Sellmyer, D.J., and Senturia, S.A., "Transport property of a memory-type chalcogenide glass", J. Non-Crystalline Solids, 4, 330 (1970).

Allgaier, R.S., A note on the temperature dependence of the electrical conductivity in amorphous semiconductor", J. Non-Crystalline Solids, 6, 240 (1971).

Amitay, M., and Pollak, M., "An experimental investigation of the Hall effect in the hopping region", Int. Conf. Phys. Semicond., J. Phys. Soc. Japan, Supplement 21, 549 (1966).

Anderson, P.W., "Absence of diffusion in certain random lattices", Phys. Rev., 109, 1492 (1958).

Anderson, P.W., "Localized magnetic states in metals", Ibid., 124, 41 (1961).

Anderson, P.W., "Theory of magnetic exchange interactions: Exchange in insulators and semiconductors", Solid St. Phys., 14, 99 (1963).

Bagley, B.C., and Bair, H.E., "Thermally induced transformations in glassy chalcogenides", J. Non-Crystalline Solids, 2, 155 (1970).

Banyai, L., "On the Theory of Electronic Conduction in Amorphous Semiconductors", Phsique des Semiconducteurs, (Paris: Dunod), p. 417 (1964).

Banyai, L., and Aldea, A., "Theory of the Hall effect in disordered systems: Impurity-band conduction", Phys. Rev., 143, 652 (1966).

Böer, K.W., Döhler, G., and Ovshinksy, S.R., "Time delay for reversible electric switching in semiconducting glasses", J. Non-Crystalline Solids, 4, 573 (1970).

Böer, K.W., "Carrier mobility in highly disordered structures", J. Non-Crystalline Solids, 4, 583 (1970).

Böer, K.W., "The electrical conduction mechanisms in highly disordered semiconductors", J. Non-Crystalline Solids, 2, 444 (1970).

Cervinka, L., Hrubý, A., Matyás, M., Simecek, J., Stourac, L., Tauc, J., and Vorlícek, V., "The structure and electronic properties of semiconducting glassses based on Cd As_2", J. Non-Crystalline Solids, 4, 258 (1970).

Cohen, M.H., Fritzsche, H., and Ovshinsky, S.R., "Simple band model for amorphous semiconducting alloys", Phys. Rev. Letter, 22, 1065 (1969).

Cohen, M.H., "Review of the theory of amorphous semiconductors", J. None-Crystalline Solids, 4, 391 (1970).

Cohen, M.H., "Electronic structure and transport in covalent amorphous semiconducting alloys", J. Non-Crystalline Solids, 2, 432 (1970).

Collins, F.M., "Switching by thermal avalanche in semiconducting glass films", J. Non-Crystalline Solids, 2, 491 (1970).

Conwell, E.M., "Theory of impurity scattering in semiconductors", Phys. Rev., 77, 388 (1950).

Conwell, E.M., "Impurity band conduction in germanium and silicon", Phys. Rev., 103, 51 (1956).

Coward, L.A., "Experimental evidence of filament forming in non-crystalline chalcogenide alloy threshold switches", J. Non-Crystalline Solids, 6, 107 (1971).

Croitorw, N., Vescan, L., Popescw, C., Lazarescu, M., "Non-ohmic properties of some amorphous semicondutors", J. Non-Crystalline Solids, 4, 493 (1970).

Csillag, A., and Jäger, H., "Energy-controlled switching process in the amorphous system Te-As-Si-Ge", J. Non-Crystalline Solids, 2, 133 (1970).

Day, G., "Estimate of the conductivity of a one-dimensional disordered chain", Proc. Phys. Soc., 87, 223 (1966).

Deis, D.W., Dancy, E.A., and Patterson, A., "On the switching characteristics and the bulk properties of chalcogenide glasses", J. Non-Crystalline Solids, 2, 141 (1970).

Deneufville, J.P., "Chemical aspects of glass formation in tellwide systems", J. Non-Crystalline Solids, 8-10, 85 (1972).

Dingle, R.B., "Scattering of electrons and holes by charged donors and acceptors in semiconductors", Phil. Mag., 46, 831 (1955).

Eckenbach, W., Fuhs, W., and Stuke, of., "Preparation and electrical properties of amorphous InSb", J. Non-Crystalline Solids, 5, 264 (1971).

Edwards, S.F., "The electronic structure of disordered systems", Ibid., 6, 617 (1961).

Evans, E.J., Helbers, J.H., and Ovshinsky, S.R., "Reversible conductivity transformations in chalcogenide alloy films", J. Non-Crystelline Solids, 2, 334 (1970).

Fagen, E.A., and Fritzsche, H., "Electrical conductivity of amorphous chalcogenide alloy films", J. Non-Crystalline Solids, 2, 170 (1970).

Fagen, E.A., and Fritzsche, H., "Optical properties of amorphous chalcognide alloy films", J. Non-Crystalline Solids, 2, 180 (1970).

Feinleib, J., and Paul, W., "Semiconductor to metal transitions in $V_2 O_3$", Physics of Solids at High Pressures", edited by C.T. Tomizuka and R.M. Emrick (New York: Academic Press), p. 571 (1965).

Feldman, C., and Moorjani, K., "Switching in elemental amorphous semiconductors", J. Non-Crystalline Solids, 2, 82 (1970).

Frisch, H.L., and Lloyd, A.P., "Electron levels in a one-dimensional random lattice", Phys. Rev., 120, 1175 (1960).

Fritzsche, H., "Resistivity and Hall coefficient of antimony-doped germanium at low temperatures", J.Phys. Chem. Solids, 6, 69 (1958).

Fritzsche, H., "Piezoresistance of n-type germanium", Phys. Rev., 115, 336 (1959).

Fritzsche, H., "Effect of shear on impurity conduction in n-type germanium", Ibid, 119, 1899 (1960).

Fritzsche, H., and Ovshinksy, S.R., "Electronic conduction in amorphous semiconductors and the physics of the switching phenomena", J. Non-Crystalline Solids, 2, 393 (1970).

Fritzsche, H., "Optical and electrical energy gaps in amorphous semiconductors", J. Non-Crystalline Solids, 6, 240 (1971).

Fröhlich, H., "On the theory of dielectric breakdown in sokids", Proc. R. Soc. A, 188, 521 (1947).

Goswami, A.K., "Switching mechanism in amorphous semiconductors", J. Non-Crystalline Solids, 2, 205 (1970).

Greenwood, D.A., "The Boltzmann equation in the theory of electrical conduction in metals", Proc. Phys. Soc., 71, 585 (1958).

Grigorovici, R., Croitow, N., Dévényi, A., and Teleman, E., "Band structure and electrical conductivity in amorphous germanium", Physique des semiconducteurs, (Pairs: Dunod), p. 423 (1964).

Hartke, J.L., "Drift mobilities of electrons and holes and space-charge-limited currents in amorphous selenium films", Phys. Rev., 125, 1177 (1962).

Henisch, H.K., Fagen, E.A., and Ovshinsky, S.R., "A qualitative theory of electrical switching processes in monostable amorphous structures", J. Non-Crystalline Solids, 4, 538 (1970).

Hindley, N.K., "Random phase model of amorphous semiconductors. I. Transport and optical properties", J. Non-Crystalline Solids, 5, 17 (1971).

Hindley, N.K., "Random phase model of amorphous semiconductors. II. Hot electrons", J. Non-Crystalline Solids, 5, 31 (1971).

Hindley, N.K., "Avalanche ionization in amorphous semiconductors", J. Non-Crystalline Solids, 8-10, 557 (1972).

Hirsch, J., "A simple ambipolar model for the electron-bombardment induced conductivity in amorphous arsenic trissulphide", J. Phys. Chem. Solids, 27, 1385 (1966).

Holstein, T., "Studies of polaron motion. II. The "small" polaron", Ann. Phys., 8, 343 (1959).

Holstein, T., "Hall effect in impurity conduction", Phys. Rev., 124, 1329 (1961).

Hori, J., "Phase theory of disordered systems", Prog. Theor. Phys., Suppl. No. 36, 3 (1966).

Hung, C.A., "Theory of resistivity and Hall effect at very low temperatures", Phys. Rev., 79, 727 (1950).

Hung, C.A., and Gleissman, J.R., The resistivity and Hall effect of germanium at low temperatures", Phys. Rev., 79, 726 (1950).

Joffe, A.F., and Regel, A.R., "Non-crystalline, amorphous and liquid electronic semiconductors", Prog. Semicond., 4, 237 (1960).

James, H.M., and Ginzbarg, A.S., "Band structure in disordered alloys and impurity semiconductors", J. Phys. Chem., 57, 840 (1953).

Jones, H., "Electrons in nearly periodic fields", Proc. R. Soc. A, 294, 405 (1966).

Kanamori, J., A Electron correlation and ferromagnetism of transition metals", Prog. Theor. Phys., 30, 275 (1963).

Kasuya, T., "A theory of impurity ocnduction, I", J. Phys. Soc. Japan, 13, 1096 (1958).

Kasuya, T., and Koide, S., "A theory of impurity conduction, II", J. Phys. Soc. Japan, 13, 1287 (1958).

Kerr, J.T., "Current-voltage characteristics of chalcogenide glass films", J. Non-Crystelline Solids, 2, 203 (1970).

Kohn, W., "Theory of the insulating state", Phys. Rev., 133, 171 (1964).

Kolomiets, B.T., "Vitreous semiconductors I", Phys. Stat. Sol., 7, 359 (1964).

Kolomiets, B.T., "Vitreous semiconductors II", Ibid., 713 (1964).

Kolomiets, B.T., and Mazets, T.F., "The thermally stimulated conductivity in vitreous and crystalline As_2 Se_3",J. Non-Crystalline Solids, 3, 46 (1970).

Kubo, R., "A general expression for the conductivity tensor", Can. J. Phys., 34, 1274 (1956).

Landauer, R., and Helland, J.C., "Electronic structure of disordered one-dimensional chains", J. Chem. Phys., 22, 1655 (1954).

Lampert, M.A., "Injection currents in insulators", Proc. Inst. Radio Engrs (USA), 50, 1781 (1962).

Lampert, M.A., "Volume-controlled current injection in insulators", Rep.-Progr. Phys. (GB), 27, 329 (1964).

Lax, M., and Phillips, J.C., "One-dimensional impurity bands", Phys. Rev., 110, 41 (1958).

Lifshitz, T.M., "The energy spectrum of disordered systems", Adv. Phys., 13, 483 (1964).

Lucas, T., "Interpretation of the switching effect in amorphous semiconductors as a recombination instability", J. Non-Crystalline Solids, 6, 136 (1971).

Mahan, G.D., "Mobility of polarons", Phys. Rev., 142, 366 (1966).

Mackenzie, J.D., "Electronic conduction in non-crystalline solids", J. Non-Crystalline Solids", 2, 16 (1970).

Mattis, D.C., and Landovitz, L.F., "New aspects of polyconductivity", J. Non-Crystalline Solids, 2, 454 (1970).

Miller, A., and Abrahams, E., "Impurity conduction at low concentrations", Phys. Rev. A., 120, 745 (1960).

Miller, A., and Abrahams, E., "Impurity conduction at low concentrations", Int. Conf. Semicond. Phys. (Prague, Czechoslovak Academy of Sciences), p. 218 (1961).

Minami, T., Hattori, M., Nakamachi, F., and Tanaka, M., "Bond structural approach to electrical conduction in vitreous semiconductors in the system Te-As-S", J. Non-Crystalline Solids, 3, 327 (1970).

Mott, N.F., "On the transition to mettalic conduction in semiconductors", Can. J. Phys., 34, 1356 (1956).

Mott, N.F., "The transition to the metallic state", Phil. Maj., 6, 287 (1961).

Mott, N.F., "Electrons in transition metals", Adv. Phys., 13, 325 (1964).

Mott, N.F., and Allgaier, R.S., "Localized states in disordered lattices", Phys. Stat. Sol., 21, 343 (1967).

Mott, N.F., and Tovose, W.D., "The theory of impurity conduction", Adv. Phys., 10, 107 (1961).

Mott, N.F., "Conduction in glasses containing transition metal ions", J. Non-Crystalline Solids, 1, 1 (1968).

Mott, N.F., and Davis, E.A., "Electronic Processes in Non-Crystalline Materials", Clarendon Press: Oxford, (1971).

Nagels, P., Callocerts, R., Denayer, M., and DeConinck, R., "Electrical properties of vitreous Tl_2 Te · As_2 Te_3", J. Non-Crystalline Solids, 4, 295 (1970).

Neale, R.G., "Device structures and fabrication techniques for amorphous semiconductor switching devices", J. Non-Crystalline Solids, 2, 558 (1970).

Nelson, D.L., "Ovonic device applications", J. Non-Crystalline Solids, 2, 528 (1970).

Ovshinsky, S.R., "Reversible electrical switching phenomena in disordered structures", Phys. Rev. Letters, 21, 1450 (1968).

Ovshinsky, S.R., "Amorphous semiconductors", Sci. J. , 5, 73 (1969).

Ovshinsky, S.R., "An introduction to ovonic research", "J. Non-Crystalline Solids, 2, 99 (1970).

Owen, A.E., and Robertson, J.M., "Electronic properties of some simple chalcogenide glasses", J . Non-Crystalline Solids, 2, 40 (1970).

Pearson, A.D., "Modern Aspects of the Vitreous State", Ed. J. D. Mackenzie (Butterworths: Washington), (1963).

Pearson, A.D., "The Hall effect-Seebeck effect sign anomaly in semiconducting glasses", of. Electrochem - Soc., 111, 753 (1964).

Pearson, A.D., "Memory and switching in semiconducting glasses", J. Non-Crystalline Solids, 2, 1 (1970).

Peck, W.F., and Dewald, J.F., "The Hall effect in semiconducting glasses", J. Electrochem. Soc., 111, 561 (1964).

Phillips, S.V., Booth, R.E., and McMillan, P.W., "Structural changes related to electrical propertives of bulk chalcogenide glasses", J. Non-Crystalline Solids, 4, 510 (1970).

Pollak, M., "Approximations for the a.c. hopping conduction", Phys. Rev., 133, A564 (1964).

Pollak, M., "Temperature-dependence of a.c. hopping conductivity", Ibid., 138, A1822 (1965).

Pollak, M., and Geballe, T.H., "Low frequency conductivity due to hopping process in silicon", Phys. Rev., 122, 1742 (1961).

Proyor, R.W., and Henisch, H.K., "Nature of the ON-state in chalcogenide glass threshold switches", J. Non-Crystalline Solids, 7, 181 (1972).

Roe, D.W., "New glass compositions possessing electronic conductivities", J. Electrochen. Soc., 112, 1005 (1965).

Roy, R., "Classification of non-crystalline solids", J. Non-Crystalline Solids, 3, 33 (1970).

Savage, J.A., "Glass formation and D.S.C. data in the Ge-Te and As-Te memory glass systems", J. Non-Crystalline Solids, 11, 121 (1972).

Sewell, G.L., "Model of thermally activated hopping motion in solids", Phys. Rev., 129, 597 (1963).

Schottmiller, J., Tabak, M., Lucovsky, G., and Ward, A., "The effects of valency on transport properties in vitreous linary alloys of selenium", J. Non-Crystalline Solids, 4, 80 (1970).

Shanks, R.R., "Ovonic threshold switching charactersitics", J. Non-Crystalline Solids, 2, 504 (1970).

Shappirio, J.R., Eckart, D.W., and Cook, C.F., "Chemical and structural characterization of amorphous semiconducting materials in the system Te-As-Se-As", J. Non-Crystalline Solids, 2, 217 (1970).

Shaw, R.F., Liang, W.Y., and Yoffe, A.D., "Optical properties, photoconductivity, and energy levels in crystalline and amorphous arsenic triselenide", J. Non-Crystalline Solids, 4, 29 (1970).

Shaw, R.R., and Uhlmann, D.R., "Effect of phase separation on the properties of simple glasses. II. Elastic properties", J. Non-Crystalline Solids, 5, 237 (1971).

Sie, C.H., "Electron microprobe analysis and radiometric microscopy of electric field induced filament formation on the surface of As-Te-Ge glass", J. Non-Crystalline Solids, 4, 548 (1970).

Sliva, P.O., Dir, G., and Griffiths, C., "Bistable switching and memory devices", J. Non-Crystalline Solids, 2, 316 (1970).

Stiegler, H., and Haberland, D.R., "The switching behaviour of chalcogenide glass with semiconducting electrodes", J. Non-Crystalline Solids, 11, 147 (1972).

Stocker, H.J., Barlow, C.A., and Weirauch, D.F., "Mechanism of threshold switching in semiconducting glasses", 4, 523 (1970).

Stocker, H.J., "Phenomenology of switching and memory effect in semiconducting chalcogenide glasses", J. Non-Crystalline Solids, 2, 371 (1970).

Stuke, J., "Review of optical and electrical properties of amorphous semiconductors", J. Non-Crystelline Solids, 4, 1 (1970).

Sugi, M., Fizma, S., and Kikuchi, M., "Kenetics of crystallization in chalcogenide glasses", J. Non-Crystalline Solids, 5, 358 (1971).

Tauc, J., Grigorovici, R., and Vancu, A., "Optical properties and electronic structure of amorphous germanium", Phys. Stat. Sol., 15, 627 (1966).

Taylor, P.L., "Energy gaps in disordered systems", Proc. Phys. Soc., 88, 753 (1966).

Uttecht, R., Stevenson, H., Sie, C.H., Griener, J.D., and Raghavan, K.S., "Electric field-induced filament formation in As-Te-Ge glass", J. Non-Crystalline Solids, 2, 358 (1970).

Walsh, P.J., Hall, J.E., Nicolaides, R., Defeo, S., Calella, P., Kuchmas, J., and Doremus, W., "Experimental results in amorphous semiconductor switching behaviour", J. Non-Crystalline Solids, 2, 107 (1970).

Warren, A.C., "Thermal switching in semiconducting glasses", J. Non-Crystalline Solids, 4, 613 (1970).

Weisberg, L.R., "Anomalous mobility effects in some semiconductors and insulators", J. Appl. Phys., 33, 1817 (1962).

Wilms, A., and Phariseau, P., "On a formal theory of conductivity in amorphous media", J. Non-Crystalline Solids, 4, 442 (1970).